

ADVANCED MASTERS IN STRUCTURAL ANALYSIS
OF MONUMENTS AND HISTORICAL CONSTRUCTIONS

Master's Thesis

Saray S. Sepulveda Cruz

Experimental investigation of
climate effects on historical
building materials: the Gothic
towers of Prague.



University of Minho

Czech Republic | 2023



DIPLOMA THESIS ASSIGNMENT FORM

I. PERSONAL AND STUDY DATA

Surname: Sepulveda Cruz	Name: Saray Soranyelly	Personal number: 520834
Assigning Department: Department of Mechanics or Department of Architecture or Department of Hydraulic Structures (select one, for ITAM use Dept. of Mech.)		
Study programme: Civil Engineering		
Study branch/spec.: Advanced Masters in Structural Analysis of Monuments and Historical Constructions		

II. DIPLOMA THESIS DATA

Diploma Thesis (DT) title: Experimental investigation of climate effects on historical building materials: the Gothic towers of Prague	
Diploma Thesis title in English: _____	
Instructions for writing the thesis: 1) calibration of the laboratory wind tunnel and development of appropriate testing methodology 2) experimental investigation of material specimen subjected to different climate scenarios 3) comprehensive review of different types of sensors will be also conducted. .	
List of recommended literature: Cacciotti, R. Brick masonry response to wind driven rain, Engineering Structures 204, 2020, 110080; Cacciotti, Riccardo - Wolf, Benjamin - Macháček, Michael - Frankl, Jiří. Innovative device for the simulation of environmental conditions and testing of building materials. Engineering mechanics 2022. Book of full texts. Prague: Institute of Theoretical and Applied Mechanics of the Czech Academy of Sciences, 2022; 15; Cacciotti, R., Pospíšil, S., Kuznetsov, S. and Trush, A.: A proposed calibration procedure for the simulation of wind-driven rain in small-scale wind tunnel. Experimental Techniques. 43 (4) 369-384 (2019)	
Name of Diploma Thesis Supervisor: _____	
DT assignment date: 14.3.2023	DT submission date in IS KOS: 6.7.2023 <i>see the schedule of the current acad. year</i>
_____	_____
DT Supervisor's signature	Head of Department's signature

III. ASSIGNMENT RECEIPT

<i>I declare that I am obliged to write the Diploma Thesis on my own, without anyone's assistance, except for provided consultations. The list of references, other sources and consultants' names must be stated in the Diploma Thesis and in referencing I must abide by the CTU methodological manual "How to Write University Final Theses" and the CTU methodological instruction "On the Observation of Ethical Principles in the Preparation of University Final Theses".</i>	
_____	_____
Assignment receipt date	Student's name

DECLARATION

Name: Saray Soranyelly Sepulveda Cruz

Email: Saray_9066@hotmail.com, sepulsar@student.cvut.cz

Title of the Msc Dissertation: *Experimental investigation of climate effects on historical building materials: the Gothic towers of Prague*

Supervisor (s): Ing. Riccardo Cacciotti PhD.

Year: 2023

I hereby declare that all information in this document has been obtained and presented in accordance with academic rules and ethical conduct. I also declare that, as required by these rules and conduct, I have fully cited and referenced all material and results that are not original to this work.

I hereby declare that the MSc Consortium responsible for the Advanced Masters in Structural Analysis of Monuments and Historical Constructions is allowed to store and make available electronically the present MSc Dissertation.

University: Czech Technical University in Prague, University of Minho

Date: 2023-04-21

Signature: _____

This page is left blank on purpose.

DEDICATION

I dedicate my thesis to my husband for being responsible for bringing me here. Thanks for his care, patience, and love, and above all thanks for his support, he was the pillar of my health in times of illness. I know that this gratitude does not do justice to everything you have done, but this dedication of my thesis is just a small form of gratitude and demonstration of the love I have for you.

I also dedicate my thesis to my teacher and above all unconditional friend Alfredo Mateus, who instilled in me a love for this area of engineering. Thank you for being a part of this process and being there every step of the way.

This page is left blank on purpose.

ACKNOWLEDGEMENTS

I give a special thanks to the company Patología e Ingeniería Estructural S.A.S. for making this Master's degree possible.

I want to express my deep gratitude to my thesis supervisor, Eng. Riccardo Cacciotti, for his guidance, constant support, and patience throughout this process.

Thanks to my parents, and my siblings for being my support and always being there for me.

This page is left blank on purpose.

ABSTRACT

In recent years, the degradation processes of construction materials such as stone have increased significantly, to which the effects of the frequency and magnitude of climatic phenomena have contributed. This can be observed today in monuments of great historical importance, which had remained in optimal conditions, are currently in a state of degradation and advanced alteration of the material that composes them, jeopardizing their structural integrity and even reaching the impossibility of preserving their historical values, either because of the irreversible state of the damage or because of the high costs of intervention.

This research focuses on the experimental investigation of the stone material using wind tunnels to simulate the effects of rain and wind on the material, in order to understand the behavior of the construction material when subjected to different environmental scenarios.

Through the investigation carried out, it was possible to determine the behavior and state of saturation within the porous materials, through the analysis of the variation of the electrical resistance for different rain loads and different speeds of the air flow, correctly detecting the storage and transport mechanisms.

The study material consisted of 4 sandstone specimens from previous studies carried out by ITAM, which were subsequently analyzed under environmental conditions of average temperature and relative humidity during the summer months in Prague. It was possible to establish a qualitative and quantitative analysis of the susceptibility index to wind and rain of the material using the calculation of the resistances obtained. Additionally, four towers built with sandstone in the Gothic style of the city of Prague were taken as a case study, of which a model was made for 1) the analysis of the action of the wind, in general of the force perpendicular to the surface of each exposed point of two of the facades of the model, 2) identification of the form of movement of the air flow through helium bubbles inside the tunnel. Finally, an analysis of the damage present in the towers was carried out, to obtain a vulnerability classification of the study structures.

This page is left blank on purpose.

SHRNUTÍ

V posledních letech se výrazně zvýšily degradační procesy stavebních materiálů, jako je kámen, k čemuž přispěly vlivy četnosti a velikosti klimatických jevů. To lze dnes pozorovat u památek velkého historického významu, které zůstaly v optimálních podmínkách, v současné době jsou ve stavu degradace a pokročilé obměny materiálu, který je tvoří, což ohrožuje jejich strukturální integritu a dokonce dosahuje nemožnosti uchování jejich historických hodnot, ať už z důvodu nevratného stavu poškození nebo z důvodu vysokých nákladů na zásah.

Tento výzkum se zaměřuje na experimentální zkoumání kamenného materiálu pomocí aerodynamických tunelů k simulaci účinků deště a větru na materiál, aby bylo možné porozumět chování stavebního materiálu, když je vystaven různým environmentálním scénářům.

Prostřednictvím provedeného průzkumu bylo možné určit chování a stav nasycení v porézních materiálech pomocí analýzy změn elektrického odporu pro různé zatížení deštěm a různé rychlosti proudění vzduchu, správně detekovat skladování a přepravu mechanismy.

Studijní materiál tvořily 4 pískovcové vzorky z předchozích studií provedených ITAM, které byly následně analyzovány v podmínkách prostředí průměrné teploty a relativní vlhkosti v letních měsících v Praze. Pomocí výpočtu získaných odporů bylo možné stanovit kvalitativní a kvantitativní analýzu indexu citlivosti materiálu na vítr a déšť. Dále byly jako případová studie brány čtyři věže postavené z pískovce v gotickém stylu města Prahy, z nichž byl vytvořen model pro 1) analýzu působení větru, obecně síly kolmé k povrchu každého exponovaného bodu dvou fasád modelu, 2) identifikace formy pohybu proudění vzduchu přes bublinky helia uvnitř tunelu. Nakonec byla provedena analýza poškození přítomných ve věžích, aby se získala klasifikace zranitelnosti studovaných struktur.

This page is left blank on purpose.

SÍNTESIS

En los últimos años se han incrementado significativamente los procesos de degradación de materiales de construcción como la piedra, a lo que han contribuido los efectos de la frecuencia y magnitud de los fenómenos climáticos. Esto se puede observar hoy en día en monumentos de gran importancia histórica, que habiendo permanecido en condiciones óptimas, se encuentran actualmente en un estado de degradación y alteración avanzada del material que los compone, poniendo en peligro su integridad estructural e incluso llegando a la imposibilidad de conservar sus valores históricos, ya sea por el estado irreversible del daño o por los altos costos de intervención. Las estrategias de prevención son necesarias para evitar una degradación excesiva y patologías graves en el material que conforma la estructura, en este enfoque es necesario investigar y caracterizar la interacción entre las propiedades del material y los factores climáticos, por lo que es importante implementar metodologías y herramientas innovadoras.

Esta investigación se enfoca en la investigación experimental del material pétreo utilizando túneles de viento para simular los efectos de la lluvia y el viento sobre el material, para comprender el comportamiento del material de construcción cuando es sometido a diferentes escenarios ambientales.

Mediante la investigación realizada se logró determinar el comportamiento y estado de saturación dentro de los materiales porosos, mediante el análisis de la variación de la resistencia eléctrica para diferentes cargas de lluvia y diferentes velocidades del flujo de aire, detectando correctamente los mecanismos de almacenamiento y transporte.

El material de estudio consistió en 4 probetas de areniscas de estudios previos realizados por el ITAM, las cuales fueron posteriormente analizadas en condiciones ambientales de temperatura media y humedad relativa durante los meses de verano en Praga. Se logró establecer un análisis cualitativo y cuantitativo del índice de susceptibilidad al viento y lluvia del material empleando el cálculo de las resistencias obtenidas. Adicionalmente, se tomó como caso de estudio cuatro torres construidas con piedra arenisca al estilo gótico de la ciudad de Praga, de las cuales se realizó una maqueta para 1) el análisis de la acción del viento, en general de la fuerza perpendicular a la superficie de cada punto expuesto de dos de las fachadas de la maqueta, 2) identificación de la forma de movimiento del flujo de aire

mediante burbujas de helio en el interior del túnel. Finalmente, se realizó un análisis de los daños presentes en las torres, para obtener una clasificación de vulnerabilidad de las estructuras de estudio.

This page is left blank on purpose.

TABLE OF CONTENTS

1	CHAPTER - PROBLEM STATEMENT	1
1.1	Questions to develop during the study	1
2	CHAPTER no.2 - METHODOLOGICAL FRAMEWORK	3
2.1	State of the art	3
2.2	Presentation of methods	5
2.2.1	Experimental methods for testing rain and wind effects	6
2.2.1.1	Moisture monitoring	6
2.2.1.2	Flow visualization	7
2.2.1.3	Wind pressure measurement	8
2.2.2	Climate simulation in small and large tunnel	10
2.2.3	Vulnerability assessment	12
2.2.3.1	Fragility Curves	14
3	CHAPTER no. 3 - EXPERIMENTAL INVESTIGATION	16
3.1	Material characterization	17
3.1.1	Typical Damage to building stone material	18
3.2	Experimental methods on sandstone samples	19
3.3	Experimental investigation with the small wind tunnel	24
3.3.1	Vulnerability assessment of the material	30
3.4	Tests in the large tunnel	36
3.4.1	Pressure measurement test	37
3.4.2	Flow visualization test	47
4	CHAPTER no. 4 - CASE OF STUDY	51
4.1	Historical Survey	51
4.2	Visual Inspection and damage survey	53
5	CHAPTER no. 5 – ANALYSIS OF THE RESULTS	57
6	CHAPTER no. 6 - CONCLUSIONS AND RECOMMENDATIONS	59
7	CHAPTER no. 6 - DIFFICULTIES AND LIMITATIONS	62
	REFERENCES	63
	DOCUMENTATION ANNEXED	67

Annex No. 1: Damage survey sheets _____ **68**

FIGURES

<i>Figure 1: Right - Some physical aggressors of buildings (Broto I). Left - Wind flow pattern around a building and raindrop trajectories in the wind flow pattern. (B. Blocken, J. Carmeliet),</i>	4
<i>Figure 2: left electronic board, Right Moisture control system sensor</i>	6
<i>Figure 3: Example of different bodies with sharp edges, where it can be seen that the detachment occurs on the first edge. Source: J. Lässig, U. Jara, A. Apcarian</i>	7
<i>Figure 4: Right-Plan view of the Vincenc Strouhal wind tunnel, designed in a near-oval closed shape adapted for aerodynamic and climatic testing. Arrows point in the wind flow direction. Left-inside the climatic section. Source: R. Cacciotti & S. Pospíšil & S. Kuznetsov1 & A. Trush</i>	9
<i>Figure 5: Pitot-Static Tube (Prandtl tube)</i>	10
<i>Figure 6: Above: isualization of main components of the SSWT. Source: R. Cacciotti a, B. Wolf a , M. Machaček.</i>	12
<i>Figure 7: failure frequency (28)</i>	15
<i>Figure 8: Classification of sandstone samples.</i>	17
<i>Figure 9: sandstone specimens.</i>	19
<i>Figure 10: specimens inside the wind tunnel</i>	20
<i>Figure 11: Schematic of rainfall simulation in sandstone specimens.</i>	20
<i>Figure 12: Drilling in the sample for electrode installation</i>	21
<i>Figure 13: Preparation of syringes for on-site injection.</i>	22
<i>Figure 14: Left-Clean specimen. Right-Check to prevent the measurement from being influenced by surface resistance values.</i>	22
<i>Figure 15: Specimens covered with aluminum</i>	23
<i>Figure 16: left - Rain simulation. Right - placement of specimens in the wind tunnel.</i>	23
<i>Figure 17: Samples in the wind tunnel and assignment of wind speed, temperature and relative humidity parameters.</i>	24
<i>Figure 18: Susceptibility index</i>	30
<i>Figure 19: Dimensional relationships from Google measurements</i>	36
<i>Figure 20: Left- Scanivalve MPS 4264 pressure transducers. Right- Pitot tube connection.</i>	37
<i>Figure 21: Sensor installation and testing</i>	38
<i>Figure 22: Distribution of sensors on facade A and B of the scale model.</i>	39
<i>Figure 23: Left-Position of the scale model inside the tunnel at 0 degrees. Right-Position of the scale model inside the tunnel rotated at 45 degrees.</i>	39
<i>Figure 24: Montaje del modelo a escala dentro del tunel de viento.</i>	41
<i>Figure 25: Pressure map at 0° degrees at different speeds. Façade A.</i>	43

<i>Figure 26: Pressure map at 0° degrees at different speeds. Façade B.</i>	44
<i>Figure 27: Pressure map at 45° degrees at different speeds. Façade A</i>	45
<i>Figure 28: Pressure map at 45° degrees at different speeds. Façade B.</i>	46
<i>Figure 29: Helium bubble generator model 5</i>	47
<i>Figure 30: General configuration of the test with tower at 0 degrees.</i>	48
<i>Figure 31: General test setup with tower at 45 degrees.</i>	48
<i>Figure 32: 2% flow visualization test.</i>	49
<i>Figure 33: 5% flow visualization test.</i>	50
<i>Figure 34: Location of the study towers.</i>	53
<i>Figure 35: Survey of damages in the study towers.</i>	54

TABLES

<i>Table No. 1: Description of the material.....</i>	<i>17</i>
<i>Table No. 2: Basic parameters of the specimen structure.....</i>	<i>18</i>
<i>Table No. 3: Most common types of injuries in stone material.....</i>	<i>18</i>
<i>Table No. 4: Input data from the tests carried out in the small tunnel.....</i>	<i>24</i>
<i>Table No. 5: Rain simulation record, experiment 1 at 700 rpm.....</i>	<i>25</i>
<i>Table No. 6: Rain simulation record, experiment 1 at 350 rpm.....</i>	<i>25</i>
<i>Table No. 7: Rain simulation record, experiment 1 at 60 rpm.....</i>	<i>25</i>
<i>Table No. 8: calculation of the averages that were used for the idealized model.....</i>	<i>37</i>
<i>Table No. 9: Pressure measurements, tower 0°.....</i>	<i>40</i>
<i>Table No. 10: Pressure measurements, tower 45°.....</i>	<i>40</i>
<i>Table No. 11: Damage found in the study towers. Source: Icomos.....</i>	<i>55</i>

LIST OF GRAPHIC

<i>Graph No. 1: Electrical resistance measurement - Especimen No.1 700 Rpm.....</i>	<i>26</i>
<i>Graph No. 2: Electrical resistance measurement - Especimen No.2 700 Rpm.....</i>	<i>27</i>
<i>Graph No. 3: Electrical resistance measurement - Especimen No.3-350 Rpm</i>	<i>28</i>
<i>Graph No. 4: Electrical resistance measurement - Especimen No.4-350 Rpm</i>	<i>28</i>
<i>Graph No. 5: Electrical resistance measurement - Especimen No.1-60 Rpm</i>	<i>29</i>
<i>Graph No. 6: Electrical resistance measurement - Especimen No.2-60 Rpm</i>	<i>30</i>
<i>Graph No. 7: MC vs T 700 rpm. Specimen 1 and 2.</i>	<i>31</i>
<i>Graph No. 8: MC vs T 700 rpm. Specimen 3 and 4</i>	<i>31</i>
<i>Graph No. 9: MC vs T 350 rpm. Specimen 1 and 2</i>	<i>32</i>
<i>Graph No. 10: MC vs T 350 rpm. Specimen 3 and 4</i>	<i>32</i>
<i>Graph No. 11: MC vs T 60 rpm. Specimen 1 and 2.</i>	<i>33</i>
<i>Graph No. 12: MC vs T 60 rpm. Specimen 3 and 4.</i>	<i>33</i>
<i>Graph No. 13: Rain Intensity</i>	<i>35</i>
<i>Graph No. 14: Wind Intensity</i>	<i>35</i>
<i>Graph No. 15: Cp vs Re 0°</i>	<i>46</i>
<i>Graph No. 16: Cp vs Re 45°</i>	<i>47</i>

1 CHAPTER - PROBLEM STATEMENT

The study focuses on the experimental investigation of material samples subjected to different climatic scenarios.

It allows proper analysis of possible pathological processes in the material due to meteorological action, as well as provides relevant clues for low-cost conservation and rehabilitation interventions that allow future reuse of the built heritage with low energy consumption and higher structural resistance. The main challenge is to establish a valid experimental methodology to support decision-making and risk management in built heritage.

1.1 Questions to develop during the study

- Question 1: Why is the study of the behavior of materials of vital importance for the structural conservation of cultural properties?

Objective: It is required to analyze the behavior of materials in response to temperature, wind-driven rain, and pressure. The analysis and characterization of the behavior of materials in the laboratory must provide visibility of the real world by generating information in a variety of environmental conditions, and contamination that allow analyzing the possible effects on the quality of the material.

- Question 2: How can different climate scenarios be effectively simulated in the laboratory and how to evaluate the effects on historic building materials?

Objective: Define parameters and procedures for the analysis of the effect of wind-driven rain in different scenarios, through experimental research.

- Question 3: Is it possible to generate solutions for the reuse of built heritage with low energy consumption to improve structural resistance and decrease the environmental impact in the field of construction?

Objective: The effectiveness of the simulation of climatic scenarios in the experimental tests on the materials will be evaluated, focusing on the behavior of moisture displacement in the material, to apply non-destructive methodologies that lead to preventing pathologies of great importance that generate massive interventions, and therefore, a high environmental impact. For this, the damage present in the towers of the case study will be analyzed and compared with the information obtained in the laboratory.

- Question 4; In the perspective of climate change, how to exploit experimental data for future risk projections and hence improve management of CH assets and their resilience?

Objective: Through the analysis of experimental tests and wind tunnel analysis, we seek to find a suitable relationship of moisture content in the material versus the intensities of factors such as rain and wind, to generate index susceptibility curves to lead to a vulnerability analysis of the study structure.

2 CHAPTER No.2 - METHODOLOGICAL FRAMEWORK

2.1 State of the art

Climate change studies focused on structures of cultural interest allow improving conservation interventions, generating greater durability and even comfort in this type of structures, achieving the future reuse of built heritage with low energy consumption to improve structural resilience, which is of vital importance, considering that the construction processes of new structures are important carbon emitters.

Numerous studies have been developed on this topic due to the awareness of the adverse effects on structures when subjected to various climate scenarios. Hans Antonson, Philip Buckland, and Roger Nyqvist (1) present a review of the treatment of climate change issues related to cultural heritage at different levels of government decision-making that deal with physical planning. In this research the need for the creation of a comprehensive manual or best practices for safeguarding heritage is evidenced, as unfortunately there is a great lack of knowledge among government officials, professionals, and entities related to the field of restoration and protection of cultural property. as Another study concentrating on how climate change can affect UNESCO cultural heritage sites in Panama (2), aims to provide guidelines and recommendations on possible measures to improve cultural heritage risk management at the European level and in support of the implementation of Priority 4 of the Sendai Framework Action Plan, focusing on the effects of climate change (3). Adaptation of cultural heritage to climate change is necessary to mitigate its effects and increase the resilience of historic sites. Therefore, organizations such as UNESCO, ICOMOS, IPCC, and the EC recommend further research on this topic (4).

The increase of CO₂ to more than 410 ppm in 2020, has resulted in unprecedented rates of environmental change (5). Climate change studies in structures of cultural interest allow to improve conservation and conditioning interventions, allowing greater durability and even comfort in this type of structures, achieving in the future to reuse the built heritage with low energy consumption to improve structural resilience, slowing down or slowing down the loss of values attributed to cultural heritage. This is of vital importance, considering that the construction processes of new structures are important carbon emitters, the adaptability,

recovery, and enhancement of this type of historic buildings are a breakthrough to reduce the carbon footprint and safeguard the environment (6).

Alterations due to chemical and environmental factors are one of the main parameters to be considered, since in many historic stone buildings a black and often irregular coloration of the surfaces can be observed, which diminishes the aesthetic impression of these objects. The cause of these thin black layers and the destruction of the stone surfaces of buildings is much more serious than the aesthetic aspect. It is related to weathering due to increased air pollution, microbial activity and climatic conditions (7), so in terms of building pathology, it is necessary to talk about the agents that generate the most important injuries in buildings, among them water (figure 1), which has a high power of dissolution of the material since it decreases its resistance, leading to processes of instability and cohesion. If acids and environmental pollutants (carbon dioxide, nitrogen oxides, etc.) are added to this agent, reactions can occur in the material, giving rise to other pathologies not only of a chemical, biological and physical type, remember that minerals and organic acids dissolve silicates and calcium aluminates, forming salts or complexes soluble in water (8)

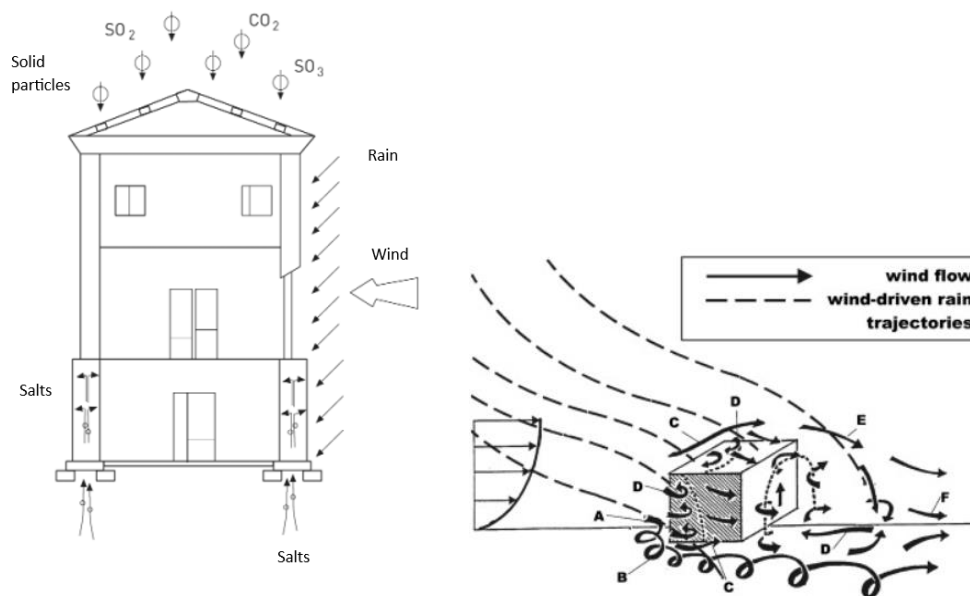


Figure 1: Right - Some physical aggressors of buildings (Broto I). Left - Wind flow pattern around a building and raindrop trajectories in the wind flow pattern. (B. Blocken, J. Carmeliet),.

The effects of biodegradation are often like those of physical degradation, microorganisms (bacteria and cyanobacteria, algae, fungi, and lichens) can attack and degrade

building materials, i.e. generate surface roughness, formation of small cracks, color change and deposition of inorganic and organic substances. For example, the swelling attack is caused by salt stress due to the attack of mineral acids (sulfuric, nitric, carbonic) and organic acids (acetic, citric, oxalic, gluconic) in which the retention of water in porous materials causes greater susceptibility to attack by freezing and thawing and favors crystallization. (9).

For a proper analysis of the effects of these agents and the damage they can cause, it is necessary to consider climatological data and environmental parameters such as humidity, temperature, and air velocity to determine the behavior of the materials and the simulation of these characteristics in the laboratory. Moisture measurement requires repeatable, minimally invasive and cost-effective solutions with regulated data collection and processing practices (10). This paper aims to conduct an experimental investigation of climatic effects on historical building materials using a laboratory size wind tunnel for the simulation of natural ventilation, relative humidity, and temperature fluctuations, as well as testing these parameters on scale models of some of the most representative towers of the city of Prague, which will be analyzed in the large wind tunnel in the city of Telc. The research aims to obtain a deeper insight into the behavior of building materials when subjected to different environmental scenarios to generate adequate and durable mitigation measures.

2.2 Presentation of methods

A factor such as moisture can cause inadequate serviceability and affect material durability and structural integrity, which, coupled with other factors, can lead to defects or sudden failure (11). To determine the interrelationship between temperature and relative humidity variations, as well as the effect of airflow velocity, the following methods have been employed in this study: 1) Experimental methods for testing rain and wind effects 2) Climate simulation in small and large tunnel 3) valuation methods for assessing vulnerability and implement proper risk management.. Sections 2.2.1, 2.2.2, and 2.2.3 describe in detail the principles behind each method.

2.2.1 Experimental methods for testing rain and wind effects

2.2.1.1 Moisture monitoring

The evaluation of the effects of wind-driven rain allows us to analyze the trends of degradation phenomena in traditional materials. This also allows us to achieve an adequate and comparative analysis of their behavior under different environmental conditions, detailed knowledge of moisture transport is essential to understand their durability (12). In this study, an electrical resistance measurement system, developed by ITAM CAS, is employed to determine the distribution of moisture inside the material in a non-destructive and repeatable way. It consists of the installation of solid copper wire sensors in the test material, connected to an electronic board and software for the moisture monitoring system (Figure 2), (13). Its principle is based on the measurement of changes in electrical resistance due to the presence of water, thus, the greater the presence of water in contact with the sensors, the greater the activation of the sensors, which record the decrease in electrical resistance at different distances from the wet face of the specimen

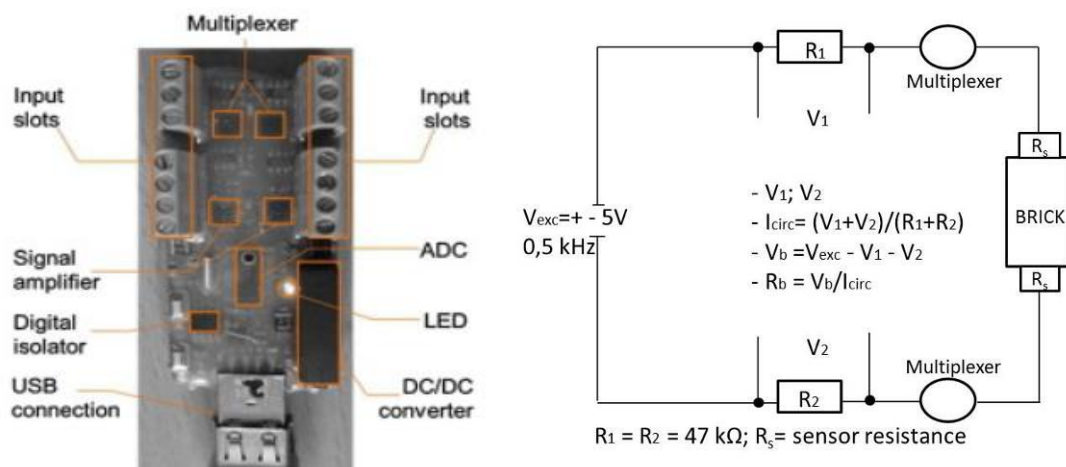


Figure 2: left electronic board, Righ Moisture control system sensor

The moisture monitoring system relies on an ammeter voltmeter method. The circuit enables the assessment of the voltage drop due to the changing electrical resistance of the material specimen. An alternating voltage $V_{exc} = \pm 5\text{ V}$ is applied with a frequency of 0.5 kHz . Voltages V_1 and V_2 are measured employing voltmeters across two resistors R_1 and R_2 of known resistance $47\text{ k}\Omega$. Depending on the direction of the current one of these measurements indicate the voltage drop because of crossing the material. To allow

simultaneous measurements at multiple points on the brick, a multiplexer is used so that several signals share the same device. The multiplexer prevents the crisscrossing of current flow among different pairs of electrodes installed..

The test instrumentation involves the installation of the electrode sensors, injection of resin mixture with graphite, cleaning of excess resin and sealing of the top of the sensor, subsequent insertion of the specimens inside the wind tunnel at laboratory conditions.

This system is used for monitoring rainwater penetration in the material during the environmental simulation in the laboratory-size tunnel.

2.2.1.2 Flow visualization

This is important when it is required to investigate the behavior of drag and adhesion of water particles and contaminant particles that can accumulate on the structure, since a turbulent flow can create low-pressure zones that tend to stabilize quickly attracting molecules from adjacent areas, which shows the importance of identifying the types of flows on the object of study. However, this type of test is possible because the air has a fluid behavior, therefore, it allows to identify of the laminar or turbulent profiles in contact with the object, identifying the points where it is difficult to adapt the air to the object (more turbulent flow), that is to say when the inertial forces are higher than the viscous forces, which is related to the separation of the boundary layer (adhered or not to the surface) in which in sections with sharp edges this separation is easily identifiable in experimental tests (wind tunnel) since it occurs in the first edge that should surround the flow ([Figure 3](#)), independent of Reynolds number, surface roughness, and wind characteristics ([21](#)). providing reliable climate simulation data in small and large tunnels.

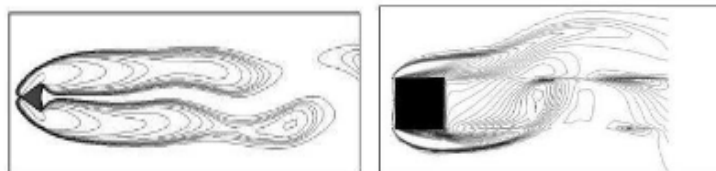


Figure 3: Example of different bodies with sharp edges, where it can be seen that the detachment occurs on the first edge. Source: [J. Lässig, U. Jara, A. Apcarian](#)

The flow visualization method using helium bubbles is used in the large wind tunnel.

For the test, a helium bubble generation console 5 was used, inside the wind tunnel without light. The console features a plug-in head and Mini-Vortex filter that produce neutral floating bubbles to seed the airflow. The plug-in head consists of a concentric arrangement of two hypodermic tubes cantilevered to a cylindrical manifold base. Inside the head, helium passes through the inner hypodermic tube, and the bubble film solution passes through the ring between the inner tube and outer tube to form helium-filled bubbles at the tip of the outer tube. As the bubbles form, a larger concentric jet of air blows them continuously from the tip of the outer tube. [Model 5 Console](#)

2.2.1.3 Wind pressure measurement

As already mentioned, wind tunnels present an adequate way to observe wind behavior, either for the calculation of the resistance of construction materials or for the design of an adequate geometry in contemporary constructions, or for the experimentation of climatic effects on historical materials as in the present study. This is possible by means of scale models, for the measurement of magnitudes such as wind speed, distribution, and value of the pressures exerted by the wind on a building through sensors located in specific areas. (24), depending on the shape, dimensions, characteristics, permeability of the material, wind direction and intensity.

Thus, it is important to understand that buildings are subjected to loads that vary, not static, either by turbulence of the incident current or the boundary layer of the object, so, for the determination of the stresses generated by the wind on the structure, it is sufficient to estimate the aerodynamic loads averaged over time. In this case, the wind action on the buildings must be known. For example, the difference in pressures on the facades is known as the aerodynamic effect (25), where the face perpendicular to the wind, i.e. windward, is the area where positive pressures (high-pressure areas) are present, where the maximum pressure depending on the angle of incidence of the wind can have a reduction of 50%. Negative pressures (low-pressure areas) occur on the opposite side of the wind, i.e. to leeward.

For the pressure coefficient, the external pressures are measured for different wind angles of attack and the total pressure on the structure is established. The external pressure coefficient C_p related to an individual shot measured with index i can be expressed as a ratio

between the difference between the actual pressure recorded at that point and the static pressure of the Pitot tube P_i and the mean reference value of the dynamic pressure P_{ref} of the Pitot tube (Figure 6).

$$C_p = \frac{p_i}{p_{ref}} \quad [1]$$

$$v_{ref} = \sqrt{\frac{2p_{ref}}{\rho}} \quad [2]$$

Where v_{ref} the mean wind velocity at the reference height z_{ref} , ρ the air density. Positive values correspond to pressures and negative values to suction.

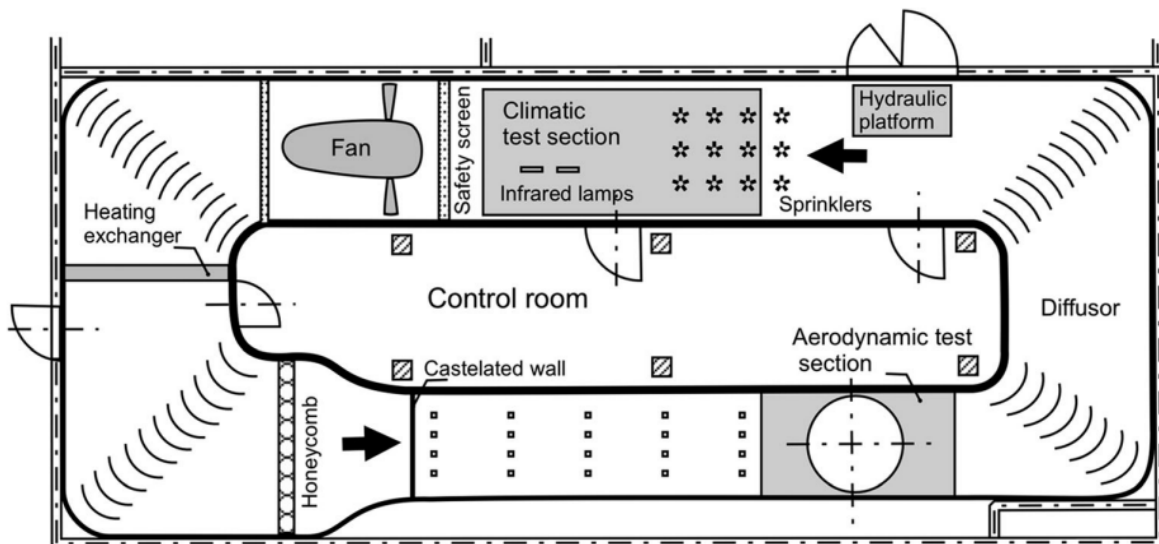


Figure 4: Right-Plan view of the Vincenc Strouhal wind tunnel, designed in a near-oval closed shape adapted for aerodynamic and climatic testing. Arrows point in the wind flow direction. Left-inside the climatic section. Source: [R. Cacciotti & S. Pospíšil & S. Kuznetsov1 & A. Trush](#)

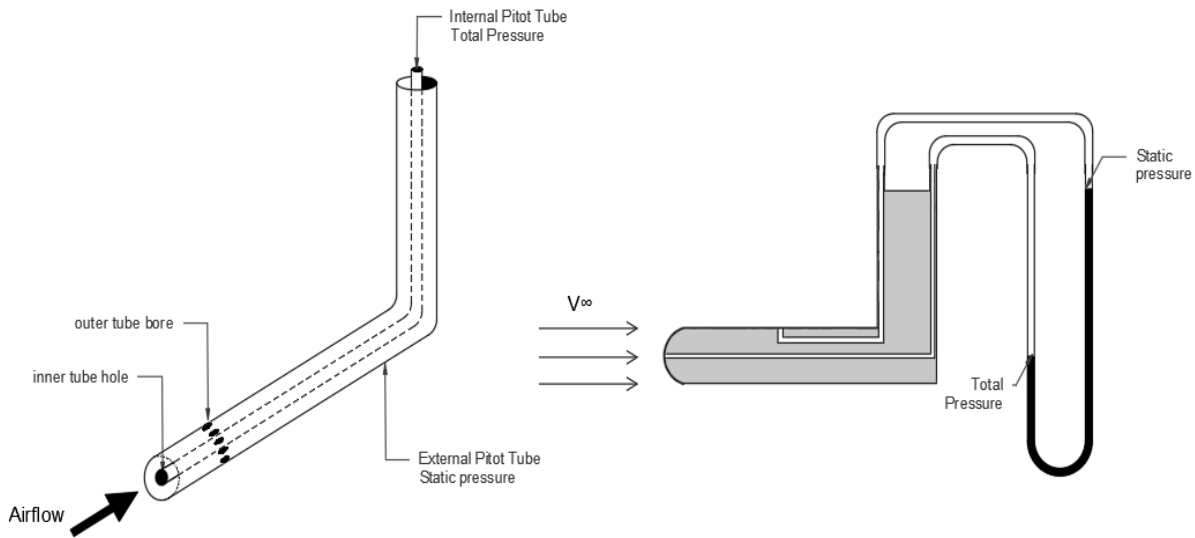


Figure 5: Pitot-Static Tube (Prandtl tube)

2.2.2 Climate simulation in small and large tunnel

Wind-driven rain is the most important source of moisture affecting the performance of building façades (14), Nevertheless, despite the acknowledgment of the relevance of this phenomenon, there are still major construction problems, damage claims, and enormous repair and replacement costs that continue to increase year after year (15). For this reason, wind tunnel tests present a very useful tool in the field of structural engineering focused on the safeguarding of architectural heritage, allowing to know the behavior of different materials subjected to different wind speeds, relative humidity, and temperature, ensuring the reproduction of a homogeneous volume of rainwater and natural distribution of raindrop size (16). This is to identify in time the possible damages that lead to an aesthetic degradation of the building and its structural integrity, as well as to develop adequate strategies for the prevention and effective solution of the existing pathologies.

The use of wind tunnels in the study of structures has been carried out for years, as is the case with the use of atmospheric boundary layer wind tunnels (17) which is important if accurate quantitative information for structural design is to be obtained from scale models (18). Various investigations have also been carried out in the field of wind tunnel simulations

to model rainfall impact rates on buildings (19), as well as tests for flow visualization using water bubbles (20) where it is possible to visualize in a practical way the airflow around a localized scale model, In this study two different devices will be employed: the laboratory-size tunnel and the large wind tunnel.

Testing of sandstone specimens for monitoring their response when subjected to different climate scenarios, is carried out in the laboratory-size tunnel. The 173 cm x 200 cm x 43.5 cm (height, width, and depth respectively) small-scale wind tunnel of the Institute of Theoretical and Applied Mechanics of the Czech Academy of Sciences is ideal for performance studies of historical building materials, presenting among its major advantages a didactic and low-budget analysis that allows simulating natural ventilation and other representative environmental conditions to which samples of building materials can be exposed for a prolonged period of time.(22). To determine the proper operation of the device, the adequacy of the environmental control system was investigated to evaluate the mutual effects between temperature (T) variations with two boundary temperatures, relative humidity (RH) and airflow velocity within the test section, it has the following characteristics: operating airflow velocity between 0.2 and 0.7m/s, operating temperature between 10°C and 35°C and allowable operating relative humidity between 30% and 99%. Its performance was validated by numerical simulation and experimental research, confirming the existence of stable wind and boundary layer conditions, and validating the correct operation of the tunnel for natural ventilation simulation for studies of the response of historical building materials under different environmental scenarios. Considering that the environmental control functionalities are subject to the operational limitations of the electronic or structural components of the circuit. (23). The description of the device components can be seen in [Figure 4](#).

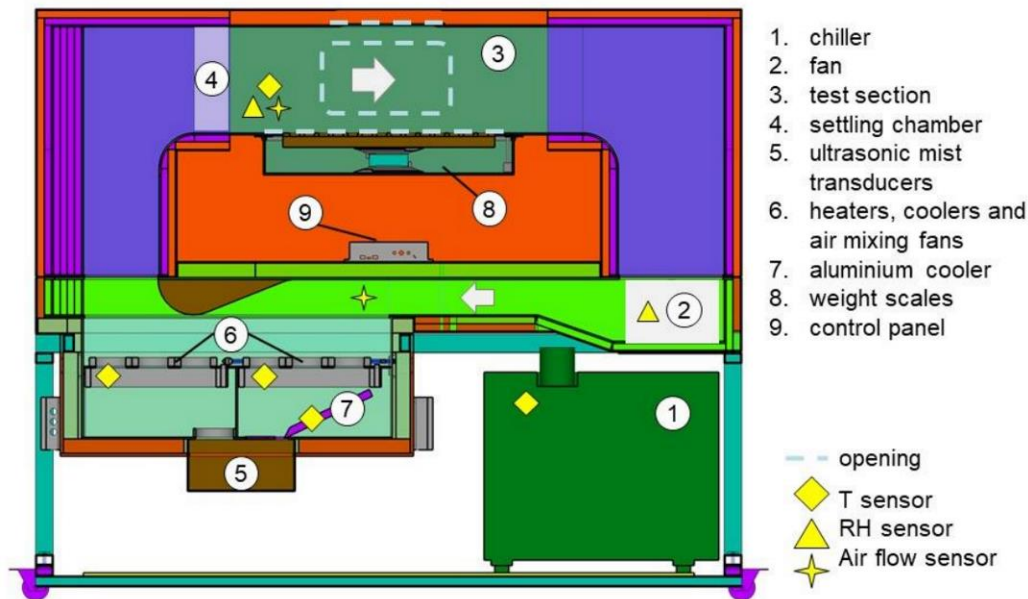


Figure 6: Above: isualization of main components of the SSWT. Source: [R. Cacciotti a, B. Wolf a , M. Macháček.](#)

Measurements of static pressures originating from the wind on the scale model of the Gothic-style towers of the city of Prague (Chapter No. 4) and flow visualization experiments are performed in the climatic section (rectangular cross-sectional dimension of 2.5×3.9 m and a length of 9.0 m) of the wind tunnel with the atmospheric boundary layer (BL) Vincenc Strouhal located at the Center of Excellence Telč, Czech Republic ([Figure 5](#)). Where the wind speed ranges from 0.6 to 15 m/s depending on the position of the vertically moving roof and the flow nozzle. Rain intensity and droplet size are regulated to simulate the effects corresponding to low or high-intensity rainfall.

2.2.3 Vulnerability assessment

Vulnerability assessment is the study of the capacity of an element to resist or mitigate the impact of an event that characterizes a hazard. It differs from risk analysis in that the latter refers to the estimation of feasible losses or consequences according to the degree of hazard considered and the level of a vulnerability existing in the exposed elements. The concepts of hazard, vulnerability, and risk are mutually conditioned. Thus, vulnerability is an internal risk factor that is mathematically expressed as the feasibility of the element under study being affected by the phenomenon that characterizes the hazard, i.e. the latent hazard or external

risk factor (probability of exceeding a certain level of occurrence of an event with a certain intensity, at a specific site and during a given exposure time). This is the potential for losses that may occur in the element of study (probability of exceeding a level of economic, social, or environmental consequences at a certain site and during a certain period of time)(26).

Some of the basic concepts to be considered are (27):

a) Hazard - H. Probability of occurrence of a potentially disastrous event during a certain period at a given site.

b) Vulnerability -V. Degree of loss of an element or group of elements under risk resulting from the probable occurrence of a disastrous event, expressed on a scale from 0 or no damage to 1 or total loss.

c) Specific Risk - R_s . Degree of expected losses due to the occurrence of a particular event and as a function of hazard and vulnerability.

d) Elements at Risk - E. These are the population, buildings and civil works, economic activities, public services, utilities, and infrastructure exposed in a given area.

e) Total Risk - R_t . The number of human losses, injuries, damage to property, and effects on economic activity due to the occurrence of a disaster, i.e. the product of the specific risk R_s , and the elements at risk E.

Natural hazard-generating phenomena or events according to their origin or main cause (26):

a) Geodynamic phenomena: These are events that can be endogenous or exogenous depending on whether they are events generated by the internal or external geodynamics of the earth (earthquakes, eruptions, mass removal, etc).

b) Hydrological phenomena: These are events related to the dynamics of water on the surface and inside the earth's crust (floods, river and lake overflows, land and coastal erosion, droughts, etc.).

c) Atmospheric phenomena: These include meteorological events such as tornadoes and gales; torrential rains and storms; climatic phenomena (frost, hailstorms, strong

temperature changes, and forest fires), oceanic-atmospheric interaction events such as hurricanes and the El Niño phenomenon. Generators of extreme hydrological and geodynamic events, exacerbated by the intensity of their effects or by global climatic changes.

d) Biological phenomena: Epidemics and plagues that may affect humans, productive animals, or crops.

In order to perform a risk analysis, the threat or hazard must be estimated, the vulnerability must be evaluated and the risk estimate must be carried out. The assessment of the vulnerability of cultural heritage is a complex process, therefore the "ProteCHt2save - Risk assessment and sustainable protection of cultural heritage in a changing environment" was created for the identification of risk areas and vulnerabilities for cultural heritage in Central Europe exposed to extreme events related to climate change. Therefore, the online tool (WGT) was created with which it is possible to visualize risk maps of Central Europe, showing the changes in specific climate parameters and extreme indices for 2 historical periods (1951-1980 and 1987-2016) and under RCP4.5 and RCP8.5 scenarios for 2 future 30-year periods (2021-2050 and 2071-2100) with respect to the historical reference (1976-2005).

The mapped indices, selected among the 27 established by the Expert Team on Climate Change Detection and Indices (ETCCDI), refer to extreme events: heavy rainfall, floods, drought, and extreme warming. With the maps, it is possible to determine how and where possible changes related to these phenomena will affect the Central European area and its heritage (27). The webGIS tool is used in the study for the evaluation of future risk projections for the case study.

2.2.3.1 Fragility Curves

Fragility curves are another way of representing physical vulnerability since they provide the probability that a type of element at risk will reach or exceed a specific damage state under a given hazard intensity. Vulnerability functions represent the interaction between the damaging event and the elements at risk employing curves that express the possible resistance of the elements to an impact. Thus, we can define (28):

- The vulnerability of an asset is the weakness and propensity to suffer negative consequences in case of a hazardous event of a given intensity.

- Risk can be analyzed as the mathematical convolution of three fundamental entities: the level of hazard, the vulnerability of the building, and the level of exposure.

$$Risk = Hazard \times Vulnerability \times Exposue$$

- Failure cause: circumstances during specification, design, manufacture, installation, use or maintenance that result in failure.
- Failure mode: manner in which the inability of an item to perform a required function occurs.
- Severity of a failure or a fault: potential or actual detrimental consequences of a failure or a fault - The severity of a failure may be related to safety, availability, costs, quality, environment, etc.

It is essential to analyze vulnerability and reduce it to mitigate the effect of the hazard on the study structure.

Curves will be used to visualize the response of sandstone samples to increasing rain load and airflow velocity in order to relate rainfall intensity to the predicted susceptibility of the material to degradation.

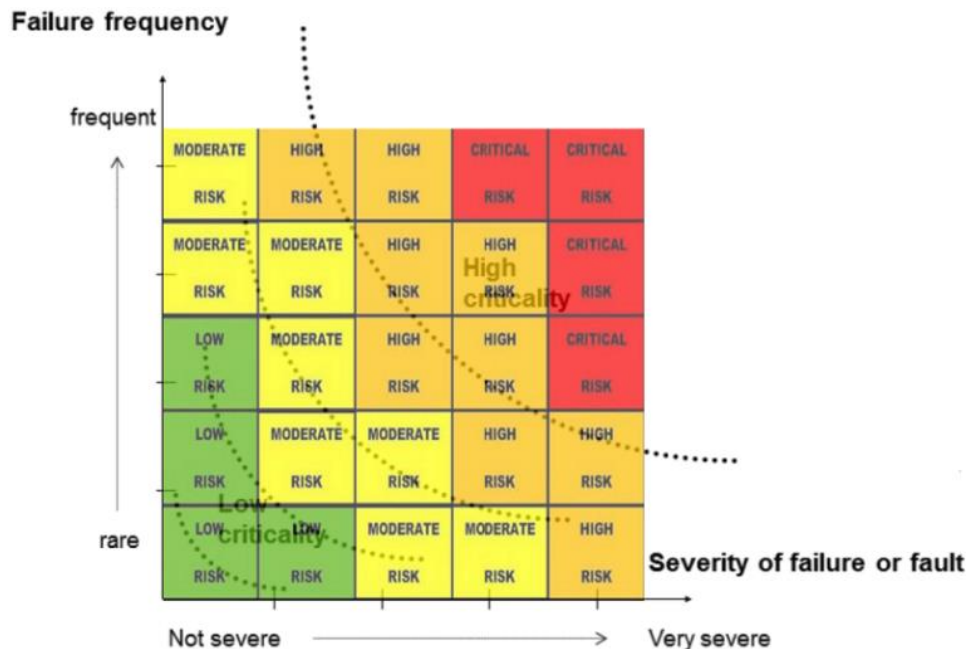


Figure 7: failure frequency (28)

3 CHAPTER No. 3 - EXPERIMENTAL INVESTIGATION

To identify the climatic effects on historical building materials, in this case, to model the impact rates of precipitation and particulate pollutants on buildings, focusing only on stone as a base building material, experimental tests were carried out in the small tunnel of the Institute of Theoretical and Applied Mechanics ITAM, with four (4) sandstone specimens. This material was obtained from the research carried out by the institute to determine the reference parameters for the evaluation of the reinforcement of the degraded sandstone masonry of the St. Vitus Cathedral of Prague Castle. (32).

As a case study, four towers built in the Gothic style in sandstone in the city of Prague were evaluated and a 1:50 scale model (96 cm height x 24 cm x 24 cm section) was made. No destructive or non-destructive samples were taken from the towers to identify the quality of the material they are made of, as this was not part of the scope of the project. Therefore, the use of this material coming from the Cathedral is accepted in relation to the existing bibliography on the construction of the city of Prague where it is stated in a taxative way *"The city of Prague is built of quarry. The cut of the tributary valley on the left bank of the Vltava exposes upper Cretaceous strata and lower layers of the Silurian Barranian, the Cretaceous formations are exploited as quarries, from which the stone for the buildings is extracted"*. (33).

With the scale model made, it was possible to obtain in the Telc tunnel the measurement of the pressures exerted by the wind on the structure through sensors located in specific areas, depending on the shape, dimensions, characteristics, direction, and intensity of the wind. Additionally, the airflow around the model was visualized in a practical way with water bubbles.

The experimental research aims to deepen the understanding of the behavior of building materials when subjected to different environmental scenarios to generate adequate and lasting mitigation measures.

3.1 Material characterization

The city of Prague is built of quarried materials. The cut of the tributary valley on the banks of the Vltava allows to see the upper strata of the Cretaceous from which the buildings were constructed, Cretaceous sandy loam was the common building stone in Bohemia, it is macroscopically characterized by a pale yellow to golden yellow color and extremely fine grain and belongs to the Upper Cretaceous sediments, it can be classified as micritic siliceous clayey limestone, with the composition of micritic calcite, clay minerals - mainly kaolinite and illite, calcite in the form of recrystallized particulate cement and calcified bioclasts, where the golden yellow color occurs due to the dispersion of opaque minerals - limonite, goethite, and anatosite. (34).

The sandstones extracted from the cathedral (used for this study) were obtained from the internal report of the research group of Dr. Jan Valek at ITAM, showed alteration on their surface at an estimated depth of at least several mm, these showed a low degree of salinity according to the ČSN P 73 0610 standard, the highest degree of sulfate content was due to surface contamination, the representation of chloride and nitrate was low.



Figure 8: Classification of sandstone samples.

Table No. 1: Description of the material

	Description
II	Very fine-grained grayish to beige quartz sandstone. Slightly to finely greenish in color.

The results obtained on the basic parameters of the structure of specimens I, II, and III (PSV1, PV2, and PV3 according to the previous report) are shown in Table 2:

Table No. 2: Basic parameters of the specimen structure

	II
Mean pore diameter (volume) (μm)	24.9
Bulk density (kg/m^3)	1831
Porosity (%)	30.2

The results yielded a unimodal pore distribution, with a similar pore size distribution from about 5 to 80 μm . The sandstones differ in pore structure and pore size:

- In sample II, according to the distribution curve it is asymmetrical, with sandstone having a significantly smaller pore size by 35 to 60 μm and on average having a smaller pore size. However, it has the largest total volume of open and interconnected pores.

Sandstone II (PSV 2) has the highest water absorption capacity and the highest open porosity and water absorption.

3.1.1 Typical Damage to building stone material

The following is a description of the most common alterations in building stone, which is a common material in historic buildings. Many of the lesions are interrelated, so that one alteration over the years leads to others that in time lead to mild to severe damage.

Table No. 3: Most common types of injuries in stone material.

DAMAGE	TYPES
Patina	Aging patina discoloration patina chromatic patina biotic patina staining patina black or dirt patina
Efflorescence	Subefflorescences
	Cryptoefflorescences
Superficial deposits	

Alveolizations	
Flakes	
Crusts	Black crusts Biotic crusts
Blisters	
Peeling and splaccations	
Disaggregation or disaggregation	sandblasting or granular disintegration, pulverization or powder disintegration
Stings	
Acanaladuras	Striations Verniculations
Cracks	Ranges from microcracks to cracks.
Erosion	
Other forms	Excoriations/stains/spalling

3.2 Experimental methods on sandstone samples

The identical specimen are marked No. 1, 2, 3, and 4 (figure 9) they are insulated on all faces except the front one and their initial conditions are the laboratory ones (i.e. $T = 23\text{ }^{\circ}\text{C}$ and $\text{RH} = 50\%$). Three experiments are conducted with three different airflow speeds: exp1 involves specimens 1 and 2 with airflow speed around 1 m/s (max fan power of 700 rpm); in exp2 specimens 3 and 4 are used with airflow speed around 0.4 m/s (350 rpm fan speed), and finally, specimens 1 and 2 were tested again after drying and exposed to an airflow speed close to 0 m/s (60 rpm fan). The environmental conditions inside the tunnel throughout the tests are $T = 23\text{ }^{\circ}\text{C}$ and $\text{RH} = 75\%$. These parameters correspond to the average relative humidity and temperature during summer months in Prague, taken as a reference location for this study. The two specimens are placed one beside the other, parallel to the direction of flow in a way that the exposed face is perpendicular to the flow.

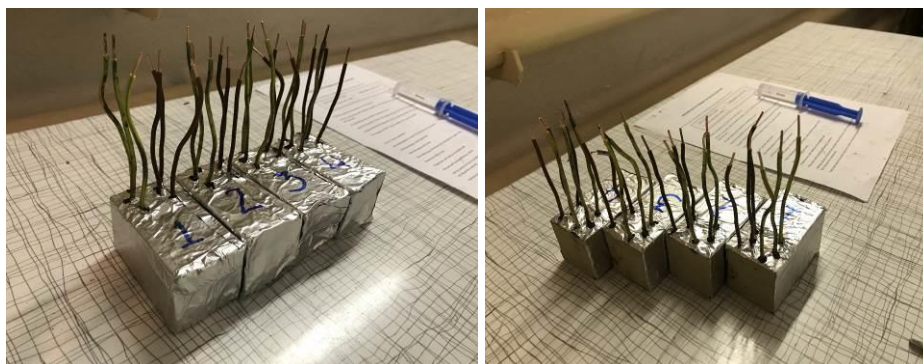


Figure 9: sandstone specimens.

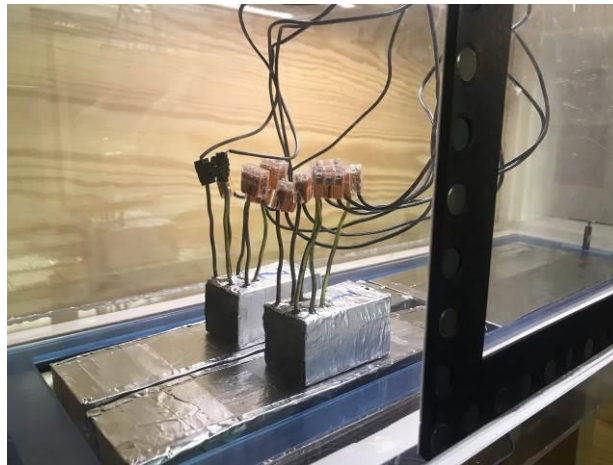


Figure 10: specimens inside the wind tunnel

For the proper analysis of the wind-driven rain simulation on the above-mentioned specimens, electrode sensors of standard dimensions (30 mm depth, 6 mm diameter) were used with epoxy resin basic mixture of 5 ml of Araldite 2020 (5.484 g) compound A, 1.5 ml of Araldite 2020 (1.468 g) compound B, plus 2.959 g of graphite powder, which allows conductivity, resistance and electrical contact quality between the specimen and the electrode. These were topped with a sealing layer of epoxy glue to prevent resistance measurements from being affected by higher conductivities on the face of the specimen at the time of the rain load simulation. (33). (Figura 11).

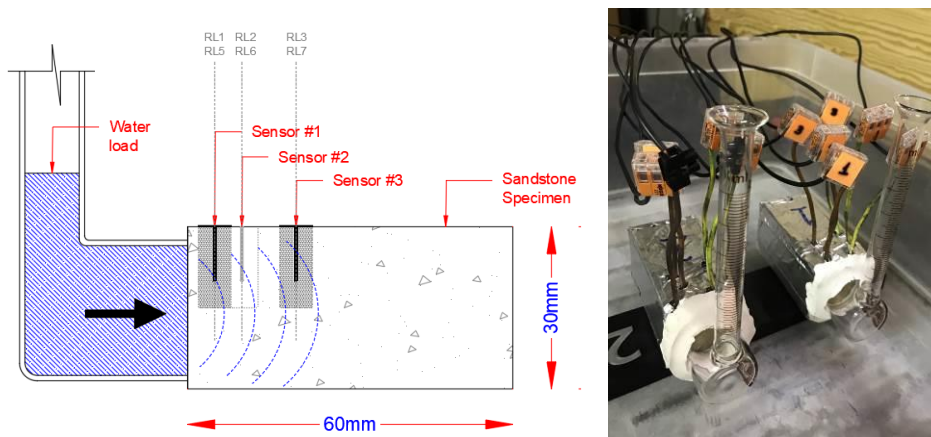


Figure 11: Schematic of rainfall simulation in sandstone specimens.

The tests performed on the four (4) specimens, are carried out applying three rain loads with three-hour intervals. Each rain load corresponds to 12 ml of distilled water. The

load is applied employing a Karsten tube (30m diameter) in order to load the whole surface of the specimens. It should be noticed that 12ml correspond roughly to the 5-ml mark (near the bottom of the tube). From the literature, this is shown to correlate to 72 km/h. These conditions allow the simulation of heavy rianfall with strong winds, even beyond the average weather data measured during summer storms in Prague. The repeated application of rainloads replicates the natural weeting cycles observed during natural phenomena. The experimental investigationis performed in a laboratory-size aerodynamic tunnel of the Institute of Theoretical and Applied Mechanics. The methodology used for the tests is explained below.

The response of sandstone samples to wind-driven rain is assessed by monitoring moisture movement using a moisture monitoring system, which records the measurement of changes in electrical resistance due to the presence of water, this is investigated by a series of capillary tests.

First, identical sandstone samples are taken and 6 mm holes are drilled into the specimen with an electric drill to the midpoint of its thickness, for installation of the electrode pairs on only one side of the sample, the hole layout configuration is shown in Figure 12. In addition, impurities inside the holes should be cleaned with compressed air, adhesive tape should be placed around the holes to protect their edges from resin injection



Figure 12: Drilling in the sample for electrode installation

The resin used is composed of two components A of 5 ml of Aradite 2020 (5.484 g) and B of 1.5 ml Araldite (1.468 g) plus 2.989 of graphite powder. First, the mixture of component A with the graphite powder is made, this mixture is made gradually until obtaining an adequate homogeneity between the two components, then the sample is placed

inside a 10 ml syringe. Pour component B into a small container with the previous mixture obtained. Mix the components thoroughly with a suitable paddle stirrer/mixer until a homogeneous mixture is obtained. Figure 13.



Figure 13: Preparation of syringes for on-site injection.

The injection must be done in a vertical position to the perforation, the application must be done slowly starting from the base of the perforation in order to generate different layers until the complete sealing of the perforation is obtained, avoiding air bubbles. Then the insertion of the solid copper wires is performed, these must be previously cut to the desired measures, additionally, the coating must be removed at one end to better grip the resin mixture, these are left to cure for about 24 hours, then the removal of the tape must be performed, The excess resin around the sensors should be removed with a file, cleaning completely any presence of the material on the face of the specimen in order to avoid that the measurement is influenced by the surface resistance values, after this the upper part should be sealed with pure epoxy glue. Figure 14.



Figure 14: Left-Clean specimen. Right-Check to prevent the measurement from being influenced by surface resistance values.

After testing, the specimens are coated in aluminum so that only the top side of the sample is exposed, this is done to ensure saturation of the sample during the experimental test. Figure 15.

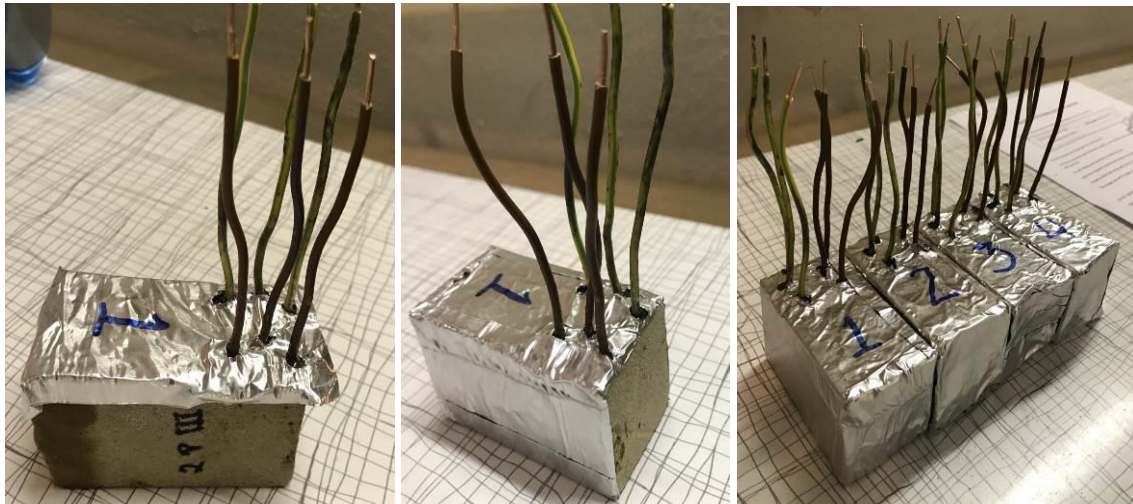


Figure 15: Specimens covered with aluminum

Once the specimens are sealed and coated, rain simulation is performed on two of the specimens employing a Karsten tube. The circular base of the Karsten tube is fixed to the surface of the aluminum-free face of the specimen utilizing plastic putty. Once the resistance gauges are installed on each of the wires, water is poured until the desired level is reached, in this case, 12 ml of distilled water was measured in a syringe, the application should be done quickly, 5 minutes of the simulation of the rain load is timed. The specimens should then be taken to the wind tunnel for wind-driven rain simulation.

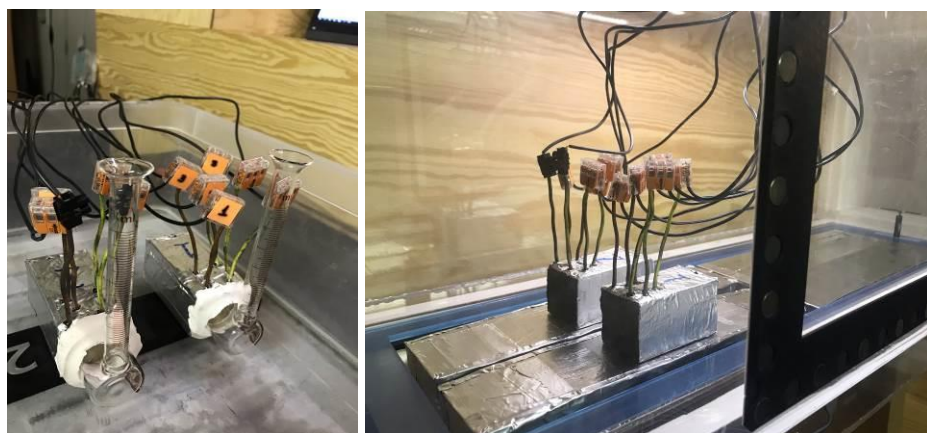


Figure 16: left - Rain simulation. Right - placement of specimens in the wind tunnel.

3.3 Experimental investigation with the small wind tunnel

The tunnel has a constant square section in its entirety, the tunnel has a circuit that has a fan to control the airflow speed, the heat and mass transfer unit where it is possible to condition the temperature and relative humidity of the air, additionally has a test section where you can place the specimens for data collection to obtain the response of the building materials, in this case for the sandstone specimens.

For the study material, three different flow velocities are used, the first at 700 rpm i.e. at 1 m/s for samples 1 and 2, the second at 350 rpm (0.4 m/s) for samples 3 and 4, and the third at 60 rpm again for samples 1 and 2. The temperature is constant and close to that of the laboratory, i.e. $T=23^{\circ}\text{C}$, and a relative humidity of 75%.



Figure 17: Samples in the wind tunnel and assignment of wind speed, temperature and relative humidity parameters.

Table No. 4: Input data from the tests carried out in the small tunnel.

Date (d/m/y)	7/06/2023		8/06/2023		9/06/2023	
Specimen No.	1 and 2		3 and 4		1 and 2	
Input Data	Des.	Real	Des.	Real	Des.	Real
Temp (C)	23	23,8	23	23,8	23	23,8
RH (%)	75	75,8	75	75,8	75	75,8
Wind RPM	700	872	350	430	60	74

Table No. 5: Rain simulation record, experiment 1 at 700 rpm.

	Cycle times					
	1		2		3	
	Start (Sp 1 and 2)	Ending	Start (Sp 1 and 2)	Ending	Start (Sp 1 and 2)	Ending
Water Injection	10:46 a. m.	10:51 a. m.	1:55 p. m.	2:00 p. m.	5:05 p. m.	5:10 p. m.
Wind tunnel	10:55 a. m.	1:50 p. m.	2:05 p. m.	5:05 p. m.	5:15 p. m.	8:15 p. m.

Table No. 6: Rain simulation record, experiment 1 at 350 rpm.

	Cycle times					
	1		2		3	
	Start (Sp 3 and 4)	Ending	Start (Sp 3 and 4)	Ending	Start (Sp 3 and 4)	Ending
Water Injection	9:15 a. m.	9:20 a. m.	12:25	12:30	3:45 p. m.	3:50 p. m.
	9:20 a. m.	9:25 a. m.	12:30	12:35	3:50 p. m.	3:55 p. m.
Wind tunnel	9:25 a. m.	12:25 p. m.	12:40	3:40	4:05 p. m.	7:05 p. m.

Table No. 7: Rain simulation record, experiment 1 at 60 rpm.

	Cycle times					
	1		2		3	
	Start (Sp 1 and 2)	Ending	Start (Sp 1 and 2)	Ending	Start (Sp 1 and 2)	Ending
Water Injection	9:15 a. m.	9:20 a. m.	12:25 p. m.	12:30 p. m.	3:40 p. m.	3:45 p. m.
Wind tunnel	9:23 a. m.	12:23 p. m.	12:38 p. m.	3:38 p. m.	3:50 p. m.	6:50 p. m.

The data of each reading for the different wind scenarios are collected in a computer for analysis and generation of resistance vs. time curves, as well as vulnerability index.

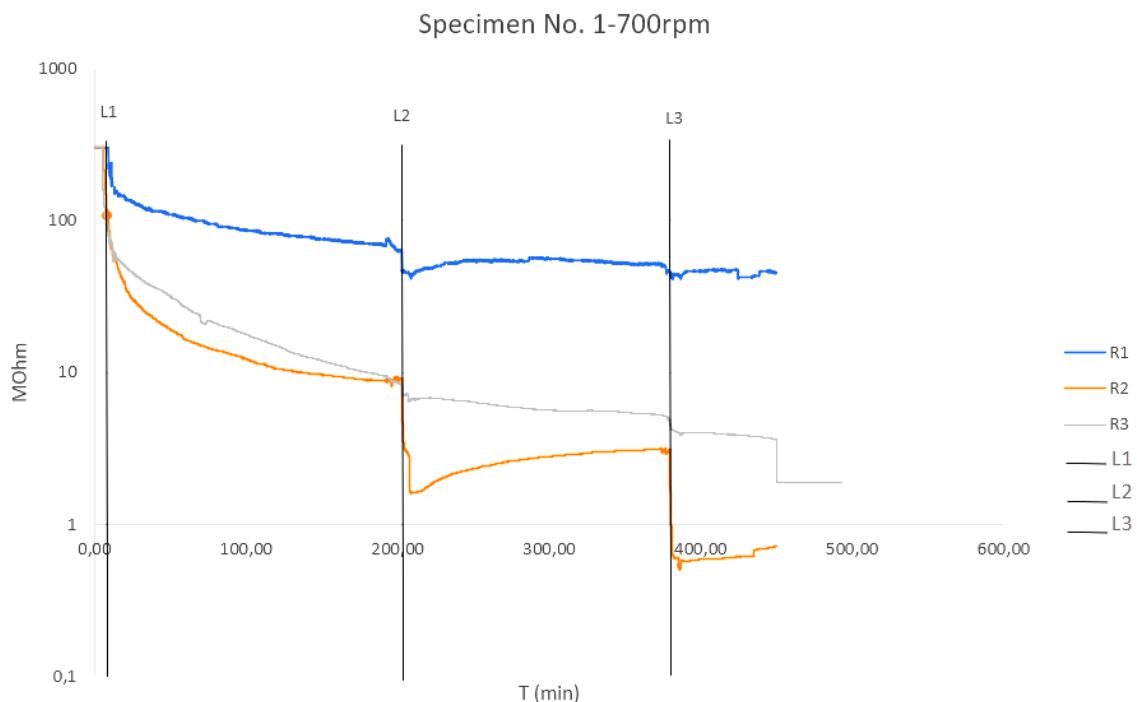
The following graphs present the results obtained from the simulation of wind-driven rain, and the ability of the sensors to measure the movement of moisture within the sandstone specimens. The reading before the wetting of the specimen starts with an electrical resistance of 300 MΩ (max detectable), while it decreases depending on the moisture content in the material. In experiment 1 specimen 1 and 2 are tested in the laboratory scale wind tunnel.

Graph 1 presents the reading of specimen No. 1 with three rainfall loads L1, L2, and L3, applied at an interval of 3 hours, for an airflow velocity of 1 m/s.

A noticeable decrease in resistance is observed after the application of L1, as the distance to the face of the water injection point increases, a decrease in resistance is denoted by a decrease of 300 rpm to $R=136$ rpm, $R_2=102$ rpm, and $R_3=104$ rpm.

Once the second rain simulation L2 is performed, a remarkable variation in the resistance of the three sensors is observed, presenting a higher peak in $R_2=1.64$ rpm, however, this is due to the previous saturation in some of the pores of the material.

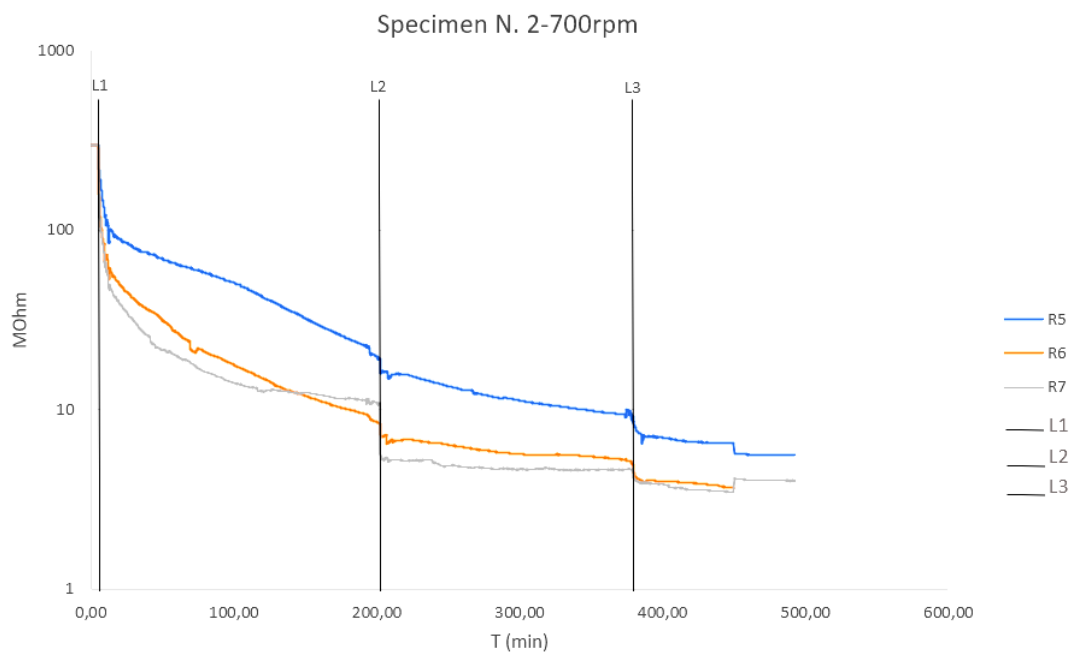
There is a noticeable change between L2 and L3 with a small increase in electrical resistance values, this may be due to a difference in the heights of the liquid that has a direct dependence on the radius of the pores and can cause no contact with the sensors $R_2=2.19$ rpm presents a behavior of increased resistance once it approaches the time $T = 400$, which may indicate that before the third rain simulation the sample at the sensor point R2 had decreased moisture content, this can be corroborated by the behavior pattern R1, between L1 and L2. The trend of $R_3=4$ rpm is of decreasing resistance during the three rainfall simulations, without abrupt changes in its values.



Graph No. 1: Electrical resistance measurement - Especimen No.1 700 Rpm

Graph 2 presents the reading of specimen No. 2 with rain loads L1, L2, and L3, spaced every 3 hours, for an airflow velocity of 1 m/s. A decreasing trend is observed in the resistance of R5, R6, and R7, among the three rain load simulations L1, L2, and L3. The greatest resistance change value occurs shortly after the first rain load in an approximate time of 5.10 minutes, presenting a greater decrease in R7=50 rpm, likewise, during the second simulation there is a greater moisture load in R7=5.16 rpm, which may be due to the size of the pores and their distribution within the material in the area where this sensor is located.

There is no evidence of an increase in resistance in any of the three rain simulations carried out, and on the contrary, this value tends to decrease, so it can be considered that the material presents a high degree of saturation.

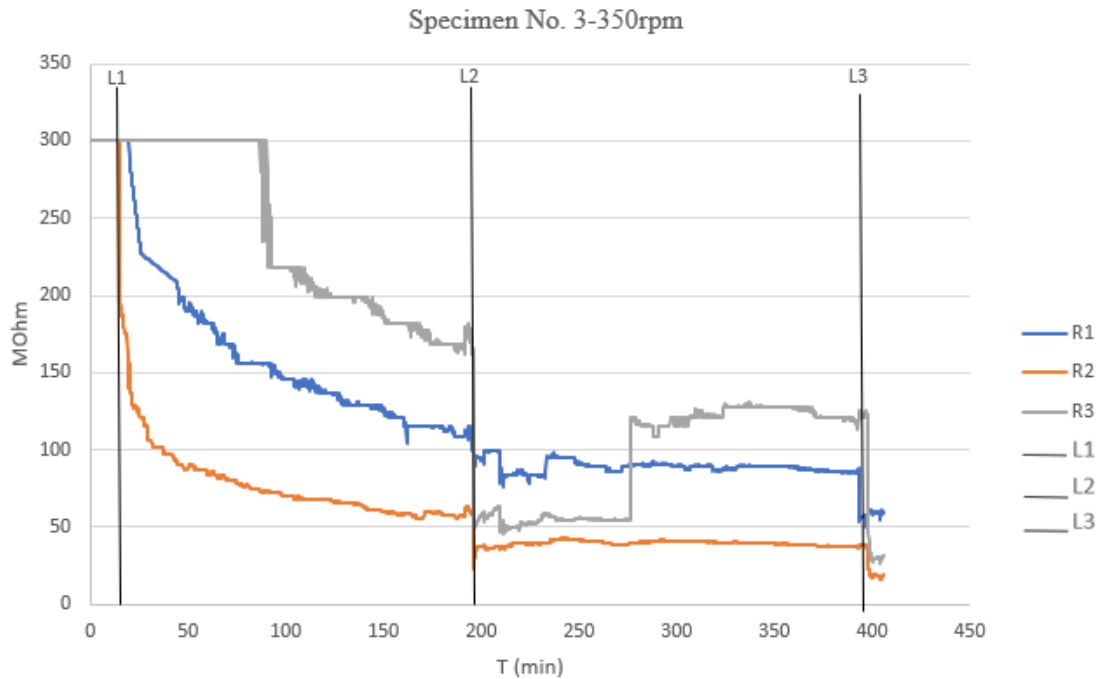


Graph No. 2: Electrical resistance measurement - Especimen No.2 700 Rpm.

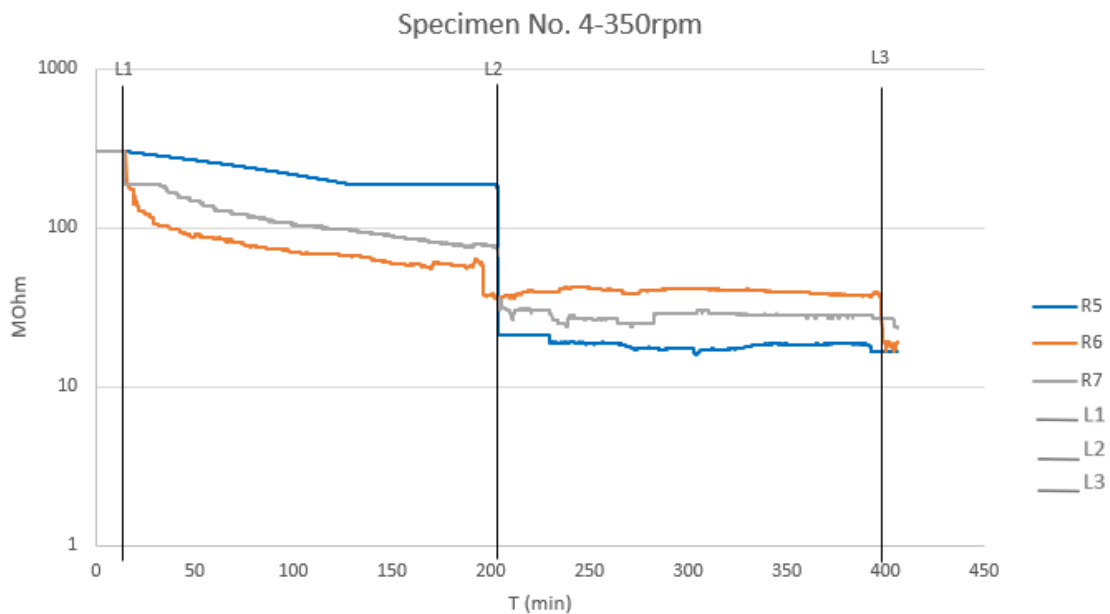
Experiment 2 considers an airflow velocity of 0.4 m/s. Two different specimens were used but exactly the same as the previous two used in experiment 1, these were named specimen No. 3 and No. 4

Graph 3 shows a considerable decrease in resistance in R1=226 rpm and R2=182 rpm, after the first rainload. The simulations were carried out with a waiting time of 5 minutes for the absorption of the liquid in the sample, to later enter the sample into the wind tunnel.

Therefore, the considerable decrease in resistance shortly after the first L1 rain simulation (approximately 15 minutes) may be due to the size of the pore and its interconnections within the material, this may be the cause of R3=235 rpm having activated up to 90 minutes and that presents a different behavior to R1 and R2 between L2 and L3.



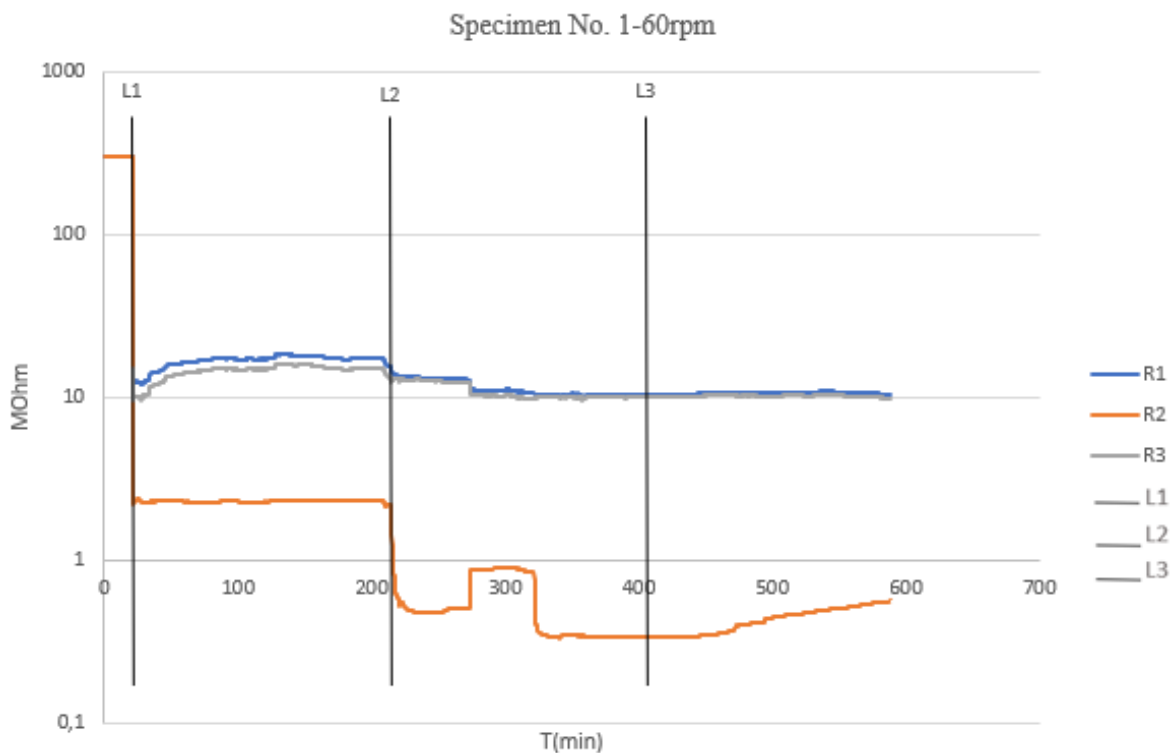
Graph No. 3: Electrical resistance measurement - Especimen No.3-350 Rpm



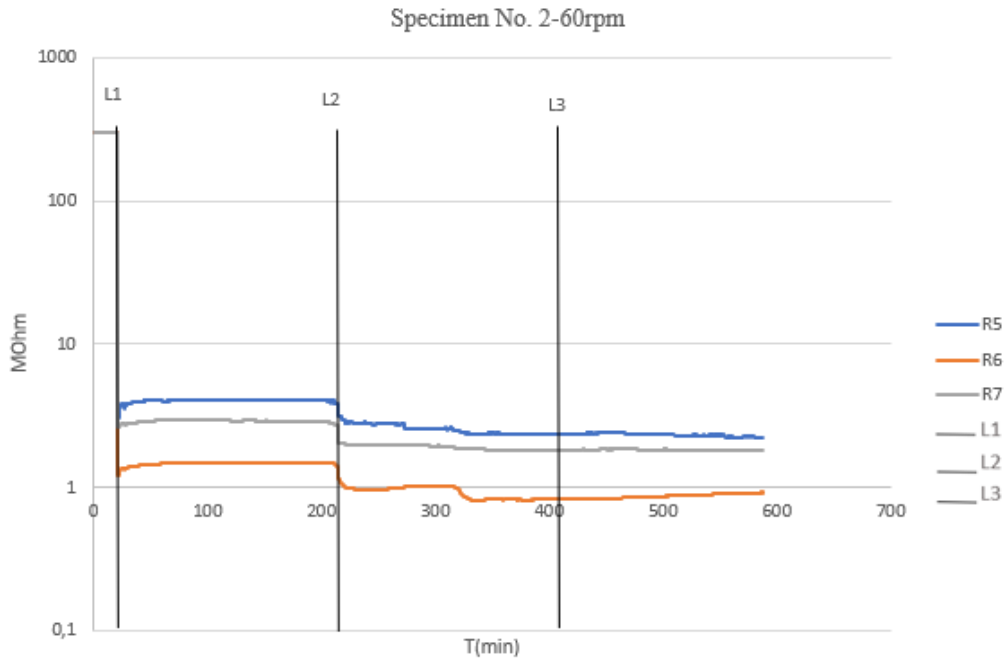
Graph No. 4: Electrical resistance measurement - Especimen No.4-350 Rpm

Graph 4 corresponds to the readings of specimen No. 4 for an airflow velocity of 0.4 m/s. There is a tendency to decrease the electrical resistance at a greater distance from the rain simulation injection point and therefore from the only face exposed for drying in the wind tunnel, the readings between L1 and L2, despite presenting the same trend, differ from the activation points of the sensors. Between L1 and L2, the greatest change in resistance occurs in R5=21 rpm, the opposite of R6=37 rpm, which presents less abrupt decreases in resistance.

Experiment3 is carried out with conditions of a temperature of 23 °C, relative humidity of RH 75%, and wind conditions of 60 rpm, the results of graphs No. 5 and No.6 are obtained for specimens 1 and 2 (the same specimens of the 700 rpm test). In these graphs it is observed that R2 always presents a lower resistance than R1, R3, R5, and R7 of graphs 5 and 6 respectively, it can also be observed that the readings do not present an initial electrical resistance of 300 MΩ, this may be due to the fact that the specimens already contained residual moisture from the tests performed during the first 700 rpm test. Likewise, it is observed that the readings R1 and R5, in approximately a time of 200 minutes (between L1 and L2) show a tendency of increasing electrical resistance which may indicate a failure in the reading of the sensors.



Graph No. 5: Electrical resistance measurement - Especimen No.1-60 Rpm



Graph No. 6: Electrical resistance measurement - Especimen No.2-60 Rpm

3.3.1 Vulnerability assessment of the material

In order to obtain the susceptibility of the material, the moisture content results were normalized by dividing each of the resistance results by the highest initial value, i.e. at 300 rpm, then the difference in resistance between R1-R2 and R2-R3 was calculated for specimens 1 and 2, and R5-R6 and R6-R7 for specimens 3 and 4. The algebraic expression presented below was used to generate a graph relating the moisture content vs. time variables according to the different wind scenarios.

$$MC = -0.123 \ln(Resist.) \quad [3]$$

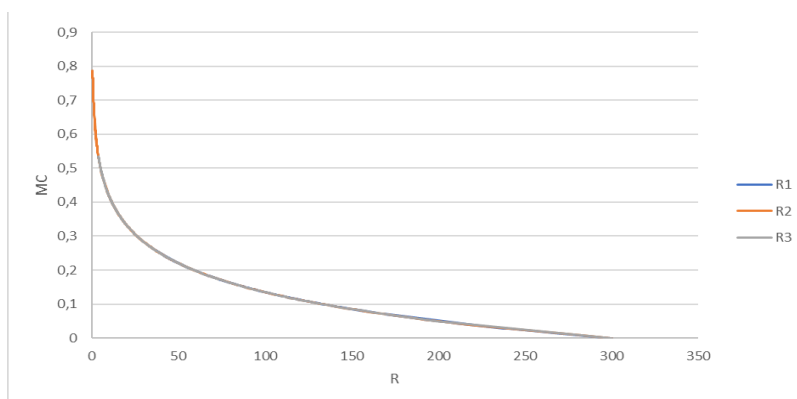
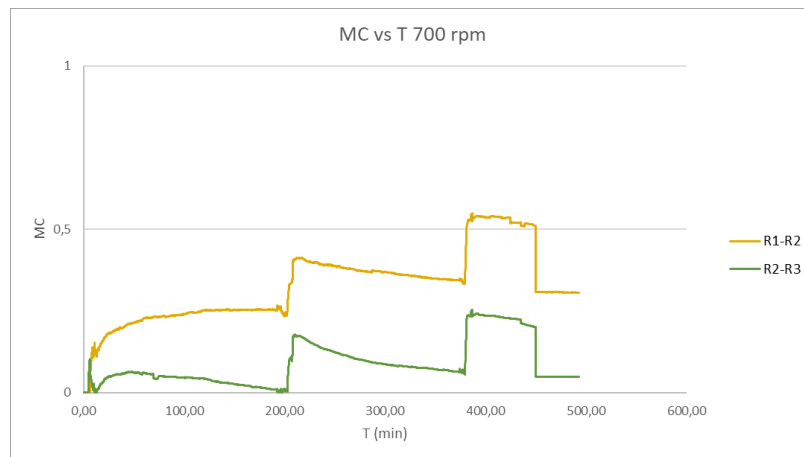


Figure 18: Susceptibility index

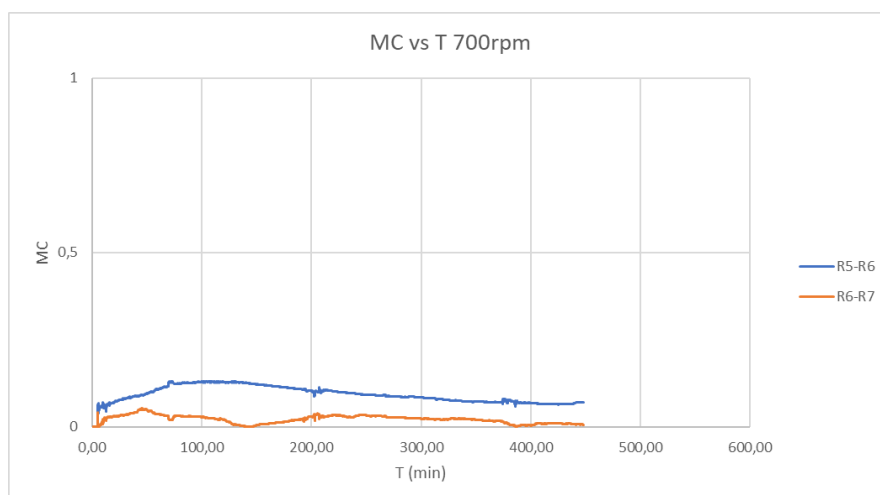
The following graphs show the total moisture content in each of the specimens at different speeds. normalizing the total moisture values of the samples between 0 and 1, being 1 when the sample is completely saturated.

Graph No. 7 shows higher moisture content at R1-R2 for 700 rpm, with a high peak after the third rainfall simulation.



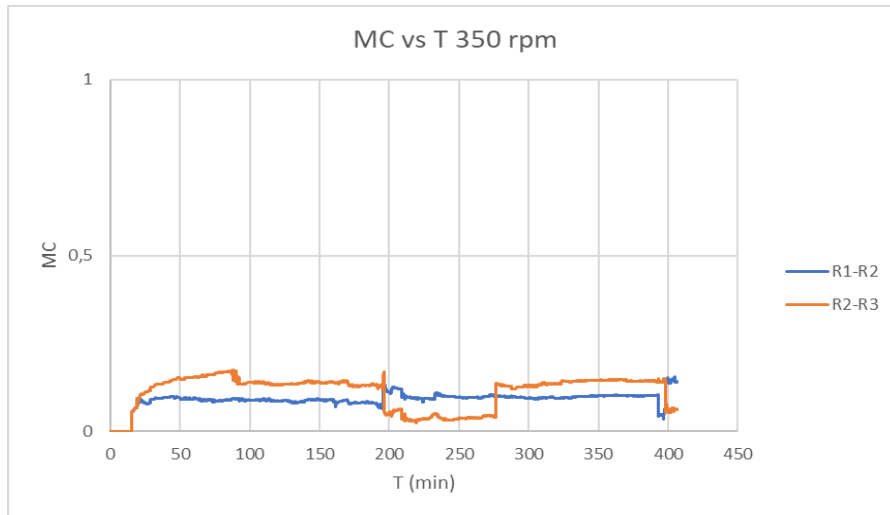
Graph No. 7: MC vs T 700 rpm. Specimen 1 and 2.

Samples R5-R6 show higher moisture content in the first rain simulation, and a continuous decrease in moisture content during subsequent rain loads.



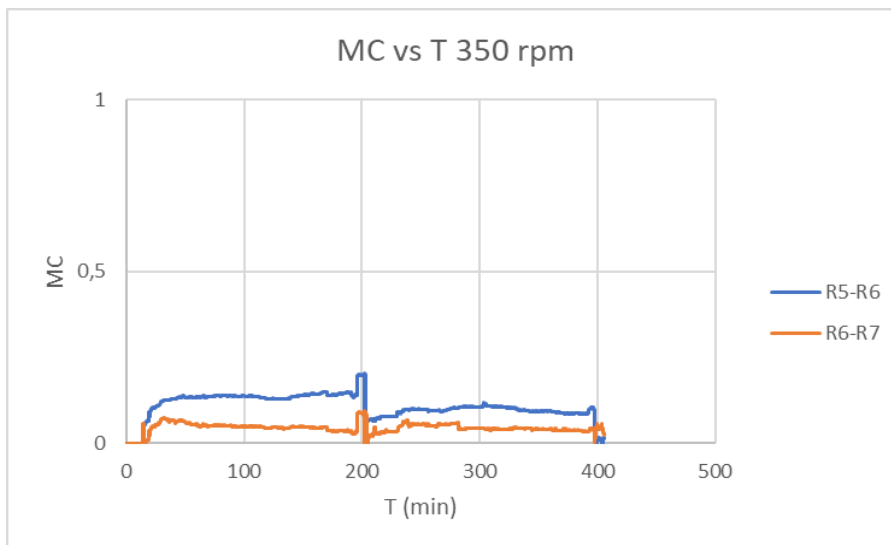
Graph No. 8: MC vs T 700 rpm. Specimen 3 and 4

Samples R2-R3 at 350 rpm show a higher moisture content between the first and second rain simulation, decreasing between the second and third rain load, and increasing again in moisture content after the third simulation. Sample R1-R2 shows a steady increase in moisture content after the second rain simulation (Grafico No. 9)



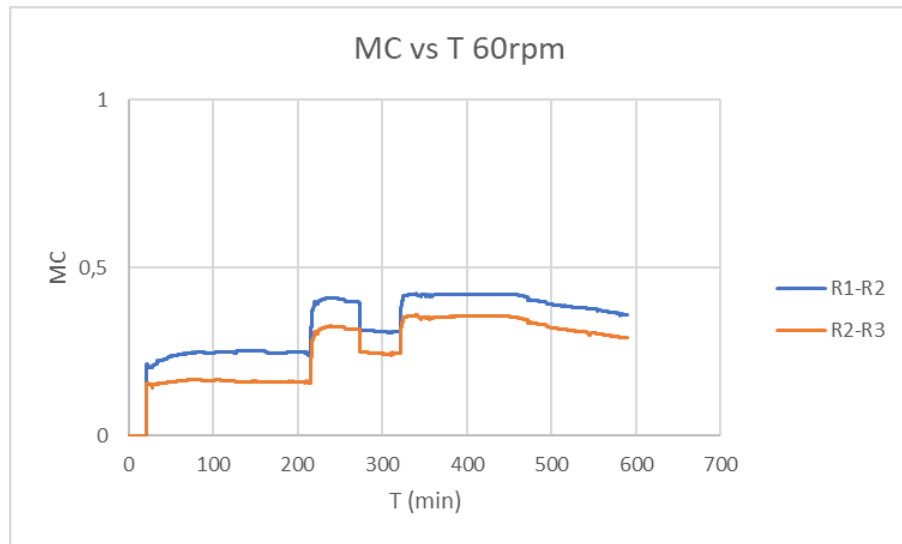
Graph No. 9: MC vs T 350 rpm. Specimen 1 and 2

Graph 10 shows a higher moisture content near the second rainfall simulation, being higher in R5-R6.



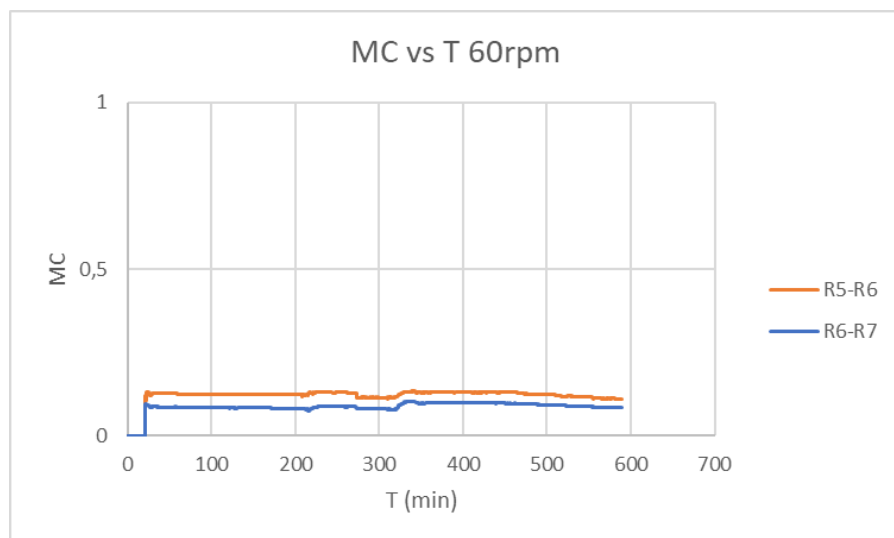
Graph No. 10: MC vs T 350 rpm. Specimen 3 and 4

Graph 11 shows a higher content in R1 and R2 for a wind speed of 60 rpm, an increasing behavior of the moisture content is observed with each of the rain loads.



Graph No. 11: MC vs T 60 rpm. Specimen 1 and 2.

For samples 3 and 4 at 60 rpm the moisture content presents a constant behavior lower than 0.5 of the moisture content, having a higher saturation R5-R6. Graph 12.



Graph No. 12: MC vs T 60 rpm. Specimen 3 and 4.

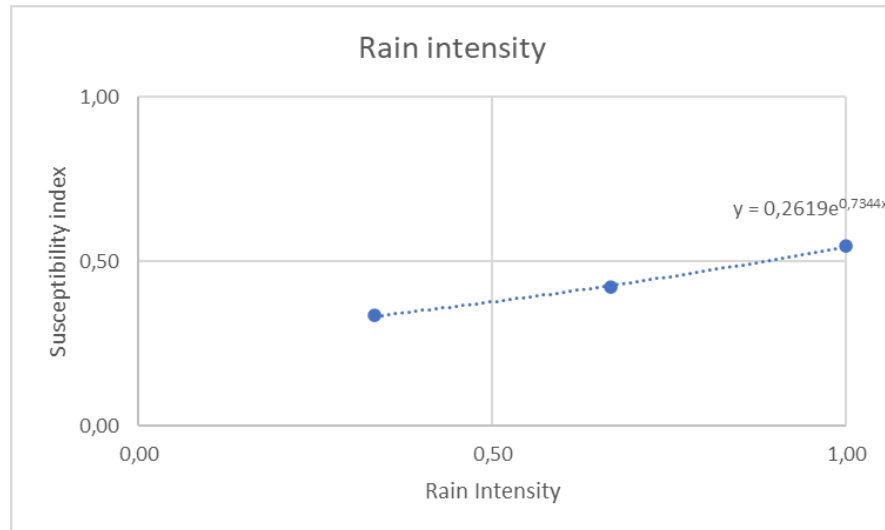
Penetration is faster for higher wind speeds. Usually in porous material wind pressure has no major effect in pushing water into the material has penetration it is mainly governed by capillary suction. The sandstone material analysed is however composed of a significant number of larger pores, reducing the capillary effect and making it more susceptible to wind pressure. This is visible comparing graphs 1-2 with 5-6: the rate of decrease in electrical resistance is much steeper for the airflow speed of 1 m/s compared to the one with no wind pressure.

Position R2 presents the lowest value of resistance, indicating a higher moisture content in the below surface section of the material.

The near-surface location, at R1, shows the effects of drying and it is visibly drier than other regions in the specimen. It is apparent that after the application of the load, this is fastly absorbed by the very porous material and driven to the below surface region; after some time, due to redistribution in the pores, the moisture is finally transported, in smaller amounts, to R3. The data provide a clear indication of the differential in moisture content among the monitored locations. Such gradient combined with the effect of other factors such as transportation of salts and pollution with water and changing temperature is expected, to trigger multiple material degradation phenomena which may lead, after many cycles, to damages such as material loss and cracking.

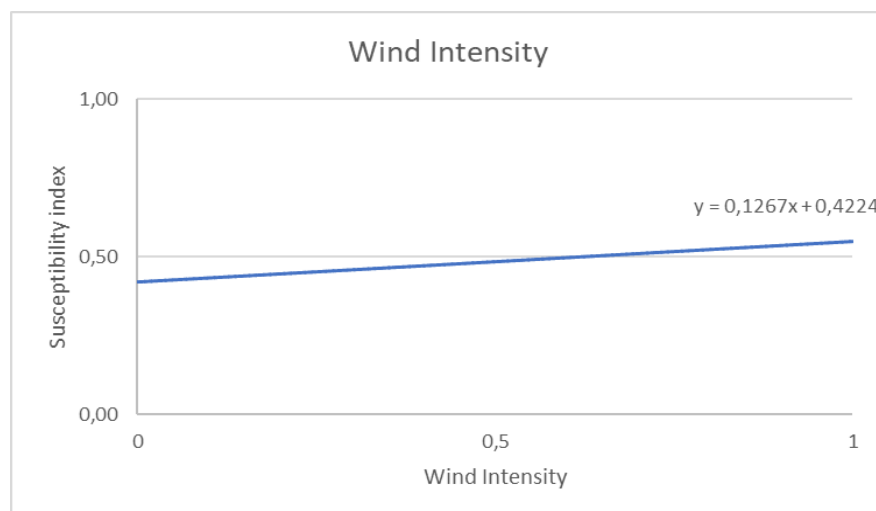
Graphs No. 13 and 14 are made to obtain the susceptibility index, in which, regardless of the position of the humidity, information is sought on the danger of damage from the intensity of the event on the material.

Graph N° 13 shows a predisposition to developing lesions coming from the effects of rain on the material, i.e., for example, the high presence of moisture inside the material can cause pressure problems in the internal walls of the material, generating cracks and fissures, in addition to crystallization processes that modify the structure of the rock, as well as other related pathologies. It is understood that water reacts with the stone substrate dissolving its components and acting as a transport vehicle. Therefore, the material can be classified with a moderate degree of susceptibility, higher than 0.50.



Graph No. 13: Rain Intensity

Graph No. 14 shows an increasing behavior of the susceptibility index at higher wind intensities. 14 presents an increasing behavior of the susceptibility index at higher wind intensities, this factor allows the transport of suspended particles that hit the stone, generating erosions in the material, which further increases the degree of damage in the presence of salts, humidity, and environments prone to contaminating agents such as sulfur compounds SO_2 , H_2S , H_2SO_4 , carbon compounds CO , CO_2 , CH_4 , HCT , nitrogen compounds NO , NO_2 , NH_3 , among others. The material is classified with a moderate susceptibility index.



Graph No. 14: Wind Intensity

3.4 Tests in the large tunnel

Pressure measurement and flow visualization tests were carried out in the atmospheric boundary layer (BL) wind tunnel of ITAM Centrum excellence Telč (CET), for a 1:50 scale model of four Gothic-style towers of the city of Prague (see table xx). The test was carried out in the climatic section, which has a rectangular cross section of 2.5×3.9 m and a length of 9.0 m. In this section, the wind speed oscillates between 0.6 and 15 m/s (depending on the position of the vertical mobile roof and the flow nozzle). The tunnel has a radiation system with four infrared lamps with a power of 8 kW and a maximum incidence of 60° with respect to the ground to simulate the intensity of the rain and the size of the drops.

For the physical model with the idealized geometry, it was necessary to compare the dimensional relationships from the Google measurements (for example, height/width), then the averages that could be used for the idealized model were calculated taking into account that it had a fixed width of the body of 30 cm.

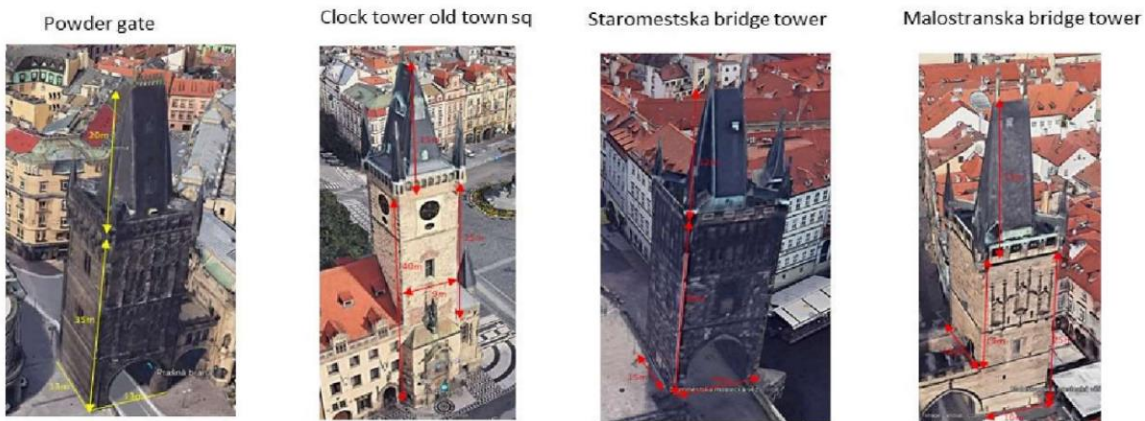


Figure 19: Dimensional relationships from Google measurements

Table No. 8: calculation of the averages that were used for the idealized model

		Real		Scale	
		Height (cm)	width (cm)	Height (cm)	width (cm)
Powder Gate	Roof	2000		40,00	26
	Structure	3500	1300	70,00	
			Σ	110,00	
Clock Tower Old town	Roof	4000		80,00	18
	Structure	1500	900	30,00	
			Σ	110,00	
Staromestska bridge tower	Roof	1200		24,00	30
	Structure	3000	1500	60,00	
			Σ	84,00	
Malostranska bridge tower	Roof	1500		30,00	20
	Structure	2500	1000	50,00	
			Σ	80,00	
		Average Roof		44	24
		Average Structure		53	
		TOTAL		96,00	

3.4.1 Pressure measurement test

As measurement equipment, the Pitot (Prandtl) tube is used, which is an instrument that allows measuring the speed of a fluid by converting the kinetic energy of the flow into potential energy. The tube allows to measure the static pressure p_s . According to Bernoulli's equation, the difference between the total and static pressure is the dynamic pressure P_d . Pressures in the model were acquired using two Scanivalve MPS 4264 pressure transducers, this is a self-contained, temperature-compensated electronic pressure scanner that can work with a maximum of 64 pneumatic inputs. The inlets are connected to the pressure taps with silicone tubes.

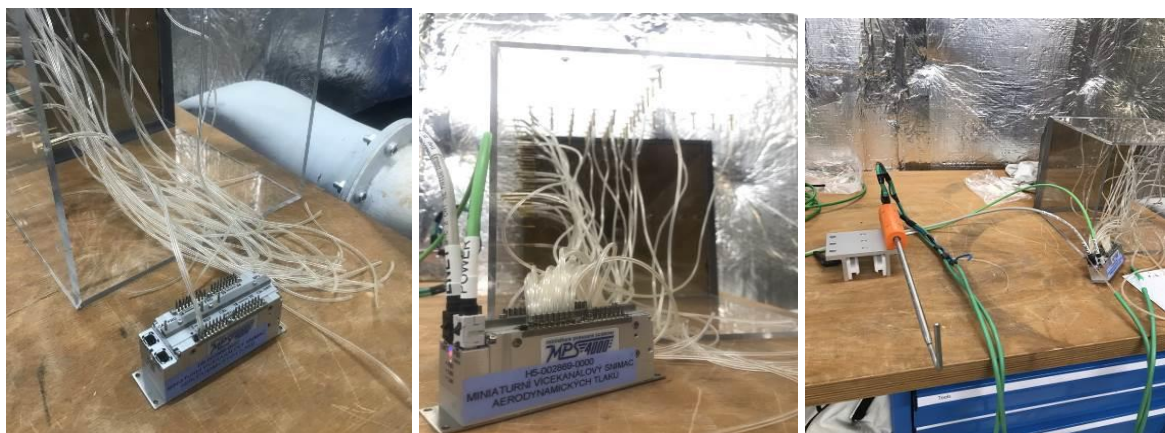


Figure 20: Left- Scanivalve MPS 4264 pressure transducers. Right- Pitot tube connection.

The 34 available channels were connected to the same reference pressure source, which was the static pressure of the Pitot-Prandtl tube placed in front of the model in free flow at a height of 27 cm. In addition, a channel was used to measure the total pressure (velocity) in the Pitot. The channels were used to acquire pressures on the surface of the model.

Pressure tappings were made as small 1 mm holes on the examined surface and 2 mm on the other side to fit the 20 mm long brass tubes that were adapters for the silicone tubes. Pressure taps were moved equidistantly along the model surfaces (if geometry allowed). The average distance between shots was 2 cm.

In order to avoid a distortion of the structural behavior of the frame, the pressure transducers cannot be mounted directly on the frame; therefore, they are connected to the intakes by means of optimized tube systems, with a length of 1000 mm. These tube systems provide a flat response of pressure signals up to 200 Hz. The tubes are attached to the taps with short brass tubes, which are glued to the inside surface of the housing.



Figure 21: Sensor installation and testing

. A total of 92 pressure taps were placed on the model, 46 pressure taps were placed on facade A and 46 on facade B (Figure 22).

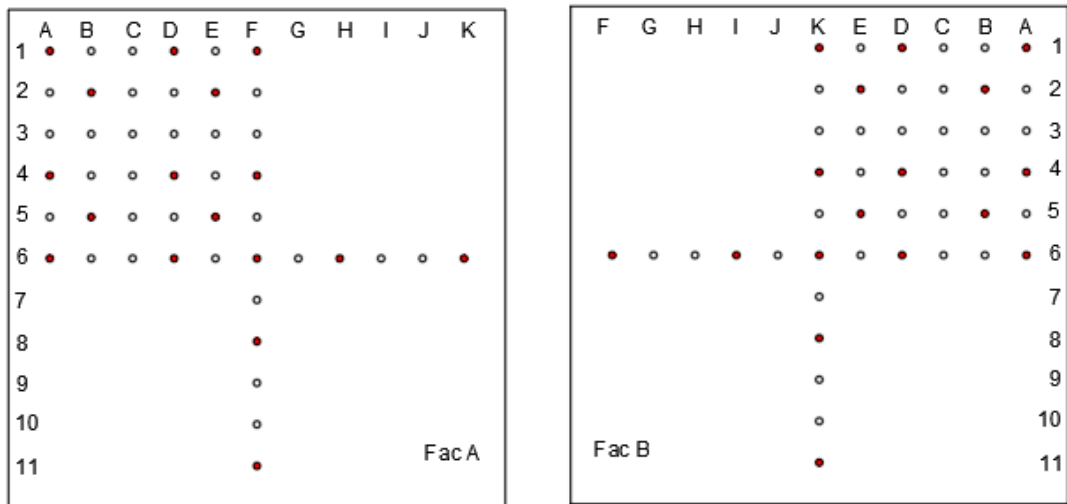


Figure 22: Distribution of sensors on facade A and B of the scale model.

Measurements were made on the unrotated model, i.e. at 0° , then the tower model was rotated 45° to cover all main wind directions. Seven measurements were performed at different percentages of wind intensities (see Table 8).

The Prandtl tube was placed 1 meter in front of the model and at a height of 27 cm from the wind tunnel floor, and was used as a reference velocity.

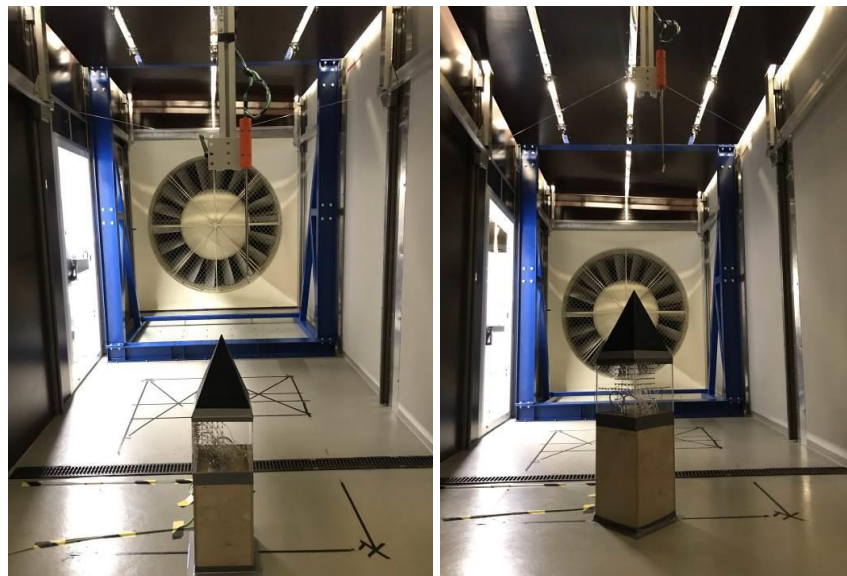


Figure 23: Left-Position of the scale model inside the tunnel at 0 degrees. Right-Position of the scale model inside the tunnel rotated at 45 degrees.

Table No. 9: Pressure measurements, tower 0°.

Pressure measurements

Climatic section

Atm. Pressure = 958,7

hPa

50 Hz, 3000 frames.

T=21, HR= 47%

Tower	Wind	m/s	Temp	HR
0°	20%	4	22,1	44,70%
	25%	4,8	22,1	44,60%
	30%	5,9	22,2	44,50%
	35%	6,9	22,4	44,10%
	40%	8	22,4	43,50%
	45%	8,9	22,6	43,10%
	50%	9,98	22,9	42,40%

Table No. 10: Pressure measurements, tower 45°.

Pressure measurements

Climatic section

Atm. Pressure = 958,4

hPa

50 Hz, 3000 frames.

T=21, HR= 47%

Tower	Wind	m/s	Temp	HR
45°	20%	3,88	22,6	43
	25%	5,01	22,6	42,8
	30%	6,00	22,6	42,7
	35%	7,00	22,7	42,4
	40%	8,05	22,8	42,1
	45%	9,10	23,1	41,5
	50%	10,00	23,4	40,8



Figure 24: Montaje del modelo a escala dentro del tunel de viento.

The external pressures were measured for different wind angles of attack and the total pressure on the structure was established. Subsequently the external pressure coefficient C_p relative to an individual shot measured with index i was calculated, it is expressed as a ratio between the difference between the actual pressure recorded at that point and the Pitot tube static pressure p_i and the mean reference value of the Pitot tube dynamic pressure P_{ref} , in this case, P_{ref} is sensor number 32.

Plots of C_p (y-axis) vs. Re (x-axis) were generated - to ensure that C_p is stable over the Re numbers tested, i.e. wind speed does not affect the flow mode of the body.

$$Re = \frac{uL}{\nu} = \frac{\rho uL}{\mu} \quad [4]$$

ρ =	density	kg/m ³
u =	Flow speed	m/s
L =	Characteristic linear dimension (m)	
μ =	Dynamic viscosity	
ν =	Kinematic viscosity	

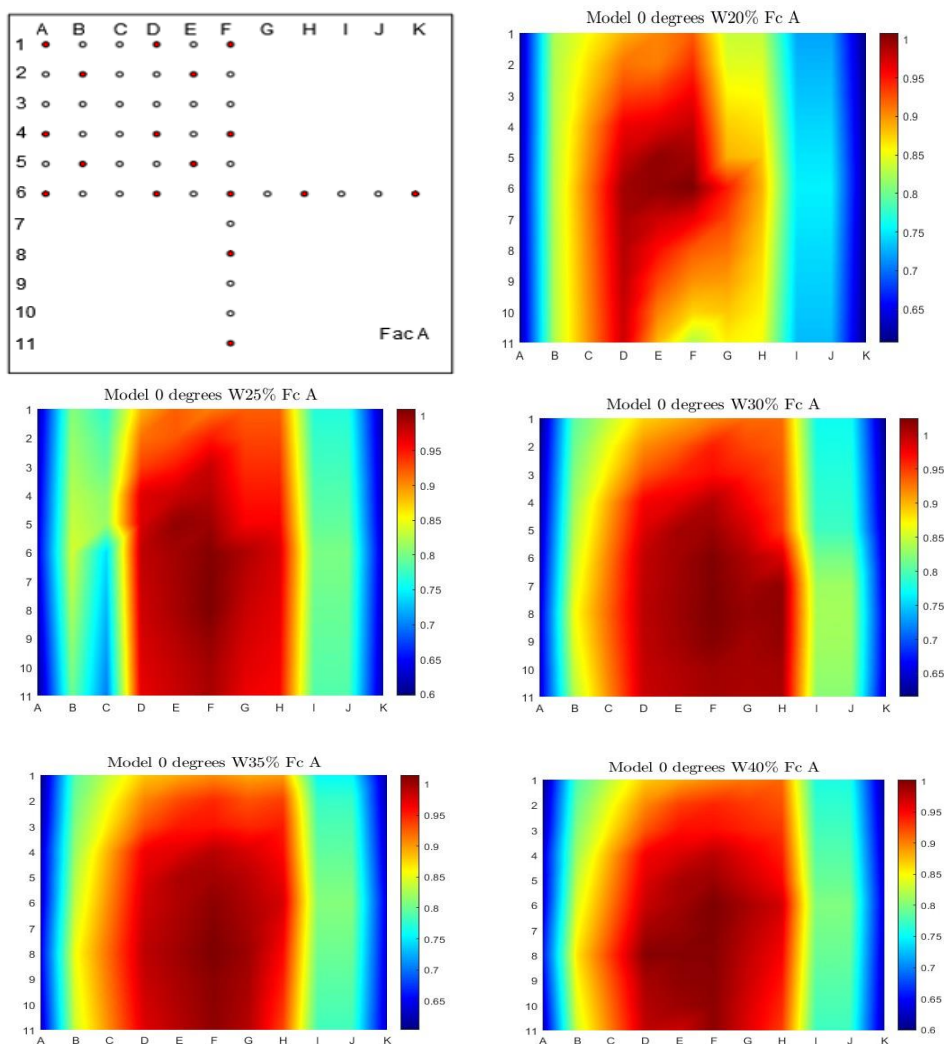
The number of Re is obtained for each of the wind scenarios and for each position of the model to scale (0 degrees and 45 degrees).

Finally, pressure maps are generated for the entire facade A and B of the model, it is necessary to interpolate the sensor data because during the test only 17 sensors for facade A and 17 sensors for facade B were connected.

Pressure measurement tests were performed on façade A and B of the model at 0 and 45 degrees perpendicular to the wind. Additionally, Flow visualization tests were performed to show the airflow patterns around the scale model of the towers.

The results are presented in terms of pressure maps to be compared at different percentages of wind speed. The model has been placed in a smooth airflow as well as a turbulent one.

Figure 25 shows the position of the face of the model perpendicular to the wind, without rotation (0 degrees) that is, to windward, this is the area where positive pressures occur (high pressure areas). As can be seen in Figure, higher pressures are observed at velocities between W30% and W35% in the center of the square section of façade A.



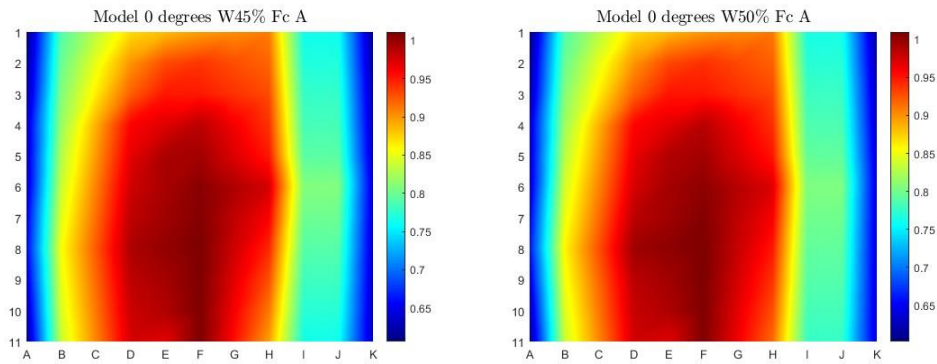
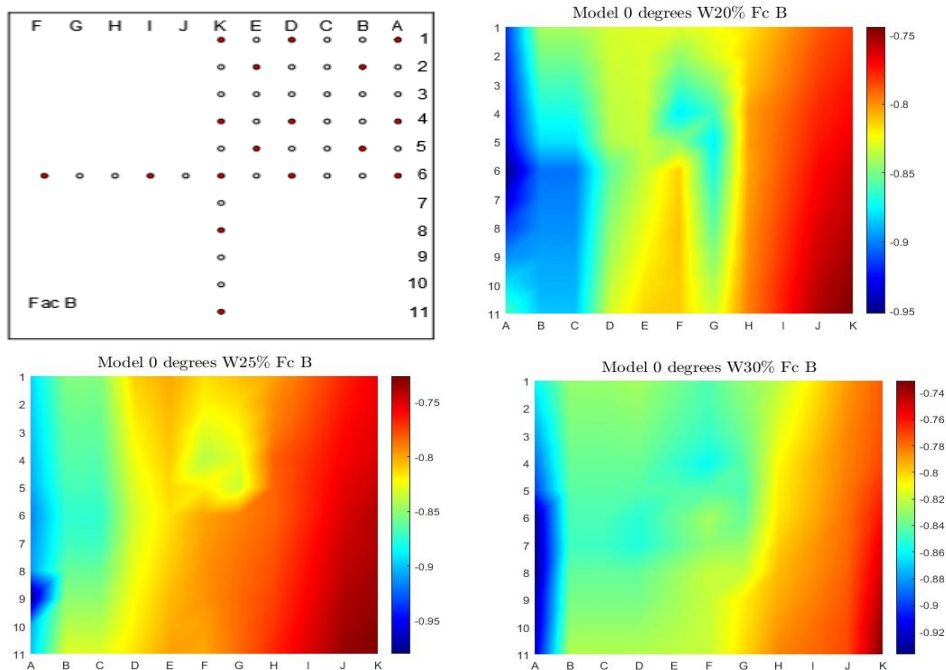


Figure 25: Pressure map at 0° degrees at different speeds. Façade A.

Figure 26 shows a greater intensity of pressures in W25% near the connection corner with façade A. Negative pressures (low pressure areas) are recorded in this area, which are consistent readings, considering that the values of Negative pressures occur on the opposite side to the wind, that is, to leeward.



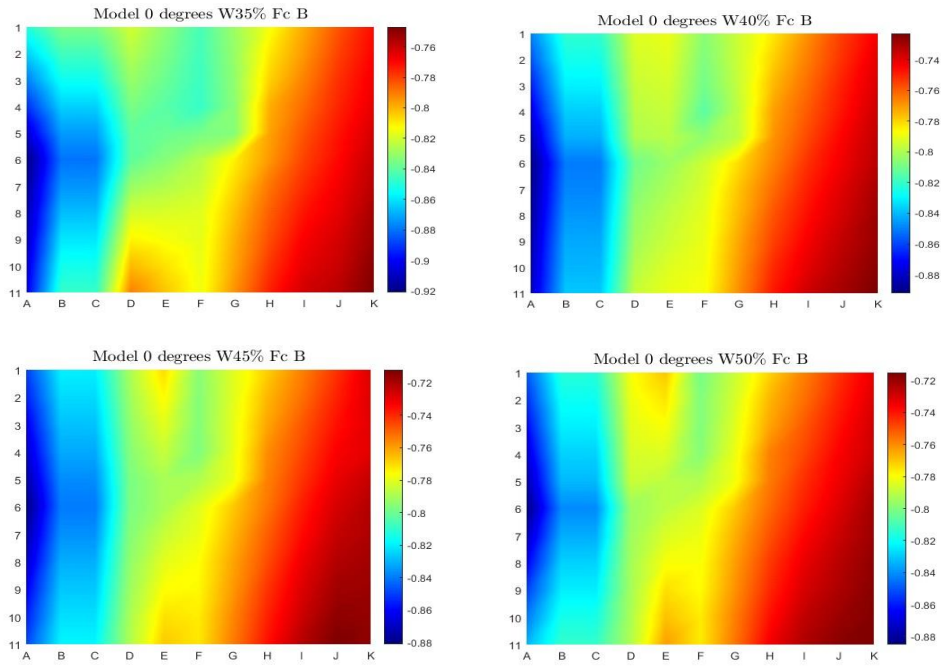
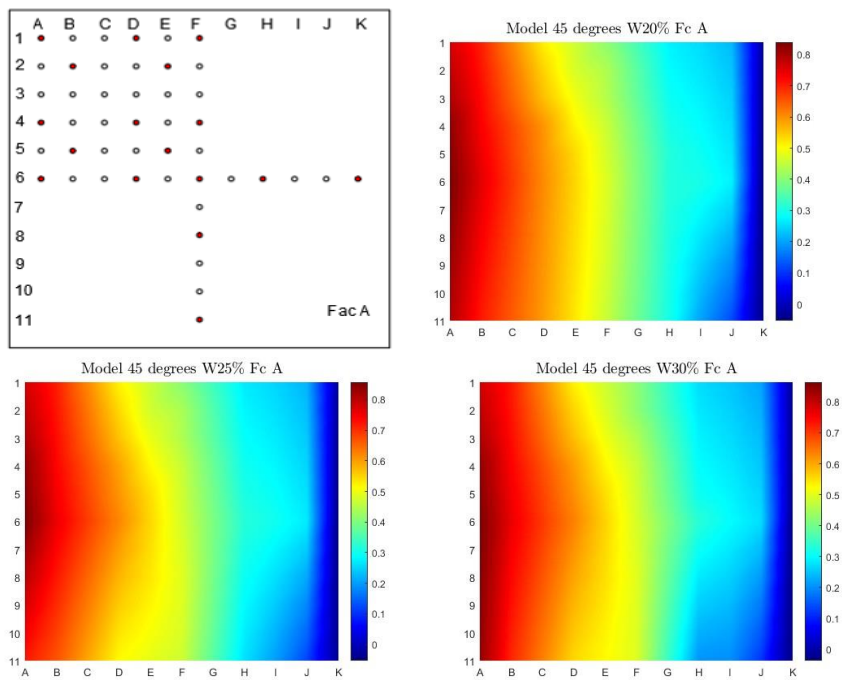


Figure 26: Pressure map at 0° degrees at different speeds. Façade B.

Figure 27 shows the position of the scale model with a 45° turn perpendicular to the wind. Similar pressure values can be observed in the different wind scenarios, having higher pressure values in the corner perpendicular to the wind of façade A with connection to façade B.



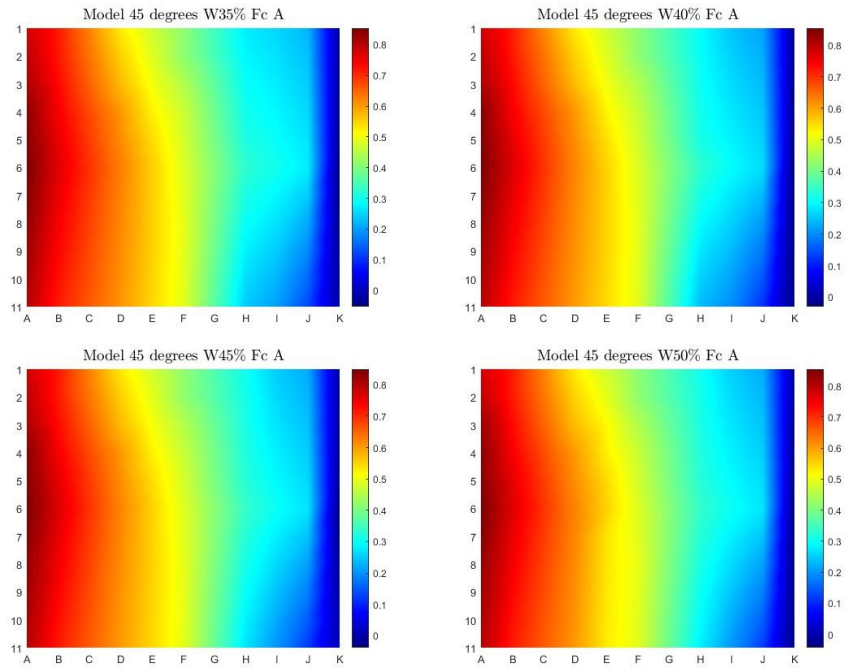
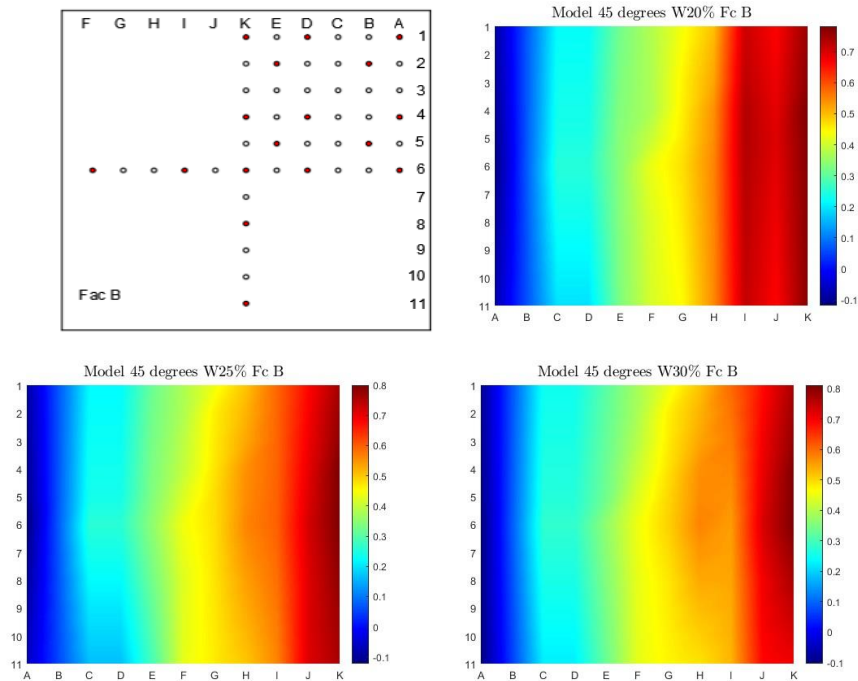


Figure 27: Pressure map at 45° degrees at different speeds. Façade A

Similar pressure values can be observed in the different wind scenarios, having higher pressure values in the corner perpendicular to the wind of façade B with connection to façade A in the W20% wind scenario.



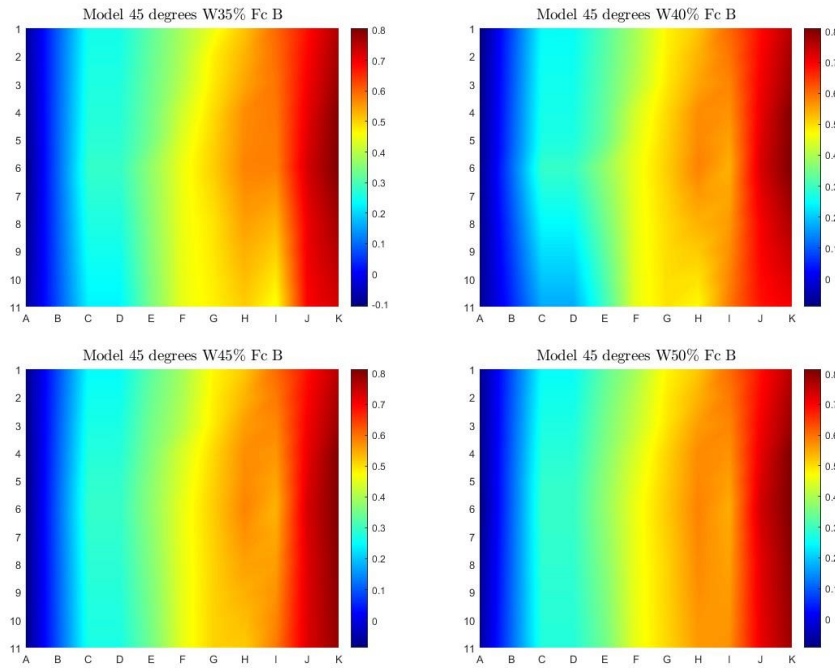
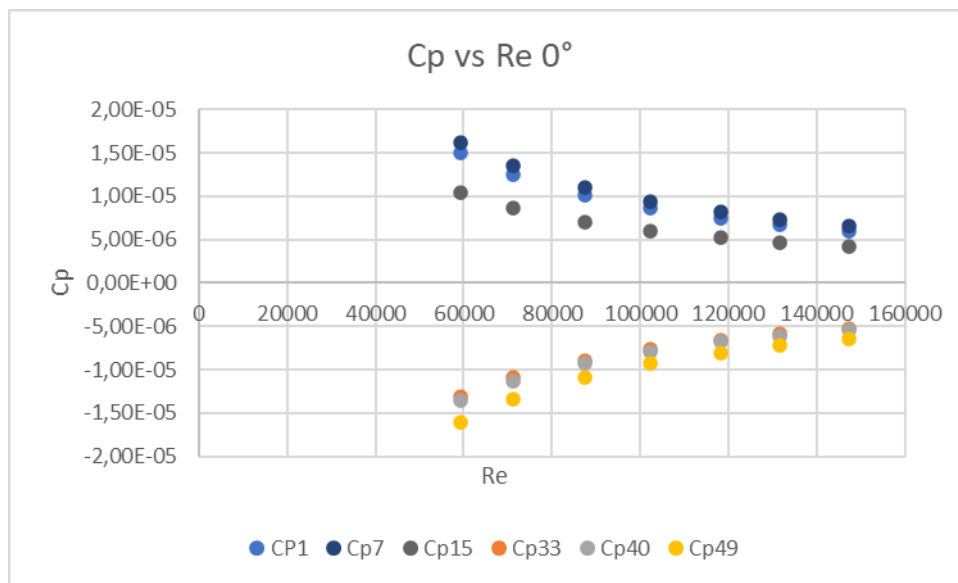
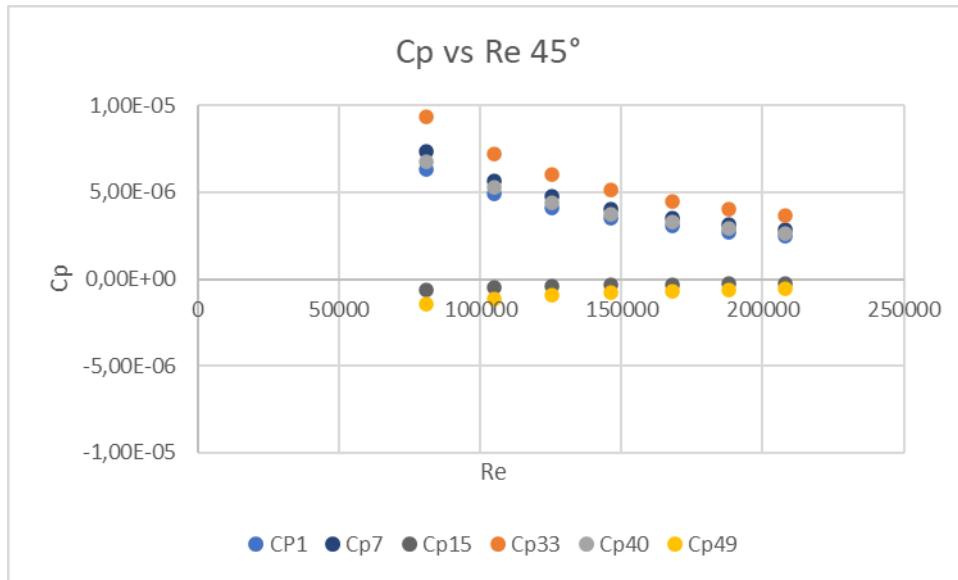


Figure 28: Pressure map at 45° degrees at different speeds. Façade B.

Graphs No. 15 and 16 show the pressure coefficients C_p (y axis) vs. Re (x axis), for the model at 0° and 45°. For this, the average C_p values of some sensors (C_{p1} , C_{p7} , C_{p15} , C_{p33} , C_{p40} , C_{p49}) were taken over the Re calculated for each speed scenario. In the graphs it is verified that C_p is stable over the numbers of Re tested, that is, the wind speed does not affect the flow mode of the body.



Graph No. 15: C_p vs Re 0°



Graph No. 16: Cp vs Re 45°

3.4.2 Flow visualization test

In order to investigate wind behavior, the Model 5 helium bubble generator was used to produce size-controlled helium-filled neutral buoyancy bubbles for visualization of laminar and turbulent airflow over the transparent plastic section of the scale model when driven by the wind. The console allows visualization of airflow patterns at velocities up to 60 m/s.



Figure 29: Helium bubble generator model 5

Inside the dark wind tunnel, a light projector is used to make the wind-driven helium bubbles glow and reflect the flow patterns, which are recorded with a digital video camera at 30 frames per second. In these, it is possible to observe the lines and curves that are generated.



Figure 30: General configuration of the test with tower at 0 degrees.



Figure 31: General test setup with tower at 45 degrees.

Employing the helium bubbles and the light it's possible to observe the airflow patterns around the scale model.

When the free wind is impeded by the sharp-edged model, it is deflected to go around it. These deviations generate pressure on the object. The air bubbles hit the side directly exposed to the flow of the wind and that opposes their free circulation (windward side). On the opposite side (leeward) the bubbles separate from the object causing suction, eddies, and turbulence to be observed. On the lateral faces, there is a pressure distribution that varies from thrust to suction. Figure 32.

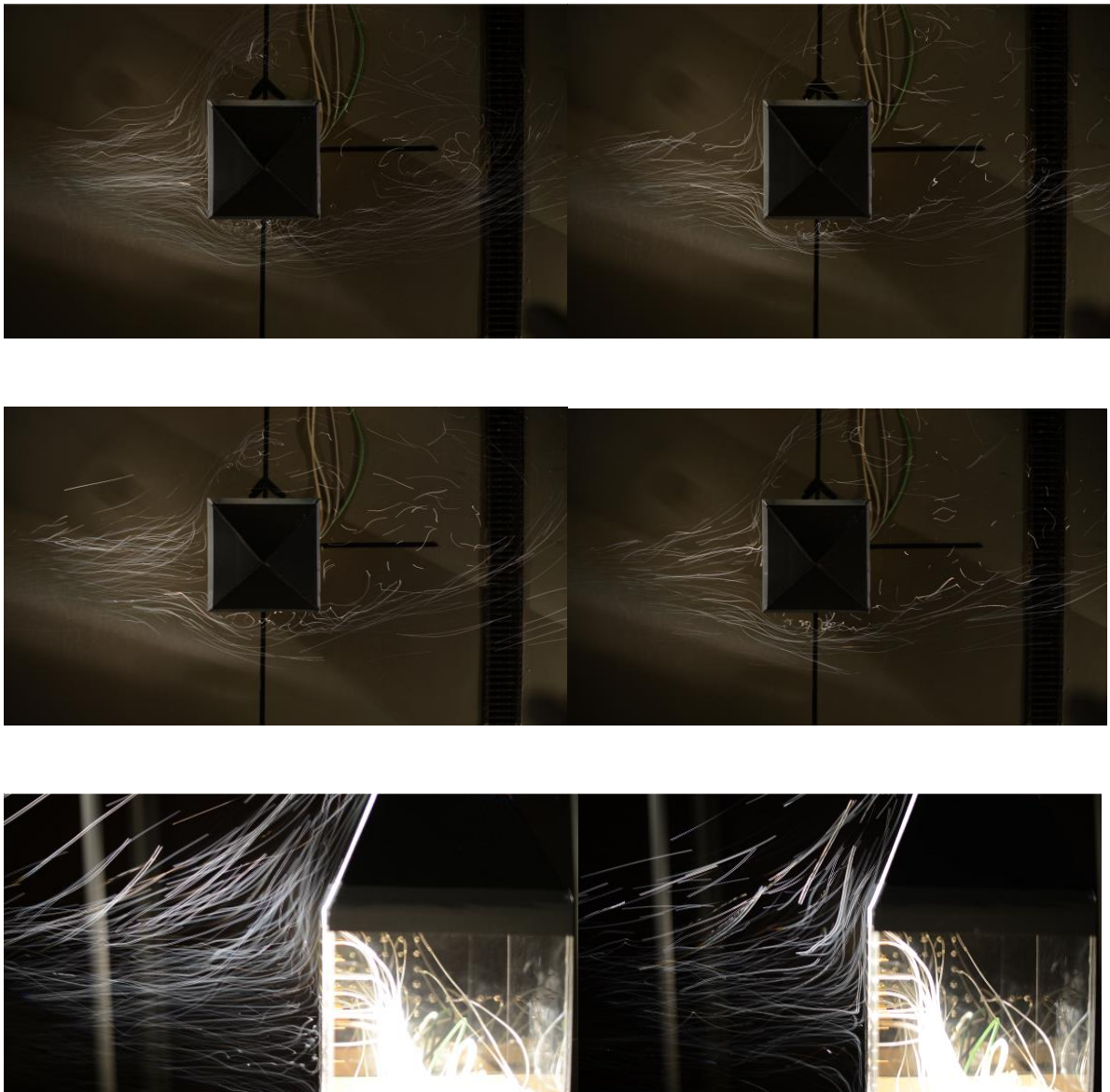


Figure 32: 2% flow visualization test.

When the free wind is hindered by the model, it attacks directly on the two facades of the model, generating pressure on them. On the two leeward sides the bubbles separate from the object causing suction, eddies and turbulence to be observed. Figure 33.

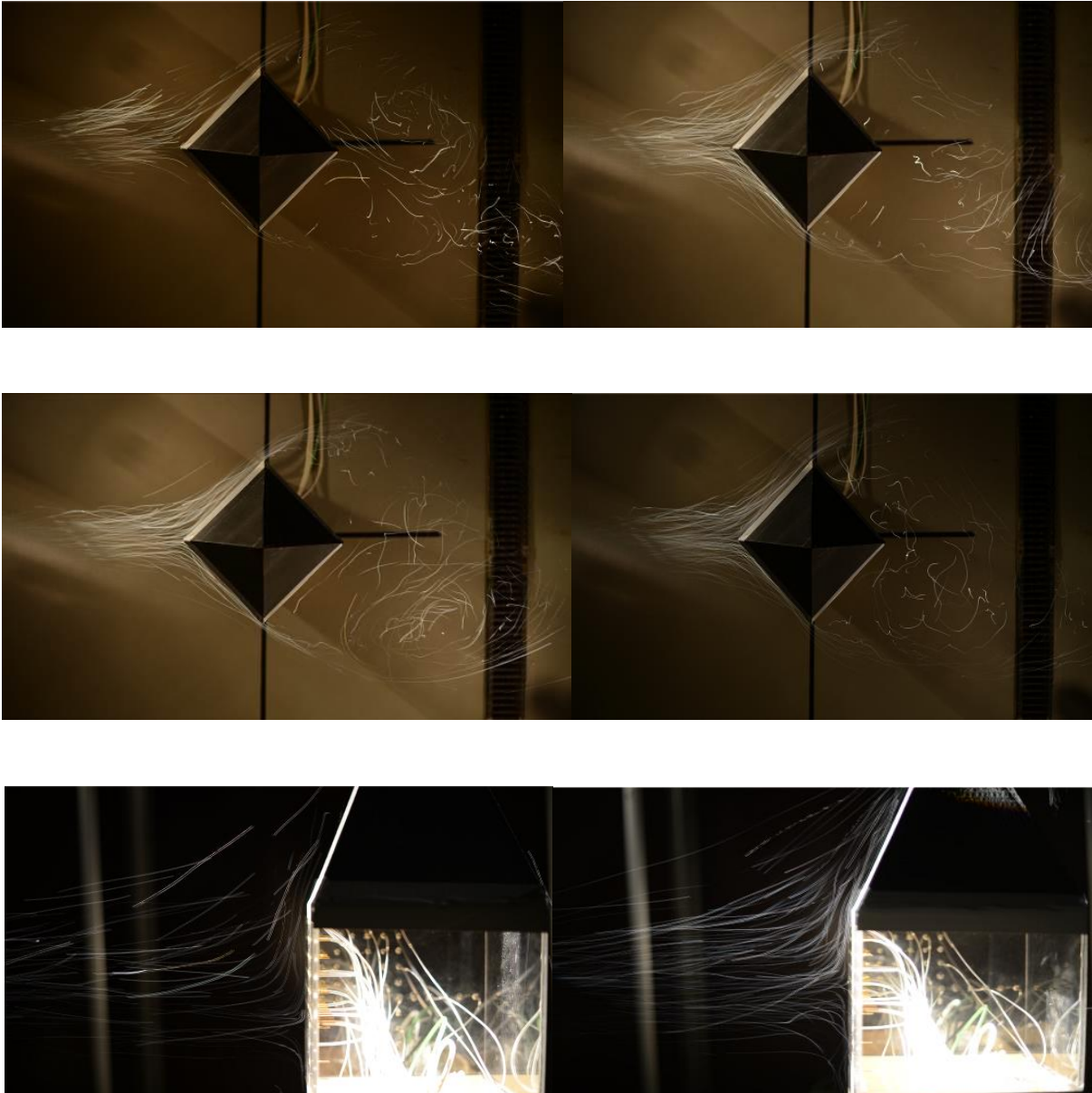


Figure 33: 5% flow visualization test.

4 CHAPTER No. 4 - CASE OF STUDY

4.1 Historical Survey

The most intense wave of reform in all of Bohemia took place in the 13th century. In 1232, by order of King Wenceslas I, a new town was prepared. The layout of the first new town was based on the town-planning concept of Wenceslas I, who decided to change the divergent layout of the old town.

During the reign of Charles IV, the second lord of the Luxembourg dynasty, king of Rome and, from 1355, Holy Roman Emperor, the urban development of Prague was generated, which later became the imperial capital and lay guide of the entire Christian world. Charles IV described the kingdom of Bohemia as a pleasant garden in the middle of his dominions. And Prague, in the heart of the kingdom, visited by countless delegates from all over the world, therefore deserved a general survey, hence the city was extended with a walled core.

The Gothic walls of the new town joined the Vysehrad fortress, rising sharply up the northern slope of the Gothic valley to the edge of Karlov, where Charles IV founded a convent of canons of St. Augustine. From here, the walls ran northward until, with insignificant deviations, they returned to the Vltava at the aforementioned point. The fortified enclosure of the new town was completed in 1353.

The architectural dominants of Gothic construction gave Prague its typical form as an urban ensemble, recognized and called the city of a hundred towers, most of which were built thanks to Charles IV. The urbanistic importance of Prague is of such a nature that the further development of the city until the second half of the 19th century can be associated with the walled spaces.

Within the Gothic architecture of Prague, the following towers should be highlighted for their architectural beauty and historical importance:

The Old Town of Prague, located on the right bank of the Vltava River, expanded around the original citadel of Vyšehrad due to its strategic position in the Vltava Valley, which crossed an important Central European trade route. With royal permission granted, the

Prague citizens founded the Town Hall, the political center of medieval Prague, on September 18, 1338. Later, as Holy Roman Emperor, he tried to make Prague the metropolis not only of the Czechs but of the entire Empire. At that time, Prague was adorned with excellent architectural monuments that are still admired today by its many visitors, who rightly gave it the title of "the Golden City", probably due to the golden roofs and gates of its castle (28).

The Gothic "Gallo" house was purchased in 1835 and the "Minuta" house was sold to the Town Hall for the extension of the Town Hall in 1896. The reconstruction of the foyer on the second floor of the Volflin house was completed with the construction of a new portal in the late Gothic style, which has been the predominant style of urban architecture in the Czech Lands for more than 100 years. The Gothic arch of the portal has richly ornamented archivolt in stone. Decorated corbels support the outer arch, which is a typical late Gothic ogee arch crowned by an imposing finial(29).

The builder renounced the traditional Gothic arch in favor of a rectangular window, embellishing the thickness of the walls with coffered pilasters. In general, the side windows maintain the same style as the original Renaissance main window, but the Gothic-style canopies over the pilaster are an exception. The Renaissance style is also evident in another window located just above the Gothic doorway of the 16th-century Volflin house.

The original structure was badly damaged by modifications in the late 18th century and eventually disappeared completely when a new neo-Gothic wing was built in the 1840s. The reconstruction also affected the historic core of the entire City Hall complex. Two neo-Gothic pediments and an oriel were added to the façade, and architect Gruber adjusted the entrance by adding two round arches. (30).

In 1357, Emperor Charles IV, ruler of Luxembourg, initiated the construction of a new bridge in Prague after the collapse of an older structure in the St. Mary Magdalene flood of 1342. Selecting a closer date for the construction of the Bridge Tower is a complex question, as the dating of its vault ranges from 1370 to 1395.

The bridge structure and towers were of Gothic architecture, the only structure linking the two integral halves of medieval Prague. Thus, the gate tower, fundamental in the surveillance and fortification of its eastern end, was originally decorated with sculptures on its eastern and western facades. The sculptures were composed of seated figures of Emperor

Charles IV and his son, King Wenceslas IV, as well as the patron saints of Bohemia. However, from an architectural point of view, one of the most important features of the bridge tower is the net vault that covers its first floor. This vault bears a strong resemblance to the choir vault of St. Vitus Cathedral, so it can be understood that the Bridge Tower was designed by the same master mason as the cathedral, Peter Parler (31).

4.2 Visual Inspection and damage survey

- Lesser Town Bridge Towers (Malostranské mostecké věže): The tower is in the late Gothic style, dates from 1464 and is based on the architecture of the Old Town Bridge Tower of Parlěř.
- Old Town Bridge Tower (Staroměstská mostecká věž): Gothic tower built by Emperor Charles IV to the designs of Petr Parlěř in the mid-14th century.
- Powder Gate Tower (Prašná brána): Late Gothic tower. Completed in 1475, the Powder Gate Tower, which formerly served as a gunpowder storehouse.
- Old Town Hall with Astronomical Clock (Staroměstská radnice s orlojem): Gothic tower with a bay chapel and a unique astronomical clock. Eastern wing of the Gothic Revival Town Hall was destroyed during the Prague Uprising on May 8, 1945.

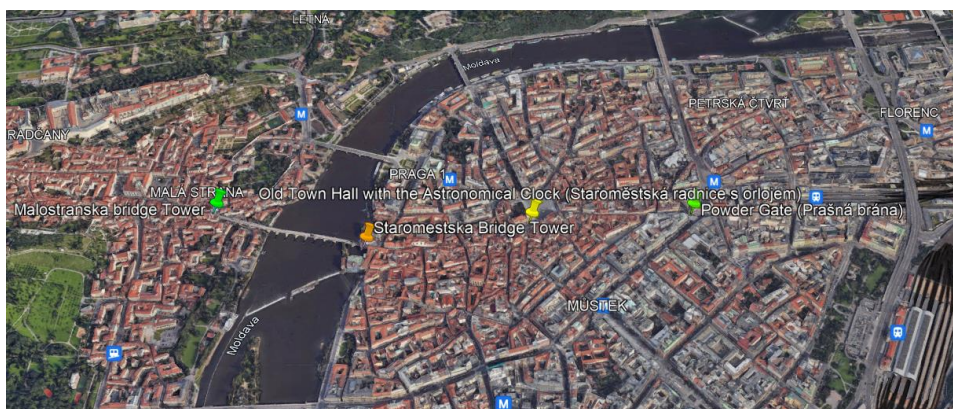


Figure 34: Location of the study towers.

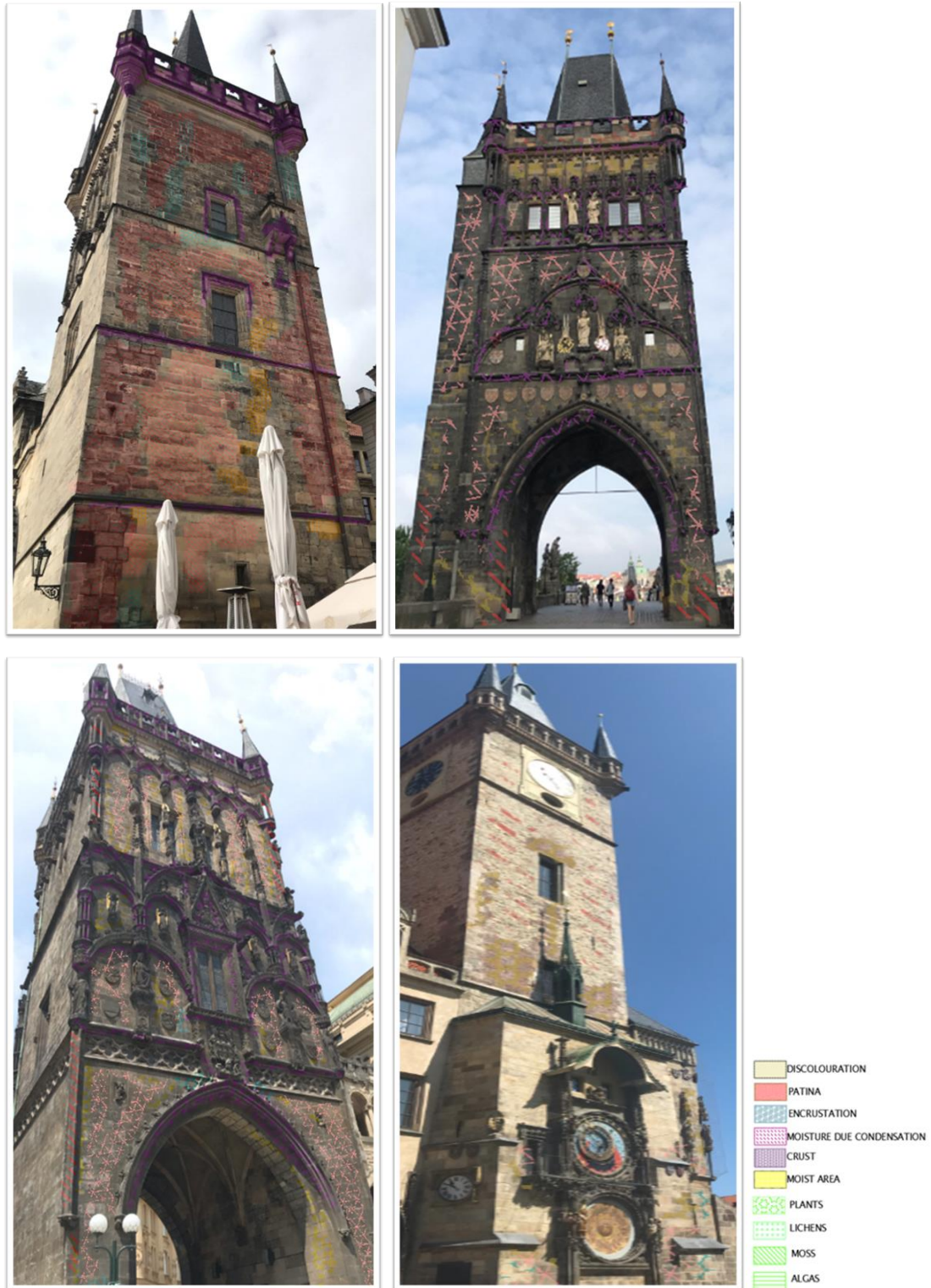


Figure 35: Survey of damages in the study towers.

The table shows the lesions found during visual inspection in each of the study towers. Injury survey sheets are attached for each of the towers with damage maps (Annex 1).

Table No. 11: Damage found in the study towers. Source: Icomos.

STONE DAMAGE	DEFINITION
Missing Part	Empty space, obviously located in the place of some formerly existing stone part.
Differential erosion	Result of selective lichen attack on calcific rocks. Differential erosion is synonymous with relief, i.e., the formation of irregularities on the surface of the stone.
Crumbling	Detachment of single grains or aggregates of grains. Crumbling: Detachment of aggregates of grains from the substrate. These aggregates are generally limited in size (less than 2 cm). This size depends on the nature of the stone and its environment.
Rounding	Preferential erosion of originally angular stone edges leading to a distinctly rounded profile. Rounding can especially be observed on stones which preferably deteriorate through granular disintegration, or when environmental conditions favor granular disintegration.
Discoloration	Change of the color of the stone in one or three of the color parameters: hue, value and chroma. Frequently produced by salts, by the corrosion of metals by micro-organisms. Some typical yellow, orange, brown and black discoloration patterns are due to the presence of carotenoids and melanin produced by fungi and cyanobacteria. Darkened areas due to moistening may have different shapes and extension according to their origin: pipe leakage, rising damp, hygroscopic behavior due to the presence of salts, condensation
Moist Area	on a sandstone rubble-built wall as a result of a concentrated discharge of rainwater from a broken downpipe.
Patina	Chromatic modification of the material, generally resulting from natural or artificial ageing and not involving in most cases visible surface deterioration.
Encrustation	Compact, hard, mineral outer layer adhering to the stone. Surface morphology and color are usually different from those of the stone.
Efflorescence	Generally whitish, powdery, or whisker-like crystals on the surface. Efflorescence is generally poorly cohesive and commonly made of soluble salt crystals

Crust	A crust is frequently dark colored (black crust) but light colors can also be found. Crusts may have a homogeneous thickness, and thus replicate the stone surface, or have irregular thickness and disturb the reading of the stone surface details.
Pitting	point-like millimetric or sub millimetric shallow cavities. The pits generally have a cylindrical or conical shape and are not interconnected. Pitting is due to partial or selective deterioration. Pitting can be biogenically or chemically induced, especially on carbonated stones. Pitting may also result from a harsh or in adapted abrasive cleaning method.
Algae	Algae are microscopic vegetal organisms without stem or leaves which can be seen outdoors and indoors. Algae form green, red, brown, or black veil like zones and can be found mainly in situations where the substrate remains moistened for long periods of time. Depending on the environmental conditions and substrate type, algae may form solid layers or smooth films.
Lichen	Vegetal organism forming rounded millimetric to centimetric crusty or bushy patches. Lichen is a common feature of outdoor stone and is generally best developed under clean air conditions, but growth may be facilitated by certain pollutant such as nitrogen oxides derived primarily from vehicle pollution or agriculture. Former lichen growth may be detected by typical pitting structures (see this term) or lobate or mosaic patterns and even depressions
Moss	Vegetal organism forming small, soft and green cushions of centimetric size. Mosses often grow on stone surface open cavities, cracks, and in any place permanently or frequently wet (masonry joints), and usually shady
Plants	Vegetal living being, having, when complete, root, stem, and leaves, though consisting sometimes only of a single leafy expansion
Perforation	A single or series of surface punctures, holes or gaps, made by a sharp tool or created by an animal. The size is generally of millimetric to centimetric scale. Perforations are deeper than wide and penetrate the body of the stone.

5 CHAPTER No. 5 – ANALYSIS OF THE RESULTS

In the scaled model, higher pressure values can be observed in wind scenarios from W25% to W35% and not in wind scenarios with higher percentages, it is observed that as the velocity increases the pressure decreases.

The points with the highest pressure are located in the center section of façade A for the 0° model. In façade B, the highest-pressure values are concentrated in the corner that connects with the façade perpendicular to the wind, which is consistent with the photographs that record the flow movement when encountering the scale model. It can be estimated that these areas are the most prone to damage and therefore to the generation of various pathologies, especially at the highest points of the model, as a result of the upward deviation of the wind, which can drag rain particles and contaminating particles that are deposited on the material.

There is greater susceptibility in the 45° model since the two facades are located perpendicular to the wind.

However, for the leeward faces there is a high degree of biological and chemical damage due to the suction process in the area, which drags the contaminating particles over the material.

In the Prague Wind Rose, a strong westerly wind is observed, so it can be inferred that the facades located in this direction may have greater mechanical and physical injuries, such as differential erosions, which could be verified with the injury surveys of the study towers.

Finally, for the evaluation of the vulnerability of the towers, understood as the extent to which the system is susceptible to damage by climate change, the three main factors were obtained. The susceptibility (RQ1) was obtained from the graphs generated in the experimental test of the material, and the exposure (RQ2) and resilience (RQ3) were analyzed according to the parameters of Protech2save through STRENCH_Vulnerability evaluation tool, according to the visual inspection performed.

Case study: Gothic Towers of the city of Prague.

Ranking of Vulnerability: $RQ1= 0.50$, $RQ2= 0.90$, $RQ3= 0.29$

Vulnerability assessment: $0.70 \times \text{Susceptibility} + 0.30 \times \text{Exposure} - 0.30 \times \text{Resilience} = 0.54$

With $0 \leq V \leq 1$ (low to high vulnerability).

Pathologies: physical damage, biological and chemical damage.

Based on the results obtained and a qualitative rating of the damage according to the visual inspection carried out, the threat to the towers is classified from moderate to severe.

slight Moderate Extensive Complete

6 CHAPTER No. 6 - CONCLUSIONS AND RECOMMENDATIONS

The moisture distribution plots within the tested specimens allowed to optimally identify how water flow is transported through the porous materials by measuring changes in electrical resistance in a non-destructive manner. The effectiveness of these readings can lead to greater use of this type of system for risk analysis in heritage structures, since it is an economical and easy-to-transport and install system that does not affect the historical and architectural values of the structure and that on the contrary can prevent severe damage leading to high costs of intervention, and therefore to construction processes that generate a high impact on the environment, where the construction sector contributes approximately 23% of air pollution, 40% of drinking water pollution, and 50% of waste in landfills.

The analysis of the measurement of electrical resistance vs. time in each of the wind scenarios with different rain simulation loads allowed to adequately determine the way in which the flow progresses and the level of saturation of the material. In addition to being able to identify the points of greatest risk, that is, in those areas where points from wet to dry and vice versa are delimited, in which there is a greater susceptibility to the appearance of pathologies in the material.

The use of the wind tunnel for the evaluation of the response of building materials under different environmental parameters, such as airflow velocity, relative humidity, and temperature, is an optimal and economical tool for the analysis of vulnerability assessment of structures, and therefore for intervention designs according to the real conditions of the project.

The mapping of the pressure coefficients represented a complex iterative process for the interpolation of the results. As part of the observations made during the pressure measurements on the scale model, interesting data on the behavior of the wind profiles at low velocities were observed. In addition, a loss of pressure values was observed on the face perpendicular to the wind in the model at 0°, between the connection angles of facades A and B.

Once the pressure coefficients of each one of the sensors installed in the model on Re were obtained, according to the density and viscosity of the flow at different speeds, it was possible to determine that the pressure coefficient C_p is stable on the numbers Re tested. , that is, the speed of the wind does not affect the flow mode of the body.

Obtaining the results of the susceptibility of the material according to the rain and wind intensity factors, as well as the analysis of the wind-rain behavior under different scenarios in a scale model of the gothic towers (built with this material) in the wind tunnel, together with the field inspection of the damages in the study structures allowed configuring a theoretical and methodological proposal for future risk projections and, therefore, improving the management of the CH assets and their resilience.

It is necessary to perform a greater number of tests to provide a more concrete analysis of the effectiveness of the results obtained.

Special care must be taken in the process of instilling the sensors and cleaning them, otherwise, errors in the readings may occur.

Within the development of the experimental research, this was carried out under limited conditions of the environmental control functionalities due to operational limitations of the electronic and structural components of the circuit, so it was not possible to perform tests to different climatic scenarios, therefore, it is possible to develop future studies focused on the adaptation and reform of the laboratory wind tunnel.

For future research, it would be convenient to obtain results of the quality of the materials of the study structures by means of non-destructive tests such as ultrasound, sclerometry and others, combined with tests such as those performed in the present study to generate mathematical models in accordance with the real conditions of the material and the state of conservation of the structure, in order to design interventions adjusted to reality. On the other hand, these studies could also be developed to check the agreement of the methods and values in the existing analysis and design codes for the different risk factors in structures of this type.

7 CHAPTER No. 6 - DIFFICULTIES AND LIMITATIONS

It was not possible to obtain material samples from the study towers, so it was necessary to use material samples from a structure with similar construction characteristics.

It was not possible to perform nondestructive testing on the walls that make up the towers due to the limited time and permits required for this process, so only a qualitative damage rating based on visual inspection was obtained.

Operational limitations of the electronic or structural components of the circuit in the small wind tunnel of the ITAM institute. The achievable temperature range is subject to the coolant temperature in the cooler, this is set at a few degrees above zero to avoid frost formation on the coolers, its upper limit is determined for safety reasons to avoid damage to the plexiglass components located around the heaters of the heat and moisture exchange unit. Therefore, it is not possible to adjust the desired temperature and obtain different climatic scenarios.

REFERENCES

1. Hans Antonson, Philip Buckland, Roger Nyqvist, *Climatic Change* (2021) 166: 18
2. Chiara Ciantelli, Elisa Palazzi, Jost von Hardenberg, Carmela Vaccaro, Francesca Tittarelli and Alessandra Bonazza. How climate change may affect UNESCO cultural heritage sites in Panama? August 2018
3. Intergovernmental Panel on Climate Change (IPCC). *Climate Change 2014: Mitigation of Climate Change*; Contribution of Working Group III to the Fifth Assessment. Report of the Intergovernmental Panel on Climate Change; Edenhofer, O., Pichs-Madruga, R., Sokona, Y., Farahani, E., Kadner, S., Seyboth, K., Adler, A., Baum, I., Brunner, S., Eickemeier, P., et al., Eds.; Cambridge University Press: Cambridge, UK; New York, NY, USA, 2014; p. 1454. ISBN 978-1-107-05821-7
4. Elena Sesana, Alexandre S. Gagnon, Chiara Bertolin and John Hughes. Adapting Cultural Heritage to Climate Change Risks: Perspectives of Cultural Heritage Experts in Europe. 14 August 2018
5. I.C. Prentice, G.D. Farquhar, M.J.R. Fasham, M.L. Goulden, M. Heimann, et al.. The carbon cycle and atmospheric carbon dioxide. *Climate change 2001: the scientific basis*, Intergovernmental panel on climate change, 2001. (hal-03333974).
6. Scott Allan Orr, Jenny Richards & Sandra Fatorić (2021) *Climate Change and Cultural Heritage: A Systematic Literature Review (2016-2020)*, *The Historic Environment: Policy & Practice*, 12:3-4, 434-477, DOI: 10.1080/17567505.2021.1957264
7. Ivana Sykorova, Martina Havelcova, Antonin Zeman, Hana Trejtnarova. Carbon air pollution is reflected in deposits on chosen building materials of Prague Castle. *Science of the Total Environment* 409 (2011) 4606-4611
8. S. Papida, W. Murphy, E. May. Enhancement of physical weathering of building stones by microbial populations. *International Biodeterioration & Biodegradation*. Volume 46, Issue December 2000, pages 305-317. ISSN 0964-8305.
9. Wolfgang Sand, Microbial mechanisms of deterioration of inorganic substrates—A general mechanistic overview. *International Biodeterioration & Biodegradation*. Volume 40, Issues 2–4, 1997. Pages 183-190. ISSN 0964-8305.
10. B. Blocken, J. Carmeliet, “A review of wind-driven rain research in building science”, November 2004, Pages 1079-1130.)

11. Broto I Comerma. *Enciclopedia Broto de patologías de la construcción*. C. (2005).
12. B. Blocken, J. Carmeliet, “A review of wind-driven rain research in building science”, November 2004, Pages 1079-1130.
13. R. Cacciotti. Brick masonry response to wind driven rain. Volume 204, 1 February 2020, 110080.
14. R. Cacciotti & S. Pospíšil & S. Kuznetsov1 & A. Trush, A Proposed Calibration Procedure for the Simulation of Wind-Driven Rain in Small-Scale Wind Tunnel. *Experimental Techniques* (2019) 43:369–384
15. R. Cacciotti. J. Valach, B. Wolf. Innovative and easy-to-implement moisture monitoring system for brick units. *Construction and Building Materials*. Volume 186, 20 October 2018, Pages 598-614
16. J. Válek, P. Kozlovcev, A. Fialová, Z. Slížková, K. Kotková, M. Svoboda, V. Koudelková. Establishment of reference parameters for the evaluation of the reinforcement of the degraded sandstone masonry of St. Vitus Cathedral of Prague Castle". ÚTAM, Praha 2021
17. Pel, Leo, Klaas Kopinga, and H. Brocken. *Moisture transport in porous building materials*. Diss. Technische Universiteit Eindhoven, 1995.
18. Bert Blocken, Jan Carmeliet, A review of wind-driven rain research in building science, *Journal of Wind Engineering and Industrial Aerodynamics*, Volume 92, Issue 13, 2004, Pages 1079-1130, ISSN 0167-6105
19. O. Birkeland, General Report, Rain Penetration, RILEM/CIB Symposium on Moisture Problems in Buildings, Rain Penetration, vol. 3, paper 3-0, Helsinki, August 16-19, 1965.
20. Cermak, J.E.; “Application of Fluid Mechanics to Wind Engineering”. A Freeman Scholar Lecture, *Journal of Fluids Engineering*, American Society of Mechanical Engineers, Vol. 97, N°1, 1975
21. M. Morales. Atmospheric boundary layer in the wind tunnel for experiments on objects. Universidad de los Andes, Bogota-Colombia. 2013
22. Flower JW, Lawson TV (1972) On the laboratory representation of the impact of rainfall on buildings. *Atmos Environment* 6:55-60

23. Rayment R, Hilton M (1977) The use of bubbles in a wind tunnel for flow visualization and possible raindrop representation. *J Wind Eng Ind Aerodyn* 2: 149-157).
24. J. Lässig, U. Jara, A. Apcarian. Determination of transverse vibrations in a building from wind tunnel tests. Vol II. 2021
25. R. Cacciotti a, B. Wolf a , M. Machaček. Small-scale wind tunnel for the investigation of the influence of environmental conditions on the performance of building materials
26. J. BLAZEK. (2001): *Computational Fluid Dynamics: Principles and Applications*, Elsevier
27. J. Arroyo, J. Benito, R. Álvarez: *Análisis de la acción del viento en los edificios*. ISSN 1133-9365, N°. 28, 1997.
28. O. Cardona A. Holistic seismic risk estimation using complex dynamic systems. Barcelona, September – 2001
29. Natural disasters and vulnerability analysis: report of Expert Group Meeting, 9-12 July 1979.
30. Risk Mapping Tool for Cultural Heritage Protection-Risk assessment and sustainable protection of Cultural Heritage in changing environment. Protecht2save © 2020 – 2022. <https://www.protecht2save-wgt.eu/>.
31. EN 13306 – Maintenance – Maintenance terminology.
32. Report number: D41.1 Affiliation: CRISMA - Modelling crisis management for improved action and preparedness. Integration project financed under the Security theme of the Cooperation Programme of the 7th Framework Programme of the European Commission. Grant agreement no 284552. November 2012.
33. Theodosiou, Efstratios & Dimitrijevic, Milan & Manimanis, Vassilios. (2009). The Astronomical Clock of Prague and the astronomical legacy of Antiquity. *European ideas, Scientific Publications of the Serbian Society for Ancient Studies*. 3. 374-391.
34. Kim, K. (2003). Czech Culture in Prague: Architecture. *International Area Review*, 6(1), 19–33. <https://doi.org/10.1177/223386590300600102>.
35. Rymarev Alexander, Petr Šamal (2008). Houses in the Old Town of Prague III. NLN - Nakladatelství Lidové noviny.
36. Gajdošová Ana (2016) “Vaulting Small Spaces: The Innovative Design of Prague’s Bridge Tower Vault” *British Archaeological Association*, 39–58.

37. J. Válek, P. Kozlovcev, A. Fialová, Z. Slížková, K. Kotková, M. Svoboda, V. Koudelková. Determination of reference parameters for the evaluation of the strengthening of degraded sandstone masonry of St. Vitus Cathedral at Prague Castle. ÚTAM, Prague 2021.
38. Pavel, Jakub. "El urbanismo de la vieja Praga." *Cuadernos de arquitectura* (1966): 37-41.
39. R. Přikryl, T. Lokajíček, J. Svobodová, Z. Weishauptová. Experimental weathering of marlstone from Přední Kopanina (Czech Republic)—historical building stone of Prague. Volume 38, Issues 9–10, 2003. Pages 1163-1171. ISSN 0360-1323,
40. Model 5 Console. [Model 5 Console - Helium Bubble Generator | Sage Action, Inc. \(sageactioninc.com\)](https://www.sageactioninc.com)

DOCUMENTATION ANNEXED

Annex No. 1: Damage survey sheets

PROJECT NAME: Malostranská bridge Tower, Prague.
 ADDRESS/ COORDINATES: Malá Strana 11800 Prague
 ELEMENT TO BE ANALYZED: Facades
 MATERIAL: Stone
 UNIT OF MEASURE: m²

ORIGINALITY: YES x
 NO
 UNKNOWN
 DATE (dd/mm/yyyy): 20/06/2023

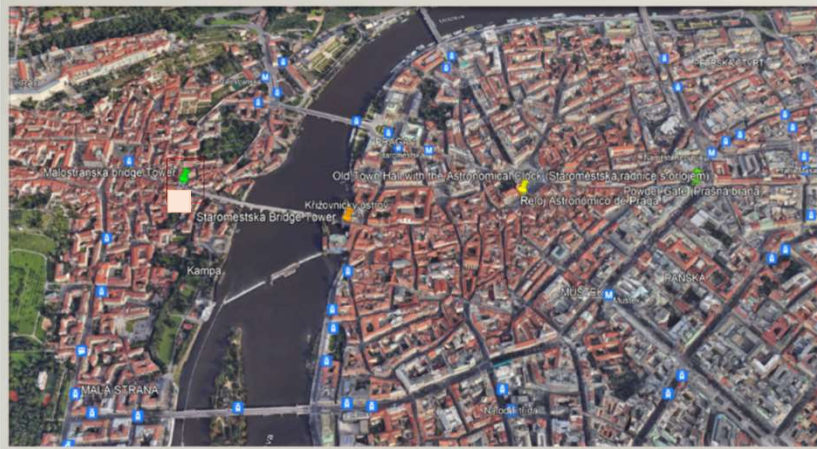
DEGREE OF DAMAGE	
X	X
X	X
X	X

CODE: E1

Format Authorship: Saray Sepulveda Cruz
 Date of creation of the forms: June 2022

Version V.1.0.

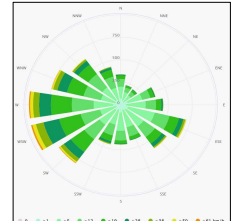
LOCALIZATION



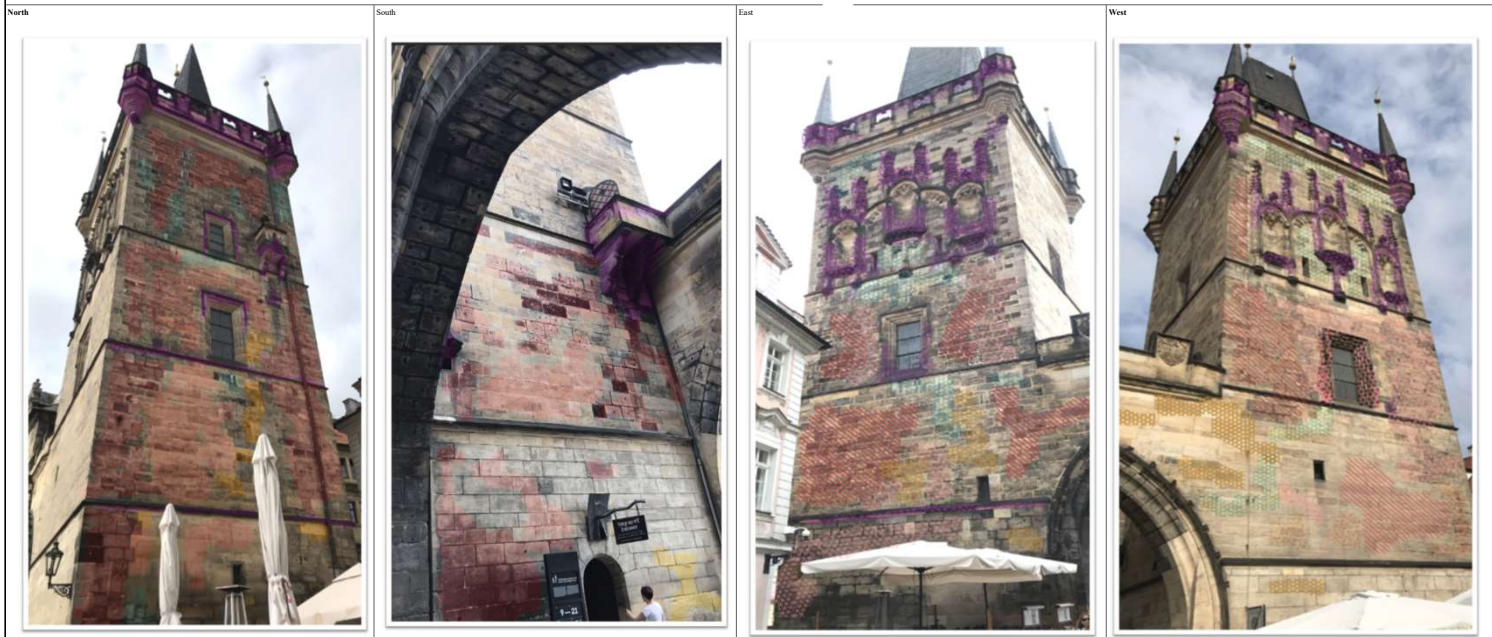
RELEVANT DATA

Coordinates
 Latitude: 50.087267°
 Longitude: 14.406845°
 Century: XIII
 Type: Late Gothic

Late Gothic tower from 1464. It is based on the architecture of the Old Town Bridge Tower in Paris. On the banks of the Vltava River and the historic center of the city.



RELEVANT DAMAGES



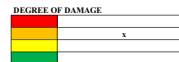
DAMAGE TYPE	DESCRIPTION
DISCOLOURATION	Change of color of the stone...
PATINA	Chromatic modification of the material...
ENCrustATION	Compact, hard, mineral outer layer adhering to the stone...
MOISTURE DUE CONDENSATION	Darkened areas due to moistening...
CRUST	A crust is frequently dark coloured (black crust) but light colours can also be found...
MOIST AREA	Darkened areas due to moistening...
PLANTS	Vegetation growing on the facade...
LICHENS	Small, leaf-like organisms...
MOSS	Small, green, leafy organisms...
ALGAS	Microscopic organisms...

PHOTO	Code	DAMAGE	DEFINITION	INTERVENTION PROPOSAL
	CD-01-05	Efflorescence	Generally whitish, powdery or whisker-like crystals on the surface. Efflorescences are generally poorly cohesive and commonly made of soluble salt crystals	The deterioration processes must be interrupted, in general the process is based on the manual cleaning of the material in order not to generate strong abrasions in the rock, it is advisable to make samplings of the dirt to determine its nature and to eradicate them in an effective way. Within this work is included the pre-consolidation, this should be done when there are pieces of great historical value where the cleaning itself can generate destruction of the element, desalination in which salts are extracted with the application on the surface of the stone of an additional absorbent material, a consolidation will be executed with the objective of increasing the cohesion of the components of the superficial zone of the stone.
	CD-01-4	Discolouration	Change of the color of the stone in one or three of the color parameters: hue, value and chroma. Frequently produced by salts, by the corrosion of metals by micro-organisms. Some typical yellow, orange, brown and black discoloration patterns are due to the presence of carbonic acids and melanins produced by fungi and cyanobacteria. Darkened areas due to moistening may have different shapes and extension according to their origin: pipe leakage, rising damp, hygroscopic behaviour due to the presence of salts, condensation	The deterioration processes must be interrupted, in general the process is based on the manual cleaning of the material in order not to generate strong abrasions in the rock, it is advisable to make samplings of the dirt to determine its nature and to eradicate them in an effective way. Within this work is included the pre-consolidation, this should be done when there are pieces of great historical value where the cleaning itself can generate destruction of the element, desalination in which salts are extracted with the application on the surface of the stone of an additional absorbent material, a consolidation will be executed with the objective of increasing the cohesion of the components of the superficial zone of the stone.
	CD-01-4.2	Patina	Chromatic modification of the material, generally resulting from natural or artificial aging and not involving in most cases visible surface deterioration.	The deterioration processes must be interrupted, in general the process is based on the manual cleaning of the material in order not to generate strong abrasions in the rock, it is advisable to make samplings of the dirt to determine its nature and to eradicate them in an effective way. Within this work is included the pre-consolidation, this should be done when there are pieces of great historical value where the cleaning itself can generate destruction of the element, desalination in which salts are extracted with the application on the surface of the stone of an additional absorbent material, a consolidation will be executed with the objective of increasing the cohesion of the components of the superficial zone of the stone.
	CD-01-4.3	Encrustation	Compact, hard, mineral outer layer adhering to the stone. Surface morphology and colour are usually different from those of the stone.	The deterioration processes must be interrupted, in general the process is based on the manual cleaning of the material in order not to generate strong abrasions in the rock, it is advisable to make samplings of the dirt to determine its nature and to eradicate them in an effective way. Within this work is included the pre-consolidation, this should be done when there are pieces of great historical value where the cleaning itself can generate destruction of the element, desalination in which salts are extracted with the application on the surface of the stone of an additional absorbent material, a consolidation will be executed with the objective of increasing the cohesion of the components of the superficial zone of the stone.
	CD-01-06	Crust	A crust is frequently dark coloured (black crust) but light colours can also be found. Crusts may have an homogeneous thickness, and thus replicate the stone surface, or have irregular thickness and disturb the reading of the stone surface details.	The deterioration processes must be interrupted, in general the process is based on the manual cleaning of the material in order not to generate strong abrasions in the rock, it is advisable to make samplings of the dirt to determine its nature and to eradicate them in an effective way. Within this work is included the pre-consolidation, this should be done when there are pieces of great historical value where the cleaning itself can generate destruction of the element, desalination in which salts are extracted with the application on the surface of the stone of an additional absorbent material, a consolidation will be executed with the objective of increasing the cohesion of the components of the superficial zone of the stone.
	PD-02-1	Differential erosion	Result of selective lichen attack on calcareous rocks. Differential erosion is synonymous with relief, i.e. the formation of irregularities on the surface of the stone.	It is important to avoid moisture, since the presence of water is the constant in almost all forms of erosion, in this sense, the right thing to do is to take measures to prevent water from stagnating on the surface through additional works on the facades, if this is not possible, water-repellent coatings should be applied, generally based on silanes without altering the breathability, and respecting the natural appearance of the bases as much as possible.
	CD-01-1	Crumbling	Detachment of single grains or aggregates of grains. Crumbling/Detachment of aggregates of grains from the substrate. These aggregates are generally limited in size (less than 2 cm). This size depends on the nature of the stone and its environment.	The deterioration processes must be interrupted, in general the process is based on the manual cleaning of the material in order not to generate strong abrasions in the rock, it is advisable to make samplings of the dirt to determine its nature and to eradicate them in an effective way. Within this work is included the pre-consolidation, this should be done when there are pieces of great historical value where the cleaning itself can generate destruction of the element, desalination in which salts are extracted with the application on the surface of the stone of an additional absorbent material, a consolidation will be executed with the objective of increasing the cohesion of the components of the superficial zone of the stone.

8	CD-01-7	Pitting	point-like millimetric or submillimetric shallow cavities. The pits generally have a cylindrical or conical shape and are not interconnected. Pitting is due to partial or selective deterioration. Pitting can be biogenically or chemically induced, especially on carbonates stones. Pitting may also result from a harsh or inadapted abrasive cleaning method.	The deterioration processes must be interrupted, in general the process is based on the manual cleaning of the material in order not to generate strong abrasions in the rock, it is advisable to make samplings of the dirt to determine its nature and to eradicate them in an effective way. Within this work is included the pre-consolidation, this should be done when there are pieces of great historical value where the cleaning itself can generate destruction of the element, desalination in which salts are extracted with the application on the surface of the stone of an additional absorbent material, a consolidation will be executed with the objective of increasing the cohesion of the components of the superficial zone of the stone.
9	BD-01-1	Algae	Algae are microscopic vegetal organisms without stem or leaves which can be seen outdoors and indoors. Algae form green, red, brown, or black veil like zones and can be found mainly in situations where the substrate remains moistened for long periods of time. Depending on the environmental conditions and substrate type, algae may form solid layers or smooth films.	Use of biocidal products with a broad disinfectant spectrum and low solubilization in water, which should not react with the products used for consolidation and cleaning of the stone. The most commonly used biocides are benzalkonium chloride, ammonia (ammonium salts), formaldehyde and sodium hypochlorite.
10	BD-01-2	Lichen	Vegetal organism forming rounded millimetric to centimetric crusty or bushy patches. Lichen is a common feature of outdoor stone and is generally best developed under clean air conditions, but growth may be facilitated by certain pollutant such as nitrogen oxides derived primarily from vehicle pollution or agriculture. Former lichen growth may be detected by typical pitting structures (see this term) or lobate or mosaic patterns and even depressions	Use of biocidal products with a broad disinfectant spectrum and low solubilization in water, which should not react with the products used for consolidation and cleaning of the stone. The most commonly used biocides are benzalkonium chloride, ammonia (ammonium salts), formaldehyde and sodium hypochlorite.
11	BD-01-3	Moss	Vegetal organism forming small, soft and green crust ions of centimetric size. Mosses often grow on stone surface open cavities, cracks, and in any place permanently or frequently wet (masonry joints), and usually shady	Use of biocidal products with a broad disinfectant spectrum and low solubilization in water, which should not react with the products used for consolidation and cleaning of the stone. The most commonly used biocides are benzalkonium chloride, ammonia (ammonium salts), formaldehyde and sodium hypochlorite.
12	BD-01-4	Plants	Vegetal living being, having, when complete, root, stem, and leaves, though consisting sometimes only of a single leafy expansion	Use of biocidal products with a broad disinfectant spectrum and low solubilization in water, which should not react with the products used for consolidation and cleaning of the stone. The most commonly used biocides are benzalkonium chloride, ammonia (ammonium salts), formaldehyde and sodium hypochlorite.

PROJECT NAME: Staroměstská Bridge Tower, Prague.
 ADDRESS/COORDINATES: 110 00 Praha 1 – Staré Město- Prague
 ELEMENT TO BE ANALYZED: Facades
 MATERIAL: Stone
 UNIT OF MEASURE: m²

ORIGINALITY YES x
 NO
 UNKNOWN
 DATE (dd/mm/yyyy): 20/06/2023

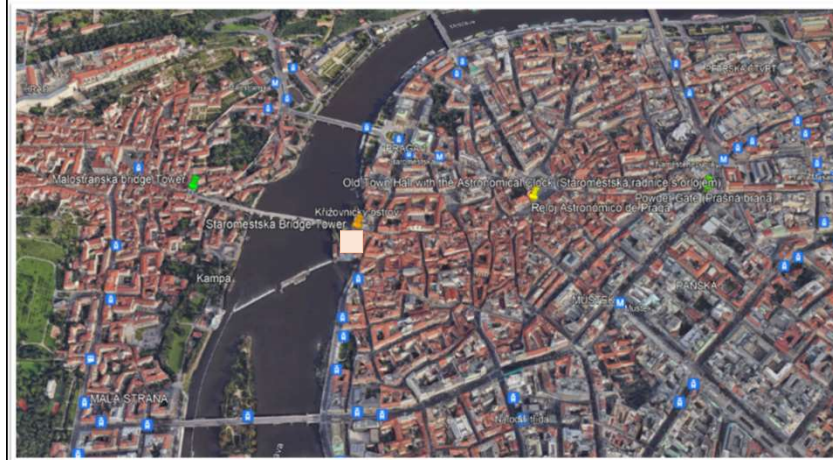


CODE: E2

Format Authority: Saray Sepuveda Cruz
 Date of creation of the formats: June 2022

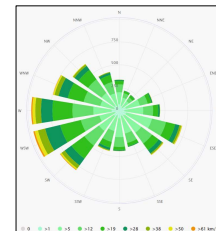
Version V.1.0.

LOCALIZATION



RELEVANT DATA

Coordinates
 Latitude: 50.086138°
 Longitude: 14.413645°
 Century: XIV
 Type: Gothic
 Built by Emperor Charles IV according to the designs of Petr Parléř in 1380



RELEVANT DAMAGES

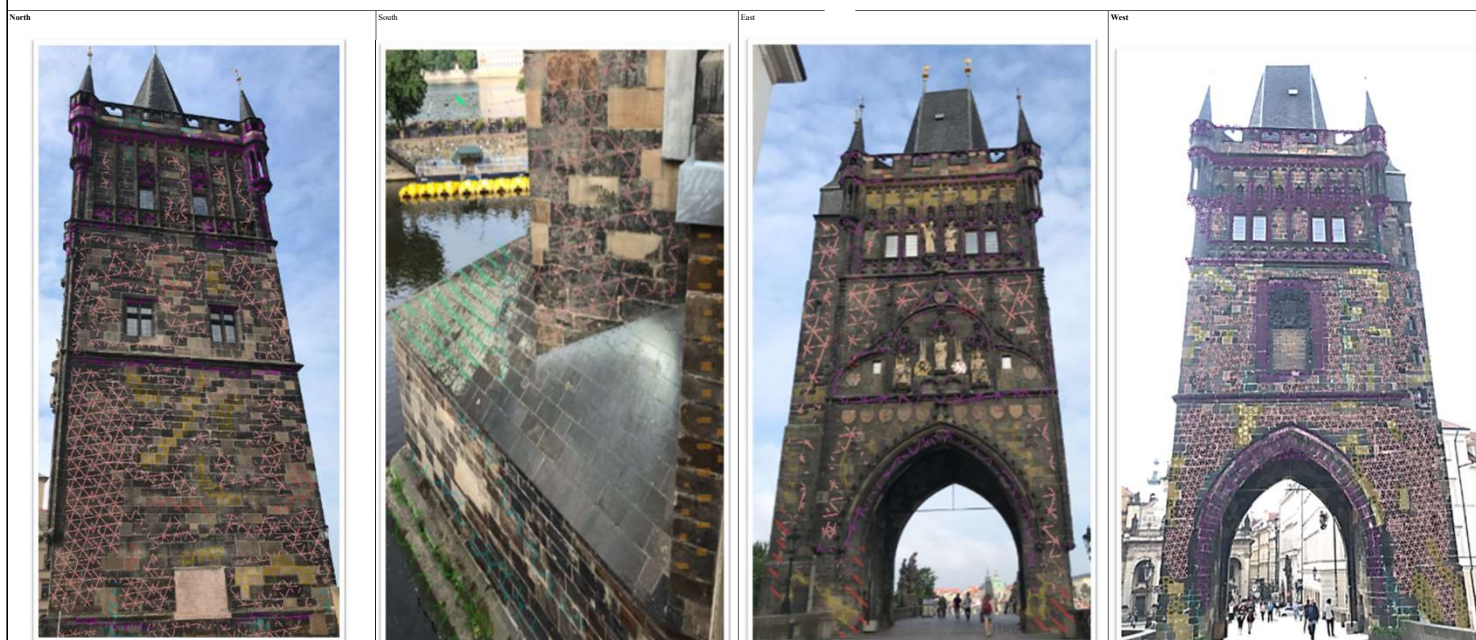


PHOTO	Cod.	DAMAGE	DEFINITION	INTERVENTION PROPOSAL
1	CD-01-05	Efflorescence	Generally whitish, powdery or whisker-like crystals on the surface. Efflorescences are generally poorly cohesive and commonly made of soluble salt crystals	The deterioration processes must be interrupted, in general the process is based on the manual cleaning of the material in order not to generate strong abrasions in the rock, it is advisable to make samplings of the dirt to determine its nature and to eradicate them in an effective way. Within this work is included the pre-consolidation, this should be done when there are pieces of great historical value where the cleaning itself can generate destruction of the element, desalination in which salts are extracted with the application on the surface of the stone of an additional absorbent material, a consolidation will be executed with the objective of increasing the cohesion of the components of the superficial zone of the stone.
2	CD-01-4	Discolouration	Change of the color of the stone in one or three of the color parameters: hue, value and chroma. Frequently produced by salts, by the corrosion of metals by micro-organisms. Some typical yellow, orange, brown and black discoloration patterns are due to the presence of carbonoids and melanins produced by fungi and cyanobacteria. Darkened areas due to mossing may have different shapes and extension according to their origin: pipe leakage, rising damp, hygroscopic behaviour due to the presence of salts, condensation	The deterioration processes must be interrupted, in general the process is based on the manual cleaning of the material in order not to generate strong abrasions in the rock, it is advisable to make samplings of the dirt to determine its nature and to eradicate them in an effective way. Within this work is included the pre-consolidation, this should be done when there are pieces of great historical value where the cleaning itself can generate destruction of the element, desalination in which salts are extracted with the application on the surface of the stone of an additional absorbent material, a consolidation will be executed with the objective of increasing the cohesion of the components of the superficial zone of the stone.
3	CD-01-4.2	Patina	Chromatic modification of the material, generally resulting from natural or artificial aging and not involving in most cases visible surface deterioration.	The deterioration processes must be interrupted, in general the process is based on the manual cleaning of the material in order not to generate strong abrasions in the rock, it is advisable to make samplings of the dirt to determine its nature and to eradicate them in an effective way. Within this work is included the pre-consolidation, this should be done when there are pieces of great historical value where the cleaning itself can generate destruction of the element, desalination in which salts are extracted with the application on the surface of the stone of an additional absorbent material, a consolidation will be executed with the objective of increasing the cohesion of the components of the superficial zone of the stone.
4	CD-01-4.3	Encrustation	Compact, hard, mineral outer layer adhering to the stone. Surface morphology and colour are usually different from those of the stone.	The deterioration processes must be interrupted, in general the process is based on the manual cleaning of the material in order not to generate strong abrasions in the rock, it is advisable to make samplings of the dirt to determine its nature and to eradicate them in an effective way. Within this work is included the pre-consolidation, this should be done when there are pieces of great historical value where the cleaning itself can generate destruction of the element, desalination in which salts are extracted with the application on the surface of the stone of an additional absorbent material, a consolidation will be executed with the objective of increasing the cohesion of the components of the superficial zone of the stone.
5	CD-01-06	Crust	A crust is frequently dark coloured (black crust) but light colours can also be found. Crusts may have an homogeneous thickness, and thus replicate the stone surface, or have irregular thickness and disturb the reading of the stone surface details.	The deterioration processes must be interrupted, in general the process is based on the manual cleaning of the material in order not to generate strong abrasions in the rock, it is advisable to make samplings of the dirt to determine its nature and to eradicate them in an effective way. Within this work is included the pre-consolidation, this should be done when there are pieces of great historical value where the cleaning itself can generate destruction of the element, desalination in which salts are extracted with the application on the surface of the stone of an additional absorbent material, a consolidation will be executed with the objective of increasing the cohesion of the components of the superficial zone of the stone.
6	PD-02-1	Differential erosion	Result of selective lichen attack on calcitic rocks. Differential erosion is synonymous with relief, i.e. the formation of irregularities on the surface of the stone.	It is important to avoid moisture, since the presence of water is the constant in almost all forms of erosion, in this sense, the right thing to do is to take measures to prevent water from stagnating on the surface through additional works on the facades, if this is not possible, water-repellent coatings should be applied, generally based on siloxanes without altering the breathability, and respecting the natural appearance of the bases as much as possible.

7	CD-01-1	Crumbling	Detachment of single grains or aggregates of grains. Crumbling: Detachment of aggregates of grains from the substrate. These aggregates are generally limited in size (less than 2 cm). This size depends on the nature of the stone and its environment.	The deterioration processes must be interrupted, in general the process is based on the manual cleaning of the material in order not to generate strong abrasions in the rock, it is advisable to make samplings of the dirt to determine its nature and to eradicate them in an effective way. Within this work is included the pre-consolidation, this should be done when there are pieces of great historical value where the cleaning itself can generate destruction of the element, desalination in which salts are extracted with the application on the surface of the stone of an additional absorbent material, a consolidation will be executed with the objective of increasing the cohesion of the components of the superficial zone of the stone.
8	CD-01-7	Pitting	point-like millimetric or submillimetric shallow cavities. The pits generally have a cylindrical or conical shape and are not interconnected. Pitting is due to partial or selective deterioration. Pitting can be biogenically or chemically induced, especially on carbonates stones. Pitting may also result from a harsh or inadapted abrasive cleaning method.	The deterioration processes must be interrupted, in general the process is based on the manual cleaning of the material in order not to generate strong abrasions in the rock, it is advisable to make samplings of the dirt to determine its nature and to eradicate them in an effective way. Within this work is included the pre-consolidation, this should be done when there are pieces of great historical value where the cleaning itself can generate destruction of the element, desalination in which salts are extracted with the application on the surface of the stone of an additional absorbent material, a consolidation will be executed with the objective of increasing the cohesion of the components of the superficial zone of the stone.
9	BD-01-1	Algae	Algae are microscopic vegetal organisms without stem or leaves which can be seen outdoors and indoors. Algae form green, red, brown, or black veil like zones and can be found mainly in situations where the substrate remains moistened for long periods of time. Depending on the environmental conditions and substrate type, algae may form solid layers or smooth films.	Use of biocidal products with a broad disinfectant spectrum and low solubilization in water, which should not react with the products used for consolidation and cleaning of the stone. The most commonly used biocides are benzalkonium chloride, ammonia (ammonium salts), formaldehyde and sodium hypochlorite.
10	BD-01-2	Lichen	Vegetal organism forming rounded millimetric to centimetric crusty or bushy patches. Lichen is a common feature of outdoor stone and is generally best developed under clean air conditions, but growth may be facilitated by certain pollutant such as nitrogen oxides derived primarily from vehicle pollution or agriculture. Former lichen growth may be detected by typical pitting structures (see this term) or lobate or mosaic patterns and even depressions	Use of biocidal products with a broad disinfectant spectrum and low solubilization in water, which should not react with the products used for consolidation and cleaning of the stone. The most commonly used biocides are benzalkonium chloride, ammonia (ammonium salts), formaldehyde and sodium hypochlorite.
11	BD-01-3	Moss	Vegetal organism forming small, soft and green cushion of centimetric size. Mosses often grow on stone surface open cavities, cracks, and in any place permanently or frequently wet (masonry joints), and usually shady	Use of biocidal products with a broad disinfectant spectrum and low solubilization in water, which should not react with the products used for consolidation and cleaning of the stone. The most commonly used biocides are benzalkonium chloride, ammonia (ammonium salts), formaldehyde and sodium hypochlorite.
12	BD-01-4	Plants	Vegetal living being, having, when complete, root, stem, and leaves, though consisting sometimes only of a single leafy expansion	Use of biocidal products with a broad disinfectant spectrum and low solubilization in water, which should not react with the products used for consolidation and cleaning of the stone. The most commonly used biocides are benzalkonium chloride, ammonia (ammonium salts), formaldehyde and sodium hypochlorite.

PROJECT NAME: Prašná Brána Tower, Prague.
 ADDRESS/ COORDINATES: 110 00 Praha 1 – Staré Město- Prague
 ELEMENT TO BE ANALYZED: Facades
 MATERIAL: Stone
 UNIT OF MEASURE: m²

ORIGINALITY YES x
 NO
 UNKNOWN
 DATE (dd/mm/yyyy): 20/06/2023

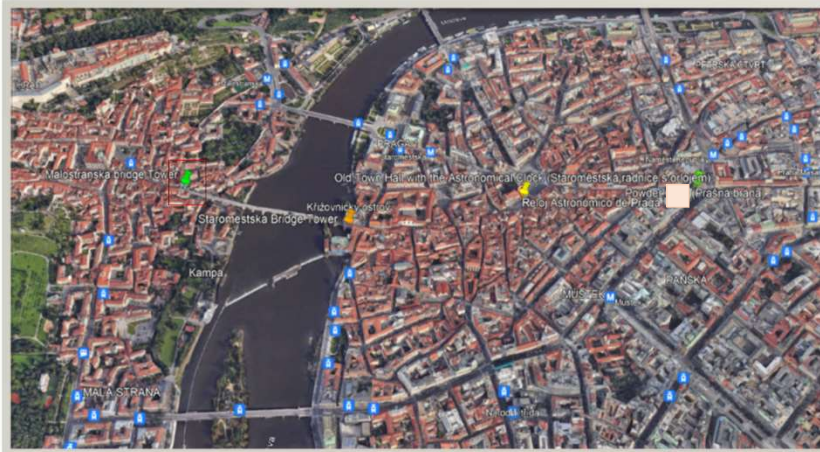
DEGREE OF DAMAGE	
X	X
X	X
X	X

CODE: E3

Format Authorship: Saray Sepulveda Cruz
 Date of creation of the formats: June 2022

Version V.1.0.

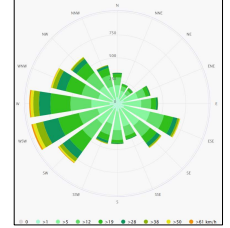
LOCALIZATION



RELEVANT DATA

Coordinates
 Latitude: 50.087243°
 Longitude: 14.427819°
 Century: XIII
 Type: Late Gothic

The Powder Tower is one of the 13 original gates of the Old Town of Prague. Its construction began in 1475.



RELEVANT DAMAGES

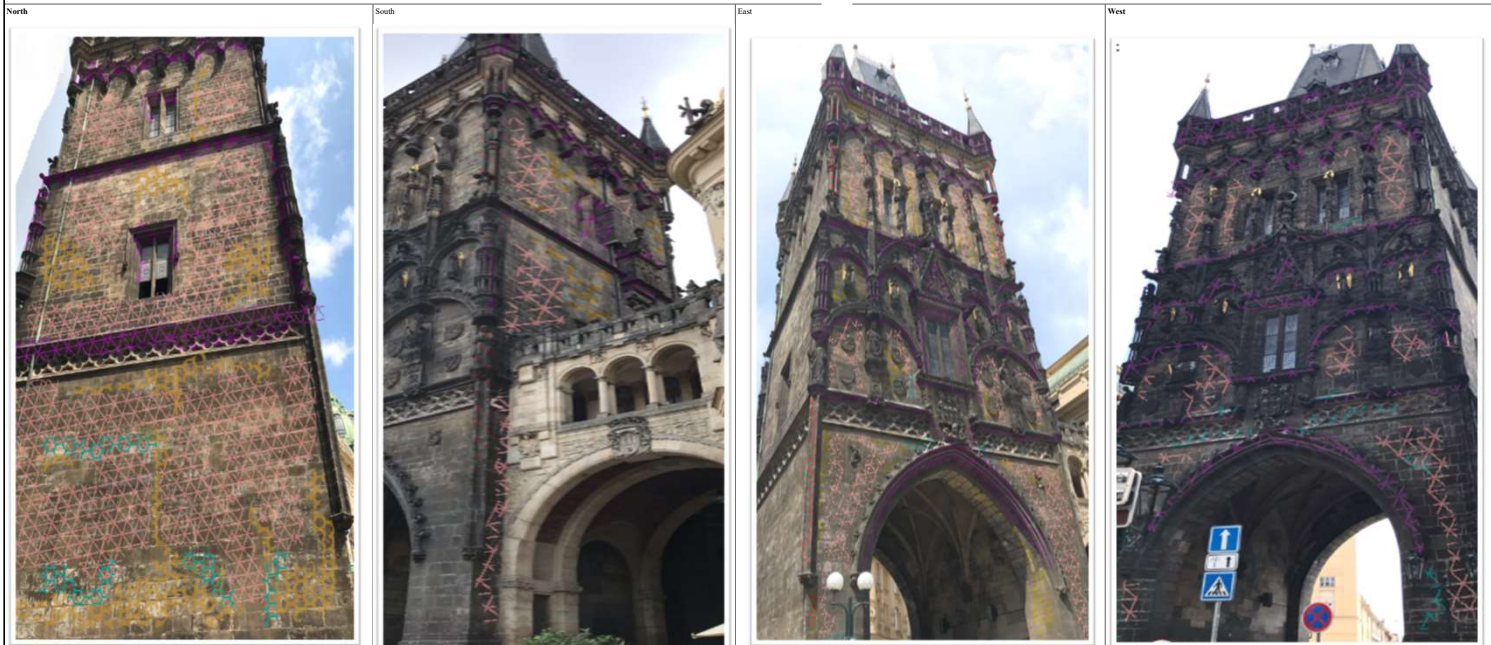


PHOTO	Cod.	DAMAGE	DEFINITION	INTERVENTION PROPOSAL
1	CD-01-05	Efflorescence	Generally whitish, powdery or whisker-like crystals on the surface. Efflorescences are generally poorly cohesive and commonly made of soluble salt crystals	The deterioration processes must be interrupted, in general the process is based on the manual cleaning of the material in order not to generate strong abrasions in the rock, it is advisable to make samplings of the dirt to determine its nature and to eradicate them in an effective way. Within this work is included the pre-consolidation, this should be done when there are pieces of great historical value where the cleaning itself can generate destruction of the element, desalination in which salts are extracted with the application on the surface of the stone of an additional absorbent material, a consolidation will be executed with the objective of increasing the cohesion of the components of the superficial zone of the stone.
2	CD-01-4	Discolouration	Change of the color of the stone in one or three of the color parameters: hue, value and chroma. Frequently produced by salts, by the corrosion of metals by micro-organisms. Some typical yellow, orange, brown and black discoloration patterns are due to the presence of carotenoids and melanins produced by fungi and cyanobacteria. Darkened areas due to moistening may have different shapes and extension according to their origin: pipe leakage, rising damp, hygroscopic behaviour due to the presence of salts, condensation	The deterioration processes must be interrupted, in general the process is based on the manual cleaning of the material in order not to generate strong abrasions in the rock, it is advisable to make samplings of the dirt to determine its nature and to eradicate them in an effective way. Within this work is included the pre-consolidation, this should be done when there are pieces of great historical value where the cleaning itself can generate destruction of the element, desalination in which salts are extracted with the application on the surface of the stone of an additional absorbent material, a consolidation will be executed with the objective of increasing the cohesion of the components of the superficial zone of the stone.
3	CD-01-4.2	Patina	Chromatic modification of the material, generally resulting from natural or artificial ageing and not involving in most cases visible surface deterioration.	The deterioration processes must be interrupted, in general the process is based on the manual cleaning of the material in order not to generate strong abrasions in the rock, it is advisable to make samplings of the dirt to determine its nature and to eradicate them in an effective way. Within this work is included the pre-consolidation, this should be done when there are pieces of great historical value where the cleaning itself can generate destruction of the element, desalination in which salts are extracted with the application on the surface of the stone of an additional absorbent material, a consolidation will be executed with the objective of increasing the cohesion of the components of the superficial zone of the stone.
4	CD-01-4.3	Encrustation	Compact, hard, mineral outer layer adhering to the stone. Surface morphology and colour are usually different from those of the stone.	The deterioration processes must be interrupted, in general the process is based on the manual cleaning of the material in order not to generate strong abrasions in the rock, it is advisable to make samplings of the dirt to determine its nature and to eradicate them in an effective way. Within this work is included the pre-consolidation, this should be done when there are pieces of great historical value where the cleaning itself can generate destruction of the element, desalination in which salts are extracted with the application on the surface of the stone of an additional absorbent material, a consolidation will be executed with the objective of increasing the cohesion of the components of the superficial zone of the stone.
5	CD-01-06	Crust	A crust is frequently dark coloured (black crust) but light colours can also be found. Crusts may have an homogeneous thickness, and thus replicate the stone surface, or have irregular thickness and disturb the reading of the stone surface details.	The deterioration processes must be interrupted, in general the process is based on the manual cleaning of the material in order not to generate strong abrasions in the rock, it is advisable to make samplings of the dirt to determine its nature and to eradicate them in an effective way. Within this work is included the pre-consolidation, this should be done when there are pieces of great historical value where the cleaning itself can generate destruction of the element, desalination in which salts are extracted with the application on the surface of the stone of an additional absorbent material, a consolidation will be executed with the objective of increasing the cohesion of the components of the superficial zone of the stone.
6	PD-02-1	Differential erosion	Result of selective lichen attack on calcitic rocks. Differential erosion is synonymous with relief, i.e. the formation of irregularities on the surface of the stone.	It is important to avoid moisture, since the presence of water is the constant in almost all forms of erosion, in this sense, the right thing to do is to take measures to prevent water from stagnating on the surface through additional works on the facades, if this is not possible, water-repellent coatings should be applied, generally based on siloxanes without altering the breathability, and respecting the natural appearance of the bases as much as possible.

7	CD-01-1	Crumbling	Detachment of single grains or aggregates of grains. Crumbling-Detachment of aggregates of grains from the substrate. These aggregates are generally limited in size (less than 2 cm). This size depends on the nature of the stone and its environment.	The deterioration processes must be interrupted, in general the process is based on the manual cleaning of the material in order not to generate strong abrasions in the rock, it is advisable to make samplings of the dirt to determine its nature and to eradicate them in an effective way. Within this work is included the pre-consolidation, this should be done when there are pieces of great historical value where the cleaning itself can generate destruction of the element, desalination in which salts are extracted with the application on the surface of the stone of an additional absorbent material, a consolidation will be executed with the objective of increasing the cohesion of the components of the superficial zone of the stone.
8	CD-01-7	Pitting	point-like millimetric or submillimetric shallow cavities. The pits generally have a cylindrical or conical shape and are not interconnected. Pitting is due to partial or selective deterioration. Pitting can be biogenically or chemically induced, especially on carbonate stones. Pitting may also result from a harsh or inadapted abrasive cleaning method.	The deterioration processes must be interrupted, in general the process is based on the manual cleaning of the material in order not to generate strong abrasions in the rock, it is advisable to make samplings of the dirt to determine its nature and to eradicate them in an effective way. Within this work is included the pre-consolidation, this should be done when there are pieces of great historical value where the cleaning itself can generate destruction of the element, desalination in which salts are extracted with the application on the surface of the stone of an additional absorbent material, a consolidation will be executed with the objective of increasing the cohesion of the components of the superficial zone of the stone.
9	BD-01-1	Algae	Algae are microscopic vegetal organisms without stem or leaves which can be seen outdoors and indoors. Algae form green, red, brown, or black veil like zones and can be found mainly in situations where the substrate remains moistened for long periods of time. Depending on the environmental conditions and substrate type, algae may form solid layers or smooth films.	Use of biocidal products with a broad disinfectant spectrum and low solubilization in water, which should not react with the products used for consolidation and cleaning of the stone. The most commonly used biocides are benzalkonium chloride, ammonia (ammonium salts), formaldehyde and sodium hypochlorite.
10	BD-01-2	Lichen	Vegetal organism forming rounded millimetric to centimetric crusty or bushy patches. Lichen is a common feature of outdoor stone and is generally best developed under clean air conditions, but growth may be facilitated by certain pollutant such as nitrogen oxides derived primarily from vehicle pollution or agriculture. Former lichen growth may be detected by typical pitting structures (see this term) or lobate or mosaic patterns and even depressions	Use of biocidal products with a broad disinfectant spectrum and low solubilization in water, which should not react with the products used for consolidation and cleaning of the stone. The most commonly used biocides are benzalkonium chloride, ammonia (ammonium salts), formaldehyde and sodium hypochlorite.
11	BD-01-3	Moss	Vegetal organism forming small, soft and green cushion of centimetric size. Mosses often grow on stone surface open cavities, cracks, and in any place permanently or frequently wet (masonry joints), and usually shady	Use of biocidal products with a broad disinfectant spectrum and low solubilization in water, which should not react with the products used for consolidation and cleaning of the stone. The most commonly used biocides are benzalkonium chloride, ammonia (ammonium salts), formaldehyde and sodium hypochlorite.
12	BD-01-4	Plants	Vegetal living being, having, when complete, root, stem, and leaves, though consisting sometimes only of a single leafy expansion	Use of biocidal products with a broad disinfectant spectrum and low solubilization in water, which should not react with the products used for consolidation and cleaning of the stone. The most commonly used biocides are benzalkonium chloride, ammonia (ammonium salts), formaldehyde and sodium hypochlorite.



PATHOLOGY DATA SHEET

PROJECT NAME: Staroměstská radnice s orlojem, Prague.
 ADDRESS/ COORDINATES: 110 00 Praha 1 – Staré Město-Prague
 ELEMENT TO BE ANALYZED: Facades
 MATERIAL: Stone
 UNIT OF MEASURE: m²

ORIGINALITY YES x
 NO
 UNKNOWN
 DATE (dd/mm/yyyy): 20/06/2023

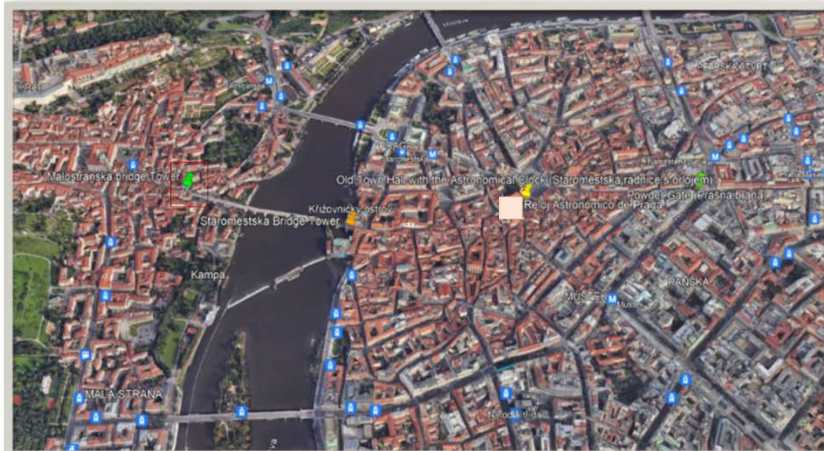
DEGREE OF DAMAGE	
	x

CODE: E4

Format Authorship: Saray Sepulveda Cruz
 Date of creation of the formats: June 2022

Version V.1.0.

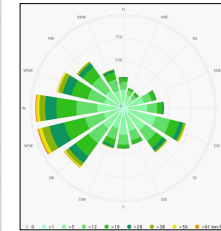
LOCALIZATION



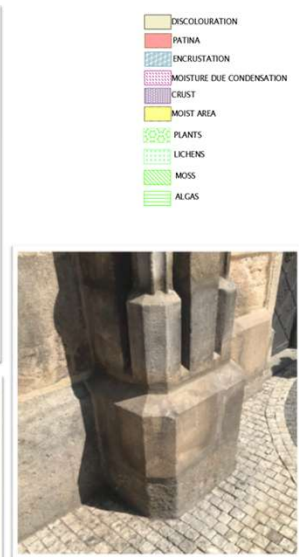
RELEVANT DATA

Coordinates
 Latitude: 50.086943°
 Longitude: 14.420722°
 Century: XIV
 Type: Gothic

Gothic tower from the 14th century. When it was built, it was the tallest building in Prague.



RELEVANT DAMAGES



- DISCOLOURATION
- PATINA
- ENCrustATION
- MOISTURE DUE CONDENSATION
- CRUST
- MOIST AREA
- PLANTS
- LICHENS
- MOSS
- ALGAS

PHOTO	Cod.	DAMAGE	DEFINITION	INTERVENTION PROPOSAL
1	CD-01-05	Efflorescence	Generally whitish, powdery or whisker-like crystals on the surface. Efflorescences are generally poorly cohesive and commonly made of soluble salt crystals	The deterioration processes must be interrupted, in general the process is based on the manual cleaning of the material in order not to generate strong abrasions in the rock, it is advisable to make samplings of the dirt to determine its nature and to eradicate them in an effective way. Within this work is included the pre-consolidation, this should be done when there are pieces of great historical value where the cleaning itself can generate destruction of the element, desalination in which salts are extracted with the application on the surface of the stone of an additional absorbent material, a consolidation will be executed with the objective of increasing the cohesion of the components of the superficial zone of the stone.
2	CD-01-4	Discolouration	Change of the color of the stone in one or three of the color parameters: hue, value and chroma. Frequently produced by salts, by the corrosion of metals by micro-organisms. Some typical yellow, orange, brown and black discoloration patterns are due to the presence of carbonates and melanins produced by fungi and cyanobacteria. Darkened areas due to soot may have different shapes and extension according to their origin: pipe leakage, rising damp, hygroscopic behaviour due to the presence of salts, condensation	The deterioration processes must be interrupted, in general the process is based on the manual cleaning of the material in order not to generate strong abrasions in the rock, it is advisable to make samplings of the dirt to determine its nature and to eradicate them in an effective way. Within this work is included the pre-consolidation, this should be done when there are pieces of great historical value where the cleaning itself can generate destruction of the element, desalination in which salts are extracted with the application on the surface of the stone of an additional absorbent material, a consolidation will be executed with the objective of increasing the cohesion of the components of the superficial zone of the stone.
3	CD-01-4.2	Patina	Chromatic modification of the material, generally resulting from natural or artificial aging and not involving in most cases visible surface deterioration.	The deterioration processes must be interrupted, in general the process is based on the manual cleaning of the material in order not to generate strong abrasions in the rock, it is advisable to make samplings of the dirt to determine its nature and to eradicate them in an effective way. Within this work is included the pre-consolidation, this should be done when there are pieces of great historical value where the cleaning itself can generate destruction of the element, desalination in which salts are extracted with the application on the surface of the stone of an additional absorbent material, a consolidation will be executed with the objective of increasing the cohesion of the components of the superficial zone of the stone.
4	CD-01-4.3	Encrustation	Compact, hard, mineral outer layer adhering to the stone. Surface morphology and colour are usually different from those of the stone.	The deterioration processes must be interrupted, in general the process is based on the manual cleaning of the material in order not to generate strong abrasions in the rock, it is advisable to make samplings of the dirt to determine its nature and to eradicate them in an effective way. Within this work is included the pre-consolidation, this should be done when there are pieces of great historical value where the cleaning itself can generate destruction of the element, desalination in which salts are extracted with the application on the surface of the stone of an additional absorbent material, a consolidation will be executed with the objective of increasing the cohesion of the components of the superficial zone of the stone.
5	CD-01-06	Crust	A crust is frequently dark coloured (black crust) but light colours can also be found. Crusts may have an homogeneous thickness, and thus replicate the stone surface, or have irregular thickness and disturb the reading of the stone surface details.	The deterioration processes must be interrupted, in general the process is based on the manual cleaning of the material in order not to generate strong abrasions in the rock, it is advisable to make samplings of the dirt to determine its nature and to eradicate them in an effective way. Within this work is included the pre-consolidation, this should be done when there are pieces of great historical value where the cleaning itself can generate destruction of the element, desalination in which salts are extracted with the application on the surface of the stone of an additional absorbent material, a consolidation will be executed with the objective of increasing the cohesion of the components of the superficial zone of the stone.
6	PD-02-1	Differential erosion	Result of selective lichen attack on calcitic rocks. Differential erosion is synonymous with relief, i.e. the formation of irregularities on the surface of the stone.	It is important to avoid moisture, since the presence of water is the constant in almost all forms of erosion, in this sense, the right thing to do is to take measures to prevent water from stagnating on the surface through additional works on the facades, if this is not possible, water-repellent coatings should be applied, generally based on siloxanes without altering the breathability, and respecting the natural appearance of the bases as much as possible.
7	CD-01-1	Crumbling	Detachment of single grains or aggregates of grains. Crumbling/Detachment of aggregates of grains from the substrate. These aggregates are generally limited in size (less than 2 cm). This size depends on the nature of the stone and its environment.	The deterioration processes must be interrupted, in general the process is based on the manual cleaning of the material in order not to generate strong abrasions in the rock, it is advisable to make samplings of the dirt to determine its nature and to eradicate them in an effective way. Within this work is included the pre-consolidation, this should be done when there are pieces of great historical value where the cleaning itself can generate destruction of the element, desalination in which salts are extracted with the application on the surface of the stone of an additional absorbent material, a consolidation will be executed with the objective of increasing the cohesion of the components of the superficial zone of the stone.
8	BD-01-1	Algae	Algae are microscopic vegetal organisms without stem or leaves which can be seen outdoors and indoors. Algae form green, red, brown, or black veil like zones and can be found mainly in situations where the substrate remains moistened for long periods of time. Depending on the environmental conditions and substrate type, algae may form solid layers or smooth films.	Use of biocidal products with a broad disinfectant spectrum and low solubilization in water, which should not react with the products used for consolidation and cleaning of the stone. The most commonly used biocides are benzalkonium chloride, ammonia (ammonium salts), formaldehyde and sodium hypochlorite.
9	BD-01-3	Moss	Vegetal organism forming small, soft and green lush ions of centimetric size. Mosses often grow on stone surface open cavities, cracks, and in any place permanently or frequently wet (masonry joints), and usually shady	Use of biocidal products with a broad disinfectant spectrum and low solubilization in water, which should not react with the products used for consolidation and cleaning of the stone. The most commonly used biocides are benzalkonium chloride, ammonia (ammonium salts), formaldehyde and sodium hypochlorite.